TECHNICAL REPORT STANDARD PAGE

1. Report No. **FHWA/LA.10/467**	2. Government Accession No.	3. Recipient's Catalog No.
4. Title and Subtitle **Performance of Buried Pipe Installation**	5. Report Date May 2010	
	6. Performing Organization Code **LTRC Project Number: 08-6GT** **State Project Number: 739-99-1520**	
7. Author(s) **Michele Barbato, Ph.D.** **Assistant Professor** **email: mbarbato@lsu.edu**	8. Performing Organization Report No.	
9. Performing Organization Name and Address **Department of Civil and Environmental Engineering** **Louisiana State University** **Baton Rouge, LA 70803**	10. Work Unit No.	
	11. Contract or Grant No.	
12. Sponsoring Agency Name and Address **Louisiana Department of Transportation and Development** **P.O. Box 94245** **Baton Rouge, LA 70804-9245**	13. Type of Report and Period Covered **Final Report** **Period Covered 01-2008 – 12-2009**	
	14. Sponsoring Agency Code	

15. Supplementary Notes
Conducted in Cooperation with the U.S. Department of Transportation, Federal Highway Administration

16. Abstract

The purpose of this study is to determine the effects of geometric and mechanical parameters characterizing the soil structure interaction developed in a buried pipe installation located under roads/highways. The drainage pipes or culverts installed as part of a roadway project are considered as holistic systems which include not only the pipes and their mechanical properties as determined by materials, geometry and manufacturing procedures, but also the natural soil and the trench into which the pipe is placed, constructed and expected to perform. The research results confirm that the performance of the soil-structure interaction system constituted by the pipe, the trench backfill and the natural soil surrounding the trench depends significantly not only on the pipe material and stiffness but also on geometric parameters defining the trench in which the pipe is installed, such as cover height, bedding thickness and trench width. Minimum requirements for these geometric parameters can be established to obtain equivalent performances of different pipe systems as function of (1) the pipe stiffness and diameter, (2) the local natural soil properties, and (3) the type of road pavement.
The results of this research can be used as guidance in establishing guidelines for the alternate selection and application of typical highway drainage products, such as pipes and culverts. This report provides initial data that can be used for a proper comparison of performance, in terms of deformations of the road surface under typical loads, of pipes characterized by different materials and different installation geometry and methodologies. This project suggests also future research directions to delineate a rigorous comparison of different soil-pipe systems under a more general definition of performance, rigorously accounting for economical factors (e.g., initial cost, life-cycle cost) and societal risk.

17. Key Words Buried pipes; culverts; soil-structure interaction; finite element method		18. Distribution Statement **Unrestricted. This document is available through the National Technical Information Service, Springfield, VA 21161.**	
19. Security Classif. (of this report)	20. Security Classif. (of this page)	21. No. of Pages 123	22. Price

Project Review Committee

Each research project will have an advisory committee appointed by the LTRC Director. The Project Review Committee is responsible for assisting the LTRC Administrator or Manager in the development of acceptable research problem statements, requests for proposals, review of research proposals, oversight of approved research projects, and implementation of findings.

LTRC appreciates the dedication of the following Project Review Committee Members in guiding this research study to fruition.

LTRC Administrator

Zhongjie "Doc" Zhang, Ph.D., P.E.
Pavement & Geotech Research Administrator

Members

Luanna Cambas
Brian Buckel
JoAnn Kurts
Steven Cumbaa
Arturo Aguirre
Khalid Farrag

Directorate Implementation Sponsor

Richard Savoie

Performance Evaluation of Buried Pipe Installation

by

Michele Barbato, Ph.D.
Marvin Bowman
Alexander Herbin

Civil and Environmental Engineering
3531 Patrick F. Taylor Hall
Louisiana State University
Baton Rouge, Louisiana 70803

LTRC Project No. 08-6GT
State Project No. 739-99-1520

conducted for

Louisiana Department of Transportation and Development
Louisiana Transportation Research Center

May 2010

ABSTRACT

The purpose of this study was to determine the effects of geometric and mechanical parameters characterizing the soil structure interaction developed in a buried pipe installation located under roads/highways. The drainage pipes or culverts installed as part of a roadway project are considered as holistic systems that include not only the pipes and their mechanical properties as determined by materials, geometry, and manufacturing procedures, but also the natural soil and the trench into which the pipe is placed, constructed, and expected to perform. The research results confirmed that the performance of the soil-structure interaction system constituted by the pipe, the trench backfill, and the natural soil surrounding the trench depends significantly not only on the pipe material and stiffness but also on geometric parameters defining the trench in which the pipe is installed, such as cover height, bedding thickness, and trench width. Minimum requirements for these geometric parameters can be established to obtain equivalent performances of different pipe systems as function of (1) the pipe stiffness and diameter, (2) the local natural soil properties, and (3) the type of road pavement.

The results of this research can be used as guidance in establishing guidelines for the alternate selection and application of typical highway drainage products, such as pipes and culverts. This report provides initial data that can be used for a proper comparison of performance, in terms of deformations of the road surface under typical loads, of pipes characterized by different materials and different installation geometry and methodologies. This project also suggests future research directions to delineate a rigorous comparison of different soil-pipe systems under a more general definition of performance, rigorously accounting for economical factors (e.g., initial cost, life-cycle cost) and societal risk.

ACKNOWLEDGMENTS

Financial support of this research project by the Louisiana Department of Transportation and Development (LADOTD) through the Louisiana Transportation Research Center (LTRC) is gratefully acknowledged.

The authors would also like to thank Zhongjie Zhang, Ph.D., P.E., LTRC project manager, who provided guidance for all phases of the research project; the project review committee members, who provided comments and feedback for the research; and Brian Felder, Joe Babcanec, and Mark Joersz from ADS/Hancor, Inc., who provided the geometrical information needed to accurately model high-density polyethylene (HDPE) pipes.

IMPLEMENTATION STATEMENT

The results of this research can be used as guidance in establishing guidelines for the alternate selection and application of typical highway drainage products, such as pipes and culverts. This report provides initial data that can be used for a rigorous comparison, in terms of deformations of the road surface and pipe ring deformation under typical loads, of the performance of pipes characterized by different materials and different installation geometry and methodologies. This project also suggests future research directions to delineate a rigorous comparison of different soil-pipe systems under a more general definition of performance, rigorously accounting for economical factors (e.g., initial cost, life-cycle cost) and societal risk.

The following specific recommendations are made for implementation:

1) The minimum cover height should be expressed as a function of the pipe diameter.
2) For flexible and semi-flexible pipes, the minimum trench width should be equal to twice the pipe diameter, while for rigid pipes a minimum trench width equal to the pipe diameter + 3 ft. is sufficient.
3) Different minimum requirements can be made for yielding and stiff soils. In the absence of specific data from in-situ tests, the more demanding requirements for yielding soil should be followed in favor of safety.
4) Different minimum requirements can be made for different road pavements with more demanding requirements for more flexible road pavements.

TABLE OF CONTENTS

LIST OF TABLES

LIST OF FIGURES

INTRODUCTION

Existing codes and recommendations often require standard/minimum values for the bedding, backfill, and fill cover geometric and mechanical properties in the installation of buried pipes under transportation facilities. These recommended values are often obtained by considering the worst-case scenario for each of the components and account only in an approximate way for the soil-structure interaction (SSI) between bedding, backfill, fill cover, and pipes of different materials and mechanical properties. Performance in terms of reliability and cost-effectiveness of the design is not fully addressed by the current specifications. The need arises for revising the current specifications to obtain a more efficient design of the installation of buried pipes.

Current design methodologies for buried pipes are still based on the Marston theory, developed between 1930 and 1960, for estimating vertical loads *[1]*. This design method is based on the assumption of an elastic, isotropic soil above and around the pipe. Such an approach has been deemed as over-conservative, given the simplifications associated with these inherent assumptions. In addition, the method does not consider the effects of different bedding material and thickness.

Some preliminary research has been performed on concrete box culverts at the University of Texas at Arlington. This research involves the experimental investigation of the shear capacity of precast reinforced concrete box culverts *[2]*. The Pennsylvania Department of Transportation has conducted a study on the effect of bedding thickness to investigate problems they experienced. This study was not published. The Federal Highway Administration (FHWA) sponsored research at UMass that investigated the use of soft bedding to reduce soil pressure at the invert, but this study did not investigate the depth of bedding as a variable. Among other results, this research led to the development of Culvert Analysis and Design (CANDE). CANDE is a two-dimensional nonlinear finite element (FE) buried pipe and culvert software application used for the structural design, analysis, and evaluation of buried pipes, culverts, and other soil-structure interaction systems *[3, 4]*. The FE program has been continuously extended (e.g., by including AutoCAD interfaces in CandeCAD Pro) and incorporates built-in linear and nonlinear soil and pipe material models to analyze almost any type of installation. FE analysis studies using the SSI program Soil-Pipe Interaction and Design Analysis (SPIDA) have been conducted for and implemented into AASHTO LRFD Bridge Design Specifications, Section 12 *[5]*. Results are used for defining standard installations, bedding thickness, and minimum compaction requirements

but are mostly obtained from conservative assumptions and referred to as deep cover situations.

The buried pipe installation considered in this project is a trench type with vertical walls and a single pipe (Figure 1). This type of installation involves the removal of a trench of natural soil in which a bedding layer, the pipe, and different layers of backfill materials are positioned. After the trench is filled and the backfill material is compacted, the sub-pavement and the road pavement (asphalt or concrete) are laid over the trench and the surrounding natural soil. The installation is characterized by shallow cover. Therefore, the live loads due to the vehicular traffic produce significant stresses on the pipe and the soil in the trench, with a stress distribution strongly dependent on the specific geometric and mechanical properties of the entire soil-pipe system.

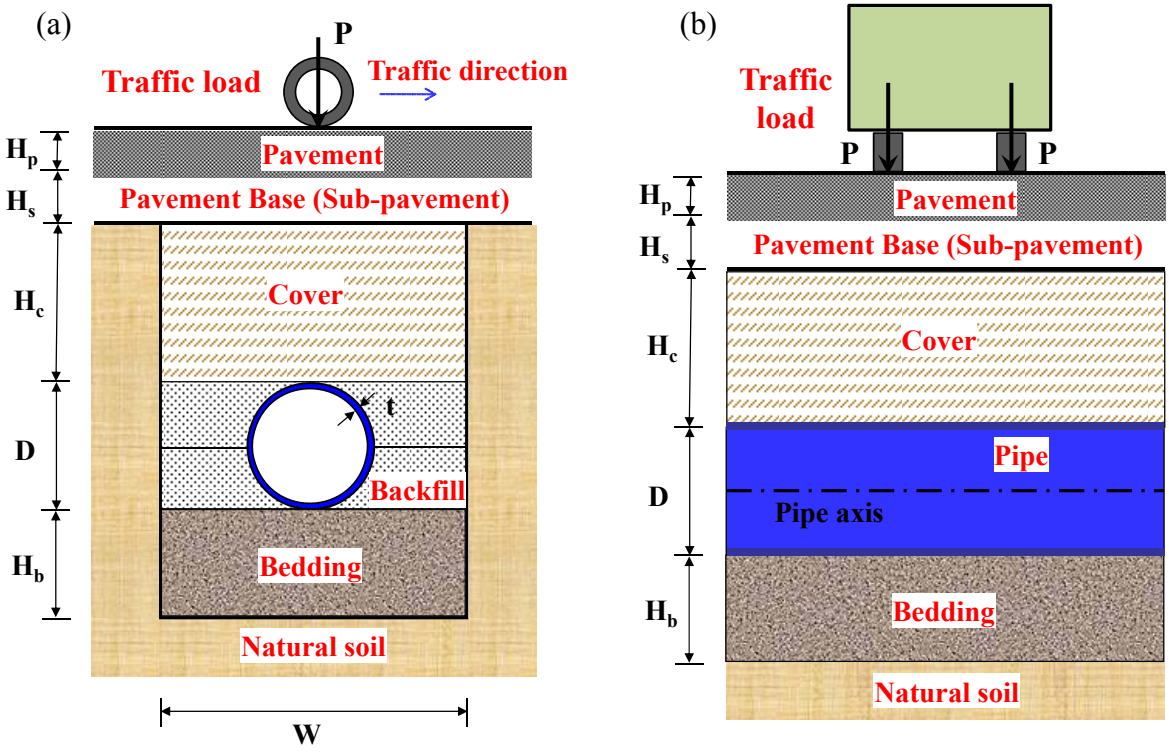

Figure 1

Buried pipe installation: (a) transversal view (cross-section) and (b) longitudinal view

This project proposes the use of a linear and nonlinear FE analysis to investigate the effects of the geometric and mechanical parameters characterizing the soil-structure interaction developed in a buried pipe installation. Adoption of FE modeling to analyze such problems in geomechanics is not new and has increased in reliability and practicality as the analysis tools and computational power have evolved. The adoption of a numerical approach is a

justifiable choice, considering the number of parameters involved and the complex interaction between the response of the soil and pipe.

This research presents several innovative aspects compared to previous similar studies. In particular, this study (a) focuses on pipes and culverts buried in shallow cover conditions; (b) considers soil conditions (i.e., soft cohesive soils) typical of Southern Louisiana; (c) models explicitly the effects of different road pavements and sub-pavements; (d) introduces a new performance parameter corresponding to the dip depth at the road surface produced by the live loads due to traffic; and (e) provides an extensive parametric study to evaluate the performance sensitivity of the soil-pipe system to material, mechanical, and geometric parameters defining pipes, trench backfills, natural soils, and road pavement types.

OBJECTIVE

The goal of this research project was to determine the effects of geometric and mechanical parameters characterizing the soil-structure interaction developed in buried pipe installations. Parameters such as pipe ring stiffness, bedding thickness, trench width, and fill cover height were considered.

The specific objectives of this study were: (1) to provide a rigorous sensitivity analysis to various geometric and mechanical parameters of the performance of buried pipe installations in terms of deformation and stresses in the pipe and deformation (dip depth) at the surface of transportation facility pavement; (2) to derive preliminary results that can be used as an initial justification for accepting/revising the current provisions for minimum bedding thickness, fill cover height, and installation quality for pipes buried under transportation facilities; and (3) to provide guidelines for developing a set of recommendations for minimum/optimal requirements on cover height, bedding thickness, and trench width that ensure similar performance for pipes of different materials, i.e., reinforced concrete (RC), steel, polyvinyl chloride (PVC), and high density polyethylene (HDPE).

SCOPE

The scope of this research included the study of the mechanical behavior of buried culvert and pipes. The considered pipes are buried in trenches excavated below roads with different levels of transit. The local soil conditions in which the pipes are installed are representative of typical locations in Southern Louisiana, i.e., with soft clay. Only single pipe installations were considered. The pipe dimensions studied cover the range between 18 in. and 60 in. of pipe internal diameters. Different materials were considered for the pipes, i.e., reinforced concrete, steel, PVC, and HDPE. This research focused on culvert pipes buried in shallow cover situations where traffic creates a high live load influence on the pipe. The geometrical properties (circular shape, thickness, and diameter ranges) considered in this investigation are representative of typical drainage pipes and culverts constructed on LADOTD projects and do not include box culvert or three sided structures.

Only loadings from traffic were considered and modeled as static equivalent loads applied on the surface of the road. These loads were amplified by using an appropriate dynamic impact factor to approximately account for dynamic effect. The soil-structure interaction behavior between the pipe, the backfill material, and the natural soil surrounding the trench was explicitly modeled and included in the study. Only short-term loading effects were considered. Effects of repeated loading cycles (i.e., fatigue) were not analyzed in this research.

The results of this research are intended to be used as input for cost-benefit analyses for alternate bidding of buried pipes of different materials. However, a complete cost-benefit analysis is outside the scope of this research. It should be noted that a complete cost-benefit analysis must consider (in addition to the direct costs of pipes and backfill material, excavation, installation of the pipe, filling of the trench, and compaction of the backfill material) costs associated with: (1) different hydraulic capacity of same-size different-material pipes (i.e., for the same transportation facility, pipes of different materials could also be a different size in order to satisfy the hydraulic requirements of the design); (2) protection from corrosion (e.g., cathodic protection and grouting) of metallic parts; and (3) other labor associated with ensuring the long-term performance of the buried pipe installations. These are not directly related to the short-term mechanical performance of buried pipe installations and were not considered in this study. However, these costs must be included in the cost-benefit analysis of a specific installation.

METHODOLOGY

A study of the SSI between pipes, trench backfill, and natural soil based on the FE method was completed during this research. The FE method allows for an accurate analysis of the complex interaction between the pipe, the trench backfill material, and the surrounding natural soil under different conditions, characterized by a wide range of geometric and mechanical parameters.

Appropriate FE models of pipes buried in shallow trenches and positioned below roadways were built using different commercial FE codes to study the sensitivity of the mechanical behavior of the soil-pipe system for a wide range of conditions typically encountered in highway projects in Southern Louisiana. A simplified linear elastic FE analysis was employed to perform an extensive parametric study and sensitivity analysis of soil-pipe installation systems. An advanced nonlinear hysteretic FE analysis was used (a) to validate the linear elastic FE analysis results under the specific conditions representing a proposed modification to the current LADOTD requirements for LADOTD highway projects, (b) to accurately evaluate the sensitivity of a buried pipe system performance to modeling parameters and SSI effects, and (c) to investigate in detail the combinations of parameter values for which the performance of the soil-pipe installation system may be unsatisfactory.

This research project studied the effects on buried pipe performance due to:

1) Excavation width (W);
2) Fill cover height (H_c);
3) Bedding height (H_b);
4) Mechanical properties (e.g., stiffness: E_s, cohesion: c_s, friction angle: ϕ_s) of the natural soil surrounding the trench;
5) Mechanical properties and grade of compaction (e.g., stiffness: E_f, cohesion: c_f, friction angle: ϕ_f) of the fill material;
6) Mechanical properties and grade of compaction (e.g., stiffness: E_b, cohesion: c_b, friction angle: ϕ_b) of the bedding material;
7) Pipe material (RC, steel, PVC, and HDPE), mechanical properties (e.g., stiffness: E, and yield strength: σ_y), and geometric properties (diameter: D and thickness: t) of the pipe;
8) Material (concrete or asphalt) and geometry of the roadway pavement (road pavement thickness: H_p) and its sub-pavement (sub-pavement thickness: H_{sp}, and sub-pavement stiffness: E_{sp}); and
9) Importance of facility (different loadings and different requirements on deformation performance).

The pipe performance has been defined in terms of relevant quantities characterizing the FE response of the soil-pipe system such as:

1) Maximum radial deformation (Δ_R) of the pipe (deformation performance); and
2) Maximum dip depth (Δ_{live}) at the surface (driver comfort and safety performance) under maximum design load.

Linear FE Modeling of Buried Pipe Installations

Linear elastic FE analyses were performed by using the commercial FE program SAP2000, typically employed in the civil engineering and structural engineering communities for FE analysis of structural and soil-structure interaction systems subjected to static and dynamic loadings *[6]*. This program was chosen for this part of the project due to its advanced and user-friendly graphical user interface, its simplicity of use, and its high computational speed, particularly for problems characterized by linear elastic behavior and large meshes (i.e., linear elastic FE models with a large number of finite elements and degrees of freedom). The next sections of this report describe the linear elastic FE models built in SAP2000, the analyses performed, the simplifying modeling assumptions adopted, and the corresponding limitations in the obtained results.

Description of the FE models Employed

Two-dimensional (2-D) models of typical cross-sections (Figure 2a) were built to study the performance of the soil-pipe installation under a wide range of different conditions and geometries. Making use of the symmetry of the cross-section model, the 2-D models included explicitly only one half of the trench. The soil-pipe system was modeled under plain strain conditions and the thickness of the model was assumed equal to one foot. The soil in the trench, the sub-pavement layer, and the road pavement were modeled using isoparametric quadrilateral elements with bilinear interpolation of the displacement fields, with the exception of the parts of the model immediately surrounding the pipe, where isoparametric triangular elements were employed (Figure 2b). The material used to fill the trench was subdivided into different layers, i.e., bedding, backfill, and cover. Different Young's moduli were employed to model the different mechanical behavior of each layer.

The pipe was modeled by using ordinary displacement-based Euler-Bernoulli frame elements. The frame element cross-sectional properties were obtained from the cross-sectional area and second moment of inertia of the pipe ring corresponding to one linear foot of pipe and computed about its centerline. The Young's modulus of the pipe was obtained

from the pipe material properties provided by American Association of State Highway and Transportation Officials (AASHTO) standards.

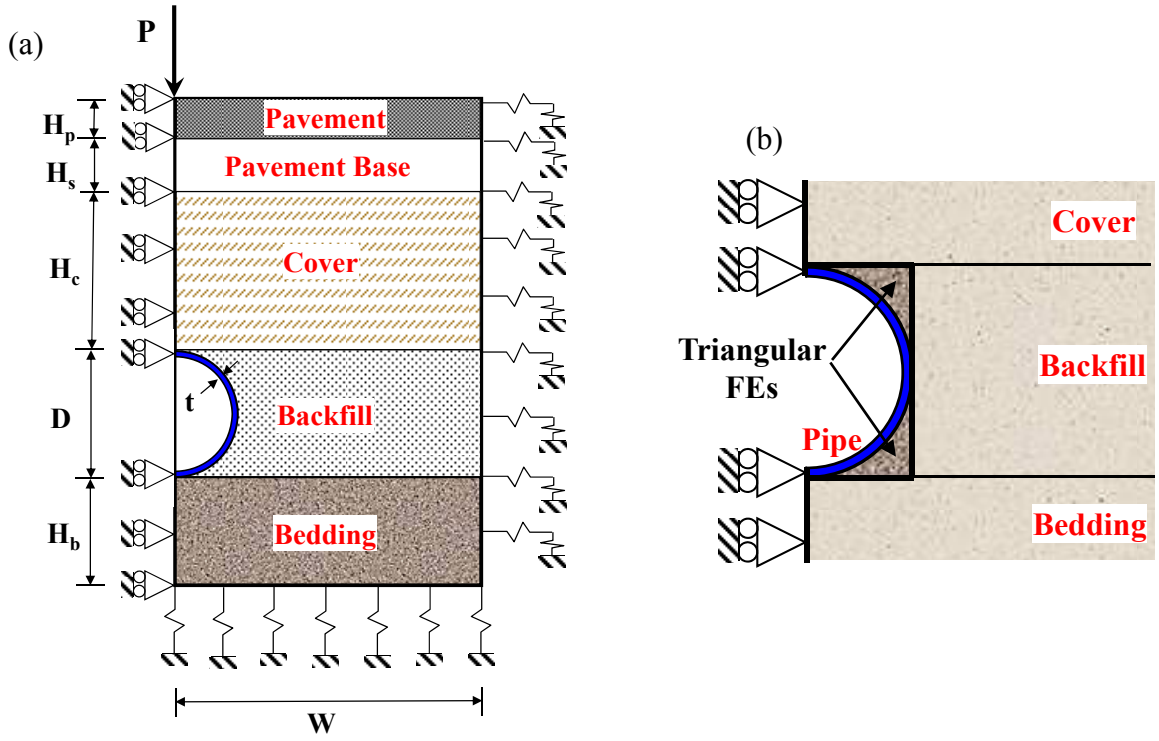

Figure 2

Description of a typical linear elastic FE model: (a) schematic representation of the regions and boundary conditions and (b) regions modeled through isoparametric triangular elements

The natural soil surrounding the trench was modeled indirectly through appropriate boundary conditions applied along the borders of the FE model of the pipe-trench system. The boundary conditions at the bottom and at the side of the trench in contact with the natural soil were imposed through linear elastic vertical and horizontal springs with stiffness defined as a function of the natural soil mechanical properties (Young's modulus). The boundary conditions along the plane of symmetry of the pipe installation were imposed in order to consistently represent the symmetry conditions, i.e., the horizontal displacements through the plane of symmetry were imposed equal to zero.

Both the self-weight of the different soil layers, pipe materials, and road surface, referred to as "gravity loads" hereinafter, and traffic live loads were considered. The gravity loads were obtained assuming a weight per unit volume equal to 124.8 lb/ft^3 for the soil materials and the weight per unit length of the pipe corresponding to the different pipe materials. The live loads were obtained considering the axle load corresponding to a standard H20 truck load as

defined in the AASHTO Standard Specifications for Highway Bridges *[7]*. The live loads were applied statically to the FE model in correspondence of the plane of symmetry as a concentrated load with intensity equal to one quarter of the AASHTO standard H20 truck axle load (i.e., 16 kips / 4 = 4 kips). A dynamic impact factor equal to 1.50 was used to approximately account for dynamic effects. It is noteworthy that the dynamic impact factor value recommended by the AASHTO code is equal to 1.33. However, this study used a value of 1.50 in order to account for below average road conditions (i.e., rough road surfaces) that may be encountered in older road facilities. Thus, the load used in the FE model is equal to 6 kips. The discretization of the considered FE model was determined so to ensure mesh independence of the response results.

Simplifying Assumptions and Limitations of the Performed Linear Elastic FE Analyses

Linear elastic FE analysis is computationally inexpensive when compared to more accurate and realistic nonlinear hysteretic FE analysis. Indeed, each linear elastic FE analysis performed in this study required less than one minute of computational time using an ordinary personal computer. The reduced computational cost of a linear elastic analysis allowed exploring a wide range of values of numerous geometric and mechanical parameters. This extensive parametric study required about 25,000 FE analyses and provided important information about the sensitivity of the performance of buried pipe installations. This information is sufficiently accurate to qualitatively assess the conditions under which pipes made of different materials can perform similarly, and thus can be used as alternative design solutions.

Nevertheless, several simplifying assumptions were employed in the linear elastic FE modeling of soil-pipe systems. Therefore, the analysis results are affected by some limitations, which are briefly described below.

1) The soil and pipe materials were modeled as linear elastic. In general, this simplification can lead to overestimating stresses and underestimating deformations. Also, long term effects, nonlinear geometry, and local buckling were not modeled.
2) The effects of imperfect interface contact between the pipe and soil were neglected. This assumption could overestimate the beneficial contribution of soil-structure interaction to the performance of buried pipe installations.
3) The live loads due to vehicular traffic were modeled as a static concentrated load magnified by a dynamic amplification factor. This approximation can lead to conservative estimates of the stresses applied on the pipe, particularly for very shallow trenches.

4) The effects of installation procedures and construction phases were neglected by simply superposing the loads due to gravity and live loads. Accurate modeling of these effects requires a staged nonlinear FE analysis faithfully reproducing the specific installation procedure.
5) The soil surrounding the trench was indirectly modeled through elastic springs applied at the boundaries of the trench model. This crude simplification can provide only a qualitative estimate of the effects of different local soil conditions on the performance of buried pipe installations.
6) Three-dimensional effects were neglected.
7) The effects of variable water elevation were not modeled explicitly. However, the range of values for the initial stiffness of the backfill material was chosen in order to include values representative of the two extreme cases of water level (below the bottom of the trench and at the road surface level).

In order to overcome the above limitations and to validate the results obtained by using linear elastic FE analysis, more advanced, accurate, and realistic nonlinear hysteretic FE models were built and analyzed. The model size for the nonlinear hysteretic models was determined based on a parametric study with respect to the dimensions of the model, referred to as the model dimension sensitivity study hereafter.

Model Dimension Sensitivity Study

A model dimension sensitivity study was performed on the linear elastic FE models of buried pipe installation systems. The objective of this sensitivity study was to determine the appropriate dimensions for a three-dimensional (3-D) nonlinear hysteretic FE model in order to obtain FE response results (e.g., pipe stresses/deformations and dip depth at the road surface) insensitive to model dimensions. This study focused on determining (a) the size of the appropriate expansion size of native soil to be included in the model in both horizontal and vertical directions and (b) the thickness of the FE model.

The first part of the model dimension sensitivity study was performed based on the original 2-D models by removing the elastic springs used as boundary conditions to model the natural soil surrounding the trench and replacing them with a FE model based on the mechanical properties of the actual native soil. The effects of both horizontal (i.e., soil region on the side of the trench) and vertical (i.e., soil region below the trench) native soil expansion were considered. The FE model was increased in both directions, both independently and simultaneously, with discrete increments equal to one quarter of the trench width in the

horizontal direction and 2 ft. in the vertical direction, until the changes in the FE results were negligible.

A second step of the model dimension sensitivity study focused on the effects due to the thickness of the FE model. The thickness of the 2-D elements was modified with discrete increments equal to 6 in. until model dimension independence of the response results was observed. The dimensions of the 2-D FE models obtained from this second sensitivity analysis step were used as the starting point for the 3-D models.

The 3-D FE models were built using solid elements for both soil and pipe components. The new FE models were obtained by extruding, in the direction parallel to the pipe axis, the elements of the 2-D models. In this case, due to symmetry, only one quarter of the physical soil-pipe system was modeled. Model dimension independence of the response results was verified under appropriate boundary conditions.

In the 3-D FE models, the intensity of the live loads was kept equal to the intensity considered in the 2-D model, while the point load was substituted by an equivalent uniformly distributed load based on the AASHTO tire-road contact dimensions for an 18 wheel truck. This contact surface is defined as a rectangular shape with sides equal to 12 in. and 7 in. *[7]*. The live loads in the 3-D model are transmitted to the road by a quarter of a tire, and the uniform pressure is obtained by distributing the corresponding 6 kips load over a rectangular area with sides equal to 6 in. and 3.5 in., respectively.

Nonlinear FE Modeling of Buried Pipe Installations

Nonlinear hysteretic FE models were built using the general purpose FE program ABAQUS. ABAQUS is a widely used FE program suitable for linear and nonlinear FE analysis of structural and mechanical systems subjected to static and/or dynamic loading conditions *[8]*. The program was chosen for the high reliability of its results, its versatility, and rich library of FEs, material constitutive models, and solution strategies.

The results obtained using linear elastic FE analyses indicate that, among the design parameters (i.e., cover height, trench width, bedding thickness, and compaction/stiffness of the backfill material), the parameter that most affects the soil-pipe system performance is the cover height, H_c. The linear FE analyses also provided a first estimate for the optimal value of H_c, (i.e., $H_c = D/4$ for RC pipes, $H_c = D/2$ for steel and PVC pipes, and $H_c = D$ for HDPE pipes). In order to improve these estimates, an additional parametric study, with H_c as a parameter, was conducted using more accurate 3-D nonlinear hysteretic FE models of the

soil-pipe systems. The ranges of H_c values considered for all materials and the corresponding FE models built and analyzed are summarized in Table 1. Based on consideration of economical constraints, a maximum value of H_c = 60 in. was assumed for all materials and all pipe diameters.

Table 1
Total number of models

Pipe Material	D (in.)	Cover Height, H_c (in.)										# of Models
		6	12	18	24	30	36	42	48	54	60	
RC	42	X	X	X	X	X	X	X	-	-	-	7
RC	60	X	X	X	X	X	X	X	-	-	-	7
Steel	42	-	X	X	X	X	X	X	-	-	-	6
Steel	60	-	X	X	X	X	X	X	X	X	X	9
PVC	42	-	-	X	X	X	X	X	X	X	X	8
PVC	60	-	-	X	X	X	X	X	X	X	X	8
HDPE	42	-	-	X	X	X	X	X	X	X	X	8
HDPE	60	-	-	X	X	X	X	X	X	X	X	8
												$\sum = 61$

Table 2
Total number of elements, nodes, and degrees-of-freedom (DOFs) with running time for each nonlinear hysteretic FE model

Pipe Material	D (in.)	H_c (in.)	Soil Elements	Pipe Elements	Total # of Elements	Total # of Nodes	Total # of DOFs	Running Time
RC	42	6	30,577	51,892	82,469	192,869	523,287	6 hrs
RC	42	42	62,045	51,892	113,937	384,822	1,036,218	15 hrs
RC	60	6	75,732	91,336	167,068	602,517	1,613,691	7 hrs
RC	60	42	91,615	91,336	182,951	698,693	1,870,683	17 hrs
Steel	42	12	116,423	50,688	167,111	701,189	1,763,535	23 hrs
Steel	42	42	138,801	50,688	189,489	778,197	2,014,589	30 hrs
Steel	60	12	187,229	72,576	259,805	1,027,624	2,593,688	30 hrs
Steel	60	60	204,789	72,576	277,365	1,187,480	3,043,976	48 hrs
PVC	42	18	24,288	1,584	25,872	152,569	404,427	6 mins
PVC	42	60	33,384	1,584	34,968	208,043	552,705	10 mins
PVC	60	18	36,828	2,352	39,180	172,884	440,148	10 mins
PVC	60	60	48,168	2,352	50,520	231,892	585,148	15 mins
HDPE	42	18	78,713	13,816	92,529	420,293	1,071,117	29 hrs
HDPE	42	60	101,989	13,816	115,805	559,517	1,443,037	61 hrs
HDPE	60	18	107,952	29,184	137,136	534,877	1,342,807	20 hrs
HDPE	60	60	132,656	29,184	161,840	684,767	1,743,197	24 hrs

Table 2 shows the number of elements, nodes, and DOFs and the approximate clock analysis time for each of the nonlinear hysteretic FE models built to perform the parametric study previously described. It was found that the clock analysis time is strongly dependent not only on the number of elements, nodes, and DOFs of the model, but also on the geometry of the interface between the pipe and the surrounding soil (outer pipe surface) and the geometry of the pipe itself (inner pipe geometry). For the RC and PVC pipes, the outer pipe surface consists of a simple cylinder surface, leading to a shorter analysis time when compared to steel and HDPE pipes. Although the RC pipe and the PVC pipe have similar outer pipe surface geometry, the reinforcement within the RC pipe increases the complexity of the inner pipe geometry, also producing a dramatic increase in analysis time. The curvature of the corrugated steel and HDPE pipes also leads to a higher computational cost for the corresponding FE analyses. More complex geometries require longer analysis time by increasing the number of iterations during each load step needed to reach convergence in the nonlinear inelastic FE analysis.

Nonlinear FE Model Description

Nonlinear hysteretic FE models of buried pipe installation systems were developed based on the 3-D models identified through the model dimension sensitivity study on linear elastic FE models of soil-pipe systems. Due to symmetry, only one quarter of the soil-pipe system was explicitly modeled.

In the following sections, the terminology used in the ABAQUS manual is employed. In particular, the following terms are defined: part, region, partition, and section. A “part” is the geometry building block of an ABAQUS FE model. Different parts can be assembled to create a FE model that can be then meshed and analyzed. A “region” is any particular portion of an ABAQUS FE model. A region can be a vertex, edge, face, cell, node, element, or a collection of these entities. Each part of an ABAQUS model can be partitioned into several regions. A “partition” is a feature that is used to divide a part into regions in which different loads are applied or different mesh attributes are assigned. Finally, a “section” is the set of data that specifies the properties of regions of an ABAQUS FE model. A section definition can contain information such as a material name, Poisson's ratio, transverse shear data, etc.

The FE model is obtained by assembling two parts, one to model the pipe (Figure 3a) and one to model the remaining components of the model (Figure 3b). The part corresponding to the pipe reproduced the geometry of the specific pipe typology, i.e., circular pipes for PVC and concrete materials, corrugated steel pipes with 2 2/3 in. x 1/2 in. corrugation pattern, and corrugated HDPE pipes (see Figure 4). The wall thickness, area of reinforcement, and

reinforcement placement for RC pipes were modeled in accordance with AASHTO M 170 *[9]*. Based on data provided by LADOTD, the thicknesses, t = 0.079 in. and t = 0.109 in., are the most commonly used in Southern Louisiana for 42 in. and 60 in. diameter corrugated steel pipes, respectively. Using the dimensions given in AASHTO M 36, the geometry of the corrugated steel pipes was modeled exactly *[10]*. The PVC pipes with D = 42 in. and 60 in. were modeled according to AASHTO M 278 with a wall thickness of 2.1 in. and 3 in., respectively*[11]*. These dimensions correspond to the pipe wall thickness t = D/20, where D is the inner pipe diameter. Finally, the HDPE pipes were modeled in compliance with AASHTO M 294 and dimensions given by Advanced Drainage Systems, Inc. (personal communication) *[12]*. The exact corrugation was scanned from an actual HDPE sample pipe and transferred into an AutoCAD file. These files were directly imported into ABAQUS in order to accurately model the geometry of the part corresponding to the HDPE pipe.
The part corresponding to the remaining components of the model was further subdivided into three regions, i.e., the surrounding native soil, the trench material, and the roadway components. In the trench region, different sub-regions were identified and modeled to represent the layers of the trench fill corresponding to bedding, haunch, backfill type A, other backfill, crown, and cover. The roadway region was further subdivided into road pavement with a thickness of 10 in. and sub-pavement with a thickness of 12 in. A schematic representation of the different sub-regions in which the models were subdivided is provided in Figure 5.

(a) (b)

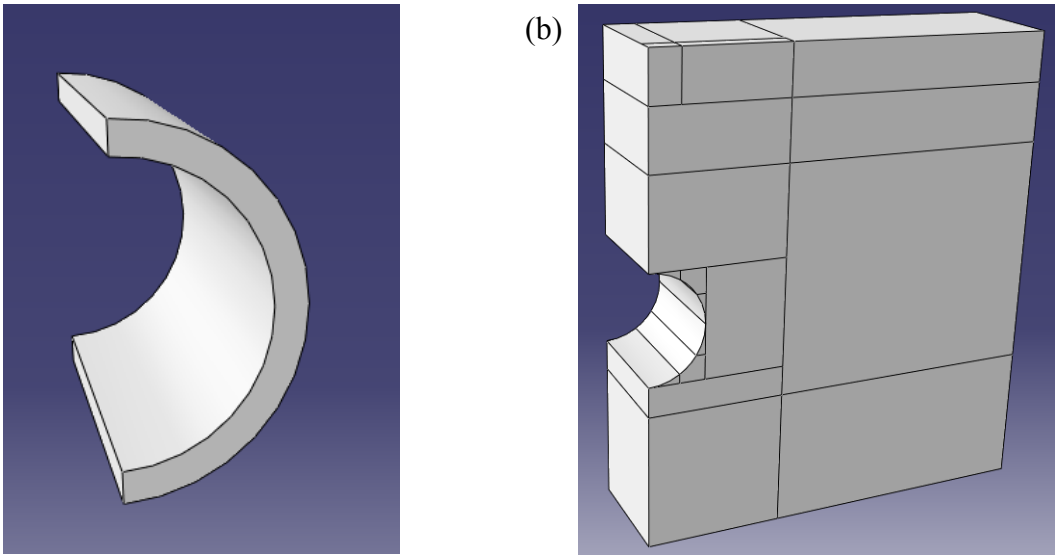

Figure 3
Subdivision into different zones (“parts” and “regions”) of the nonlinear FE model in ABAQUS: (a) part modeling the pipe and (b) part modeling the remaining components of the system

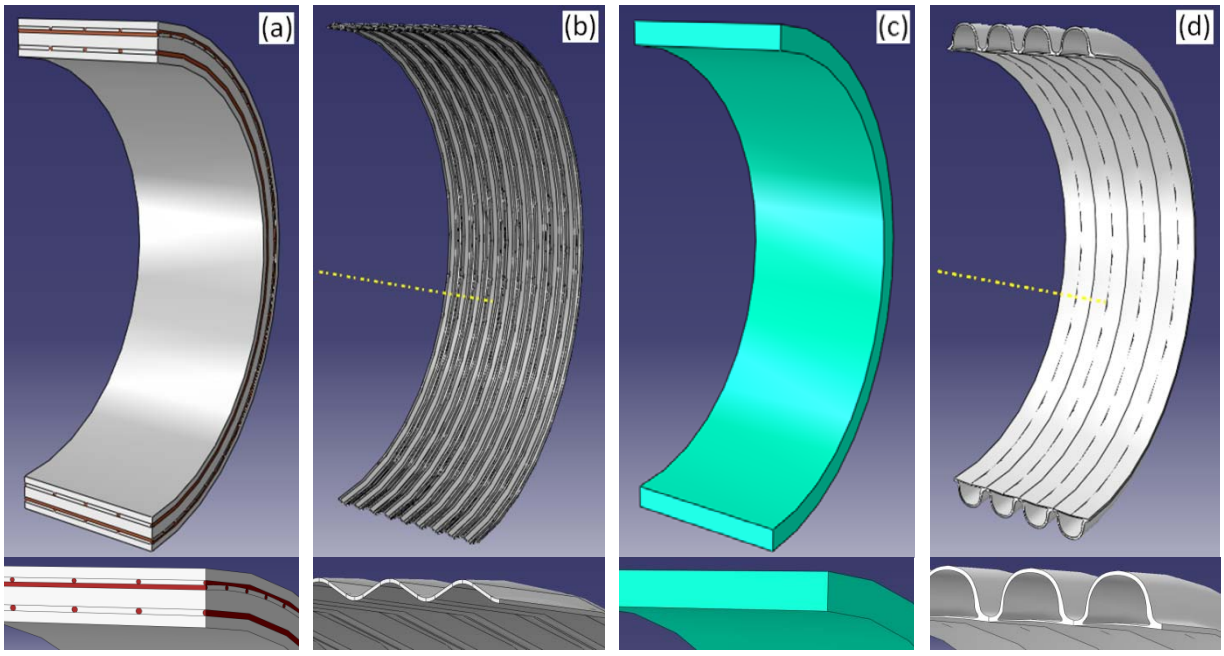

Figure 4
Pipe profiles: (a) RC pipe, (b) steel pipe, (c) PVC pipe, and (d) HDPE pipe

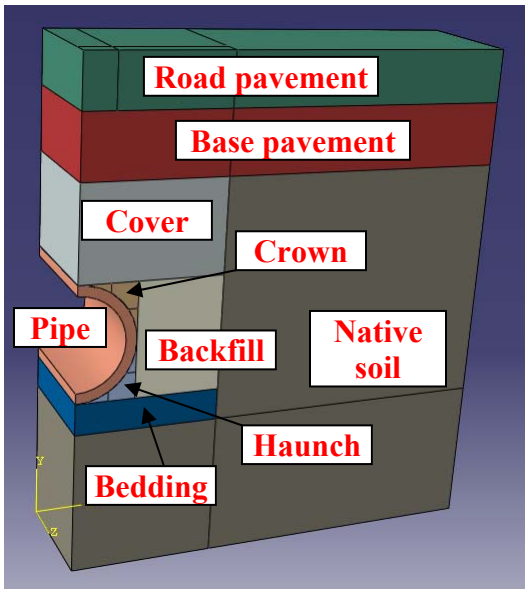

Figure 5
Different sub-regions in the nonlinear FE models

The FE model dimensions in the transversal directions were expressed as a function of the trench width, with the native soil region extending by one trench width in the horizontal direction and half a trench width below the trench. In the longitudinal direction, a fixed thickness of 2 ft. was used for all developed FE models *[13]*.

The FE model was built using (a) wedge elements for the crown and the haunch (element C3D6, i.e., a 6-node linear triangular prism, see Figure 6b); (b) hexahedral elements (element C3D8I, i.e., an 8-node linear brick with incompatible modes, see Figure 6a) for all other regions when the geometry of the region allowed compatible discretization; and (c) tetrahedral elements (element C3D4, i.e., a 4-node linear tetrahedron) for the steel and HDPE pipes in order to accurately reproduce the corrugation patterns of these pipe typologies. An automatic meshing technique, available in ABAQUS, was employed to generate meshes with variable size of the FEs. Smaller FEs (e.g., side length = 0.05 in.) were employed in the pipe and the sub-regions immediately surrounding the pipe, where changes in stress were larger and smaller elements were required for higher accuracy. Larger FEs were used for the native soil with elements of side length increasing from 2 in. near the trench to 6 in. at the boundaries of the FE model.

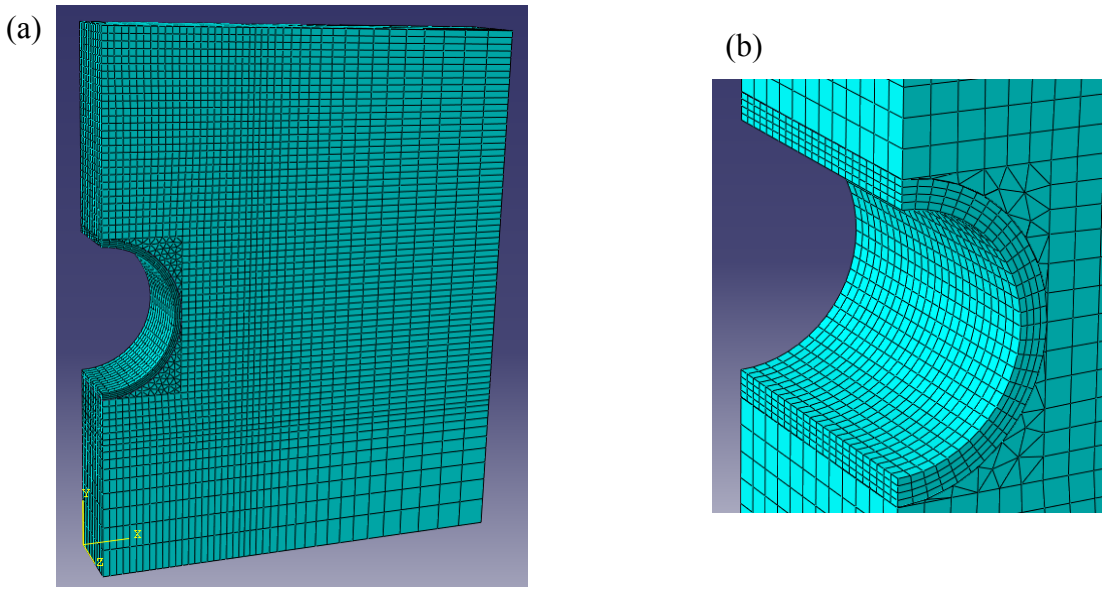

Figure 6
Nonlinear FE model mesh: (a) complete model and (b) zoom view of the pipe, haunch, and crown regions

Different boundary conditions were used along the boundary surfaces of the model. In particular, the bottom surface (Figure 7a) was fixed (i.e., fixed constraint in horizontal, vertical, and transversal directions), the front and back surfaces (Figure 7b) were constrained in the transversal direction only, and the side surfaces (Figure 7c) were constrained in the horizontal direction only. In Figure 7, the highlighted areas indicate the constrained surfaces for each specific boundary condition.

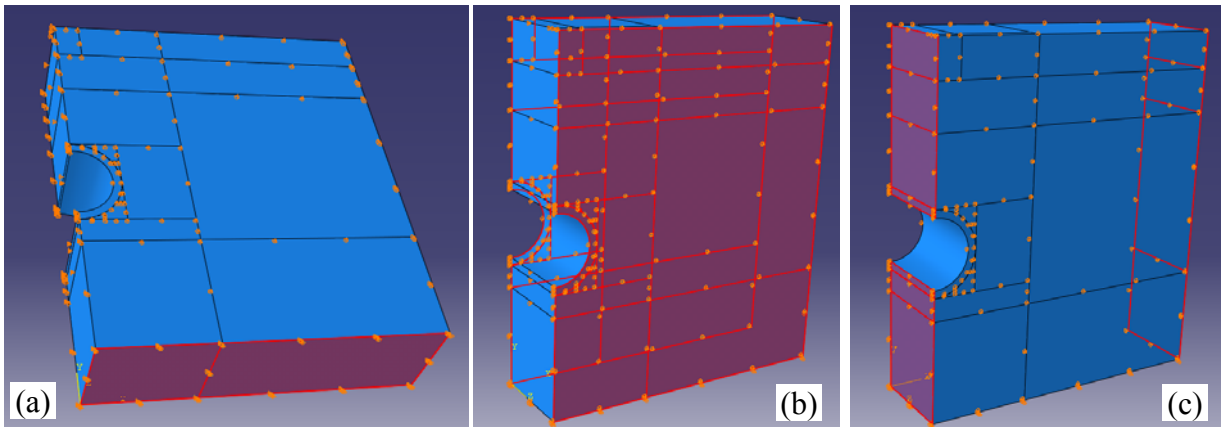

Figure 7
Boundary conditions: (a) bottom surface, (b) front and back surfaces, and (c) side surfaces

The contact interaction between the pipe structure and the surrounding soil was modeled introducing a contact surface characterized by frictional properties. Both tangential and normal contact interactions were explicitly modeled. For the tangential behavior, a friction coefficient of 0.6 was used to represent the ratio between (a) the shear stress at which relative slip occurs and (b) the normal pressure between the pipe and the soil. For the normal behavior, a "hard" contact interaction was assumed. The hard contact relationship avoids compenetration of different parts through the contact surface under compressive conditions and does not allow the transfer of tensile stress across the interface.

Nonlinear Hysteretic Material Constitutive Models

Appropriate and well-established nonlinear hysteretic constitutive models were adopted for all different materials used in the FE models of buried pipe installations. The nonlinear hysteretic constitutive models available in ABAQUS are based on classical plasticity theory and are appropriate for a wide range of elasto-plastic material behaviors, including metals, concrete, cohesive, and granular soils. The elasto-plastic constitutive models were employed and the corresponding materials were:

1) A classical multi-axial J_2 plasticity model with nonlinear hardening for steel and thermoplastic (PVC and HDPE) materials *[14]*;
2) A multi-axial plastic damage model in compression and semi-brittle behavior in tension for the concrete material, referred to as the concrete damaged plasticity (CDP) model in ABAQUS *[15]*.
3) An elasto-plastic model with a Mohr-Coulomb yield surface for the soil materials *[16]*; and
4) A linear elastic material for the asphalt of the roadway pavement.

The nonlinear material properties for steel, PVC, and HDPE were taken from the AISC steel manual, AASHTO M 278, and AASHTO M 294, respectively *[17], [11], [12]*. The most important parameters defining the Mohr-Coulomb yield surface are the cohesion and the friction angle. The native soil was modeled as a cohesive soil material, i.e., the friction angle was assumed equal to zero. The materials used to fill the trench and to build the road sub-pavement were modeled as non-cohesive granular materials, i.e., the cohesion was set equal to zero and the friction angle was obtained based on the assumed grades of compaction for each different soil layer. Higher grades of compaction correspond to higher values of the friction angle. For high grades of compaction, i.e., compaction larger than 80%, dilation was also modeled.

Loading Conditions and Nonlinear FE Staged Analysis

The nonlinear FE models previously described were subjected to two different sets of static loads, i.e., (a) gravity loads due to own weight of the pipe and the trench soil and (b) live loads due to vehicular traffic. The gravity loads were obtained from the densities of the different materials. The live loads were modeled as a uniform pressure applied at the road pavement surface over a surface corresponding to the tire print based on the AASHTO tire-road contact dimensions for an 18 wheel truck. The live loads corresponding to AASHTO H20 truck load was magnified by using a dynamic impact factor equal to 1.50.

The loadings were applied in different subsequent stages, in order to account for the actual installation procedure. The first loading stage involved applying the gravity load to the entire model with exclusion of the native soil region. This first stage reproduced the excavation of the trench; the installation of the bedding, pipe, backfill, and cover material inside the trench; and the construction of the sub-pavement and the roadway pavement. The second loading stage applied the live loads. The third and final load stage removed the live loads to evaluate the plastic deformations produced by the vehicular traffic.

It is noteworthy that, since all materials are modeled as isotropic, the need for a nonlinear FE analysis involving 3-D FE models derives from the following: (1) live loads are applied only on a limited portion of the road surface (i.e., the tire print area) and (2) live loads contribute significantly, in the case of shallow trenches, to the stresses present in the FE model. Thus, the FE model of pipes buried in shallow trenches cannot be rigorously represented by using a simpler 2-D plane strain model, as is commonly done when considering pipes deeply buried into the soil.

DISCUSSION OF RESULTS

The results of this research are presented in four different sections. The first section presents a sensitivity study based on a linear elastic FE analysis of buried pipe installations with respect to geometric and mechanical parameters describing the pipe, the trench, the native soil, and the road surface. The second section identifies the combinations of geometric and mechanical parameters that can produce unsatisfactory performance of buried pipe installations. The third section gives the model dimension sensitivity analysis results. Finally, the fourth section provides the validation and verification of the presented results by using nonlinear hysteretic FE analysis.

Sensitivity Analysis of Buried Pipe Installation Performance Based on Linear Elastic FE Analysis

The sensitivity of the performance of buried pipe installations has been studied with respect to several mechanical and geometric parameters defining the pipe structure, the trench where the pipe is installed, and the natural soil surrounding the trench. For each combination of these parameters, a linear elastic FE model of the soil-pipe system was prepared and analyzed. Both gravity loads and live loads are considered in the analysis. Several quantities obtained from the response of the linear elastic FE models of the soil-pipe system have been recorded and analyzed, including: (a) maximum stress, σ_{max}, reached in the pipe due to both gravity and live loads, (b) maximum static (elastic) deflection, Δ_{max}, at the road surface due to both gravity and live loads, (c) pipe ring deflection due to both gravity and live loads, (d) increment of pipe ring deflection due to live loads, (e) maximum stress increment, $\Delta\sigma$, due to live loads, and (f) maximum deflection increment, Δ_{live}, at the road surface due to live loads. The maximum deflection increment, Δ_{live}, has been chosen as the reference performance parameter for the linear elastic FE response of the soil-pipe system based on the following considerations:

1) It provides information on both soil and pipe behavior at the same time, differently from stress and ring deflection performance measures.
2) It is a deformation measure that can be related to the generation of potholes and dips on the road surface.
3) It depends on the short term mechanical properties of the pipes, which are used to define the FE models employed in this study.

The performance of the soil-pipe systems improves for decreasing values of Δ_{live}. Thus, it is of interest to determine the sensitivity of Δ_{live} on the different geometric and mechanical parameters describing the pipe, the material used to fill the trench in which the pipe is buried, the soil surrounding the trench, and the type of road surface. Four different pipe materials are considered, i.e., (a) reinforced concrete with initial stiffness E = 2,900 ksi *[9]*; (b) steel with Young's modulus E = 29,000 ksi *[17]*; (c) PVC with initial stiffness modulus for short term behavior E = 400 ksi *[11]*; and (d) HDPE with initial stiffness modulus for short term behavior E = 140 ksi *[12]*.

Table 3
Linear elastic FE analyses parameters

Pipe Materials	RC	Steel	PVC	HDPE		∑
# of Pipe Thicknesses	3	3	2	2		10
Trench Widths (in.)	18	30	60			3
Backfill Heights (in.)	12	24	36			3
Backfill Materials (ksi)	10	30	45			3
Bedding Materials (ksi)	5	30				2
Native Soil Materials (ksi)	1	5	10			3
Pipe Diameters (in.)	18	36	42	48	60	5
Pavement Types	4" Asphalt	10" Asphalt	8" Concrete			3
				Total # of Models		24,300

The results of this sensitivity study are based on about 25,000 linear elastic FE analyses. Table 3 provides the list of sensitivity parameters and their values together with the total number of analyses performed. It is noteworthy that additional linear elastic FE analyses were carried out to study the response sensitivity to the bedding thickness, corresponding to bedding thicknesses of 6 in., 12 in., and 24 in. However, in order to reduce the total number of FE analyses, the parametric study with respect to all other parameters was performed by using a fixed bedding thickness of H_b = 6 in., due to the fact that the bedding thickness was

found to be a minor parameter in affecting the FE response. They are summarized and discussed herein, using as a reference the FE model defined as follows: pipe diameter D = 60 in., trench width W = 2D = 120 in., cover height of backfill material H_c = 12 in., bedding thickness H_b = 6 in., initial stiffness of the natural soil surrounding the trench E_s = 5 ksi, initial stiffness of the backfill material E_f = 30 ksi, and initial stiffness of the bedding material E_b = 5 ksi. The pipes are modeled as plain wall pipes with constant wall thickness, t. The pipes used in the reference FE model are: (a) reinforced concrete pipes with D/t = 10 (RC), (b) steel pipes with D/t = 50 (steel), (c) PVC pipes with D/t = 10 (PVC), and (d) HDPE pipes with D/t = 10. The road surface considered as reference is made by a sub-pavement base of thickness equal to 10 in. and a road pavement made of a 4-in. layer of asphalt. In the following sections, each mechanical and/or geometric parameter is varied, one at a time, over an appropriate range. The combined effects of the variation of two parameters at the same time are also highlighted whenever important.

Sensitivity to Trench Excavation Width: W

Figures 8 to 10 show the dependency of Δ_{live} on the trench excavation width W for pipes made with different materials buried in trenches surrounded by natural soils with different initial stiffnesses. This dependency is given by plotting Δ_{live} as a function of the quantity (W – D)/2, which represents the minimum width of the backfill material on one side of the pipe. Three values of (W – D)/2 are considered, i.e., 18 in., 30 in., and 60 in., corresponding to W = 96 in., 120 in., and 180 in., respectively. The value (W – D)/2 = 18 in. is considered as the smallest space sufficient to ensure accessibility of the trench and, thus, appropriate positioning and compaction of the backfill material.

Figure 8 provides the results for a moderately stiff natural soil (E_s = 5 ksi) for which the ratio between the initial stiffnesses of the backfill material (E_f = 30 ksi) and the natural soil is equal to 6. It is observed that, under the considered conditions, increasing the trench width has a practically negligible effect on Δ_{live}.

Figure 9 provides the same results for a moderately stiff natural soil (E_s = 5 ksi) and a stiffer backfill material (E_f = 45 ksi) for which the ratio between the initial stiffnesses of the backfill material and the natural soil is equal to 9. In this case, the effects of different trench widths on Δ_{live} are still very limited, even though slightly larger than for the case of firm natural soil. It is observed that the best performance of the buried pipe systems are achieved for a trench width equal to two pipe diameters, i.e., (W – D)/2 = 30 in. The performance improvement from (W – D)/2 = 18 in. to (W – D)/2 = 30 in. is more significant for pipes made of more flexible material.

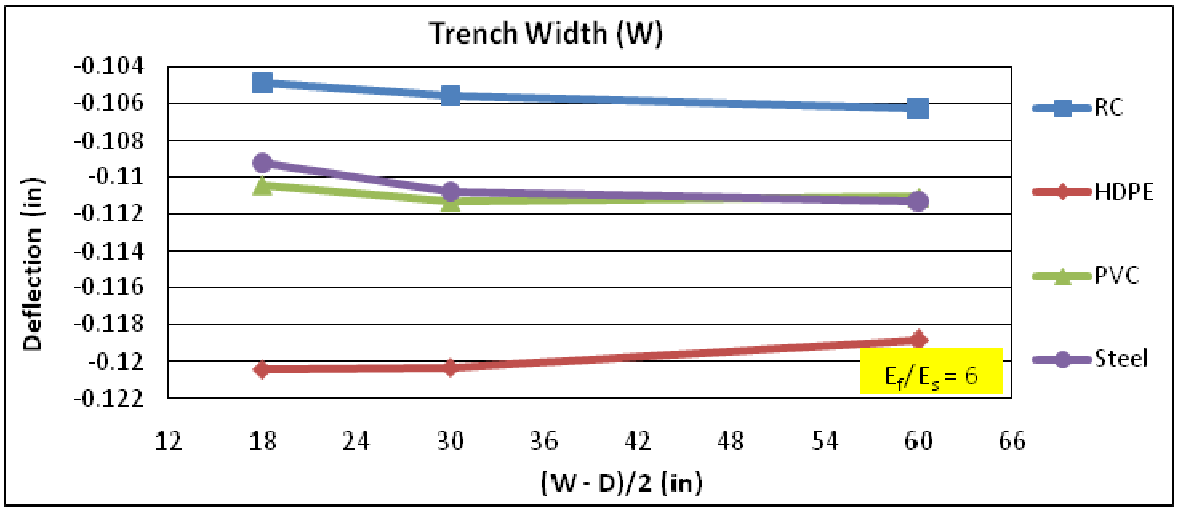

Figure 8

Sensitivity study: effects of trench excavation width (moderately stiff natural soil)

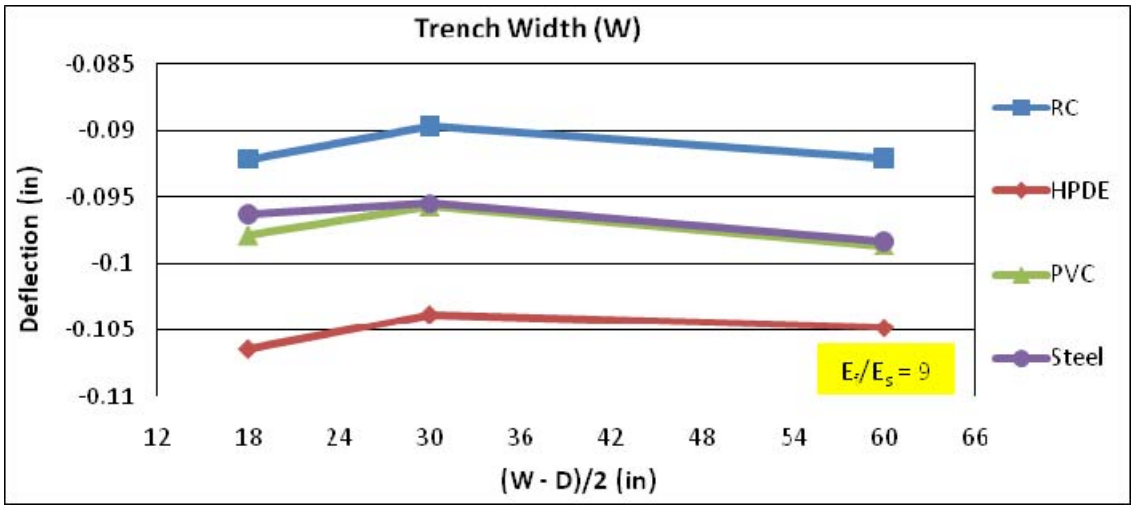

Figure 9

Sensitivity study: effects of trench excavation width (moderately stiff natural soil and very stiff backfill material)

Figure 10 provides the dependency of Δ_{live} on the trench width in the case of a trench surrounded by yielding natural soil (E_s = 1 ksi) for which the ratio between the initial stiffnesses of the backfill material (E_f = 30 ksi) and the natural soil is equal to 30. In this case, the performance of all soil-pipe systems considerably improves for increasing trench excavation width, particularly for trench widths smaller than 2D. Also in this case, the performance improvement is more significant for flexible pipes.

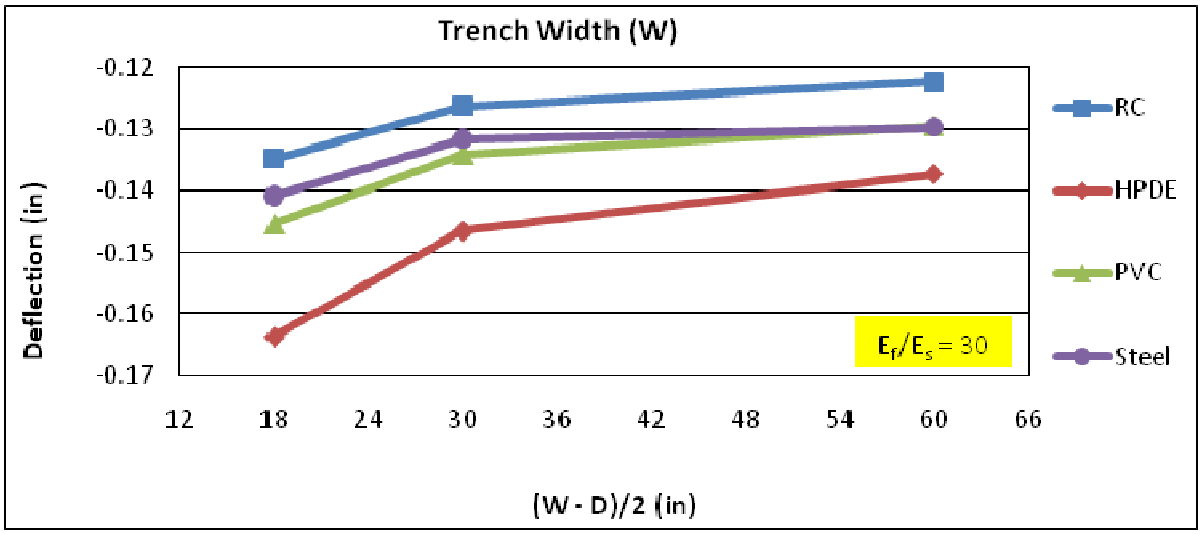

Figure 10

Sensitivity study: effects of trench excavation width (yielding natural soil)

Similar results are obtained considering different pipe diameters, different D/t values for the various pipe materials, different natural soil, and backfill material combinations. The results obtained using linear elastic FE analysis show that the excavation width W has, in general, a relatively small influence on deformation performance of soil-pipe interaction systems for W > 2D, in which D denotes the pipe diameter. However, the improvement in performance can be significant for W ≤ 2D, particularly for flexible pipes and yielding natural soil. The effectiveness of increasing the excavation width substantially decreases for decreasing ratio between the backfill stiffness and the natural soil stiffness and, in minor grade, for increasing stiffness of the pipe. This phenomenon is due to the better confinement provided to the sides of the pipe by a wider trench with filling material that is stiffer than the natural soil surrounding the trench. It appears that for rigid pipes, such as reinforced concrete pipes, the trench width can be chosen so to allow accessibility of the sides of the trench for the correct positioning and compaction of the backfill material, e.g., W = D + 36 in. For other pipes (i.e., steel, PVC, and HDPE), the best performance in terms of maximum deflection increment at the road surface due to live loads, Δ_{live}, is obtained for a trench width W = 2D.

Sensitivity to Soil Cover Height: H_c

Figure 11 shows the maximum deflection increment at the road surface due to live loads, Δ_{live}, as a function of the cover height above the pipe of trench backfill material, H_c. Three values of cover height are considered, i.e., H_c = 12 in., 24 in., and 36 in. It is observed that the performance of the soil-pipe system is significantly improved for increasing values of H_c for all pipes. The more flexible the pipe, the higher is the performance improvement for the same increase of H_c. The performance improvement marginally decreases for increasing H_c. Thus, for each pipe, it is possible to find an optimal cover height, H_c, beyond which the performance improvement of the soil-pipe system is negligible.

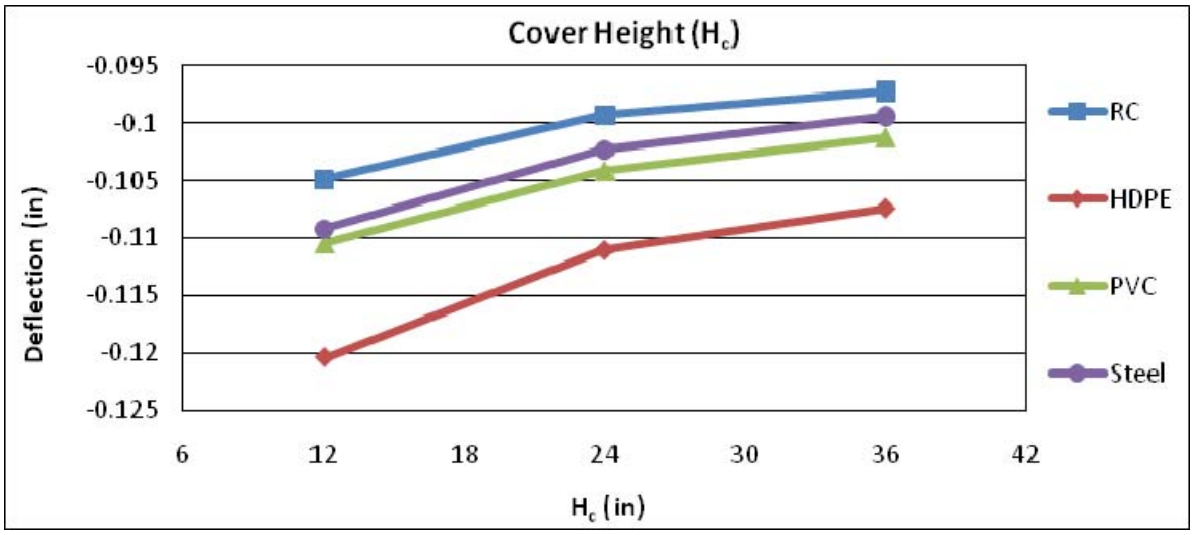

Figure 11
Sensitivity study: effects of soil cover height

Sensitivity to Bedding Thickness: H_b

Figures 12 and 13 plot the maximum deflection increment at the road surface due to live loads, Δ_{live}, as a function of the bedding thickness, H_b. Three bedding thicknesses are analyzed, i.e., 6 in., 12 in., and 24 in.

Figure 12 provides the Δ_{live} results for a soft bedding material (E_b = 5 ksi = E_s), while Figure 13 plots the same results for a stiff bedding material (E_b = 30 ksi = 6 E_s). The effect of different bedding thicknesses on Δ_{live} is negligible for all pipes when the bedding material is soft, while it is relatively small but not negligible for stiff bedding material.

It was found that the use of stiff bedding material can cause a significant stress concentration at the bottom of the pipe, particularly if the backfill material at the haunch is not well compacted. It is concluded that the stiffness of the bedding material is not an appropriate design variable for improving the performance of buried pipe installations in terms of maximum deflection increment at the road surface. The bedding thickness and bedding material stiffness should be determined in order to ensure that the bedding of the pipe is stable. This bedding must be able to redistribute the stresses transferred from the pipe and the loading acting above the pipe as uniformly as possible.

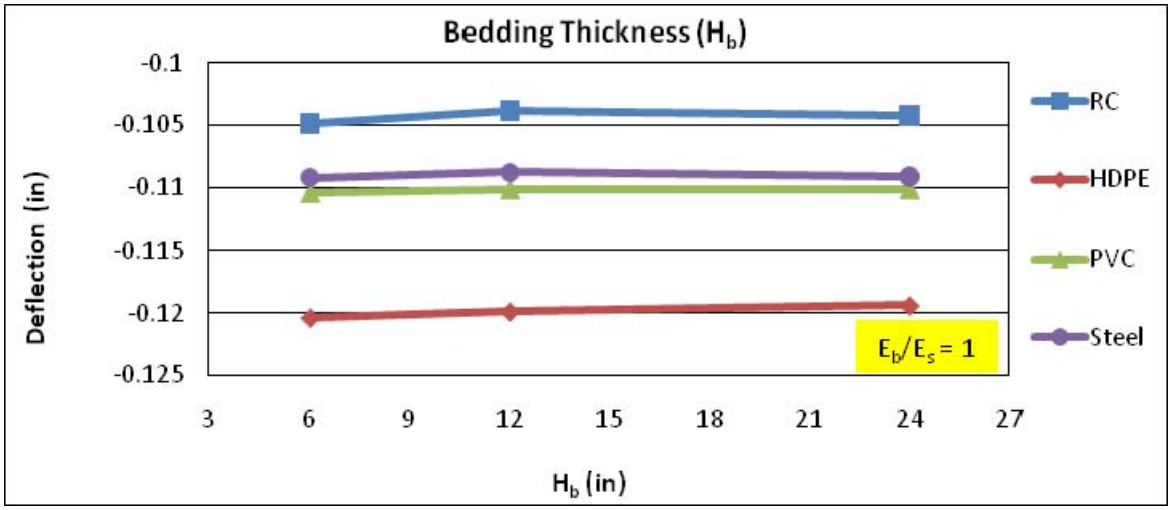

Figure 12
Sensitivity study: effects of bedding thickness with soft bedding material

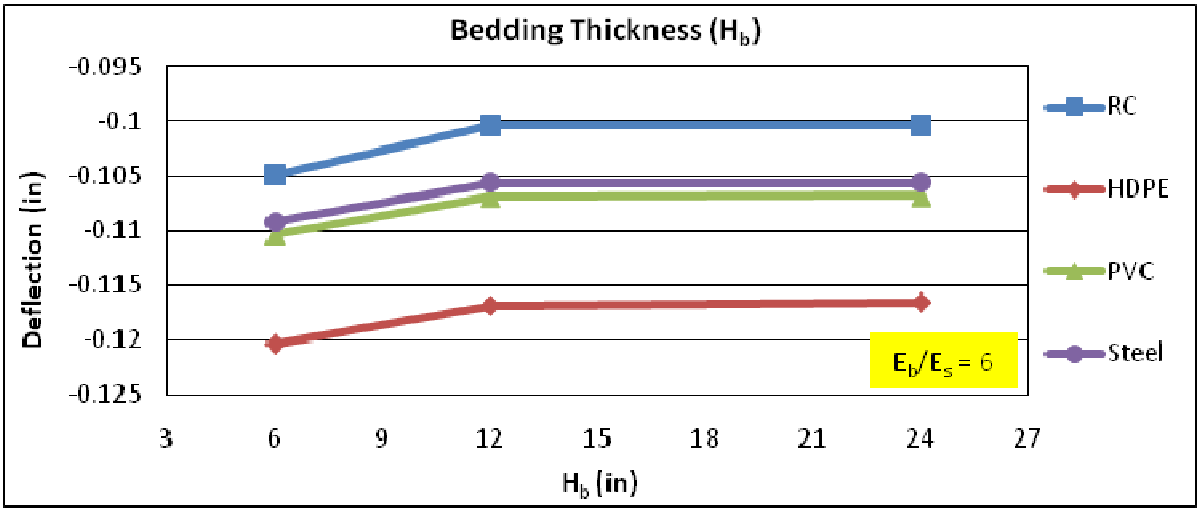

Figure 13
Sensitivity study: effects of bedding thickness with stiff bedding material

Sensitivity to Initial Stiffness of Natural Soil Surrounding the Trench: E_s

Figure 14 plots Δ_{live} as a function of the natural soil stiffness for pipes made with different materials. Three different natural soil conditions are considered, i.e., yielding soil (E_s = 1 ksi), moderately stiff soil (E_s = 5 ksi), and stiff soil (E_s = 10 ksi). The choice of the natural soil stiffnesses is made based on typical conditions encountered in Southern Louisiana, where very soft clay, often organic, is commonly found.

It is observed that Δ_{live} is very sensitive to the stiffness of the surrounding soil, increasing by a factor up to 70% for E_s decreasing from 10 ksi to 1 ksi. The performance improves less than linearly for increasing soil stiffness. This improvement is more significant for flexible pipe materials.

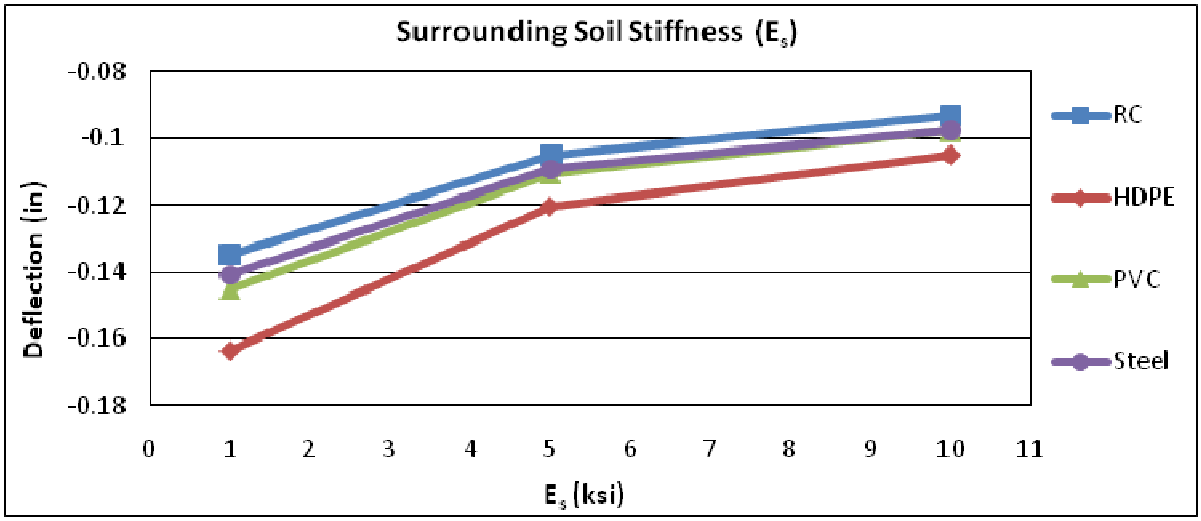

Figure 14

Sensitivity study: effects of initial stiffness of natural soil surrounding the trench

Sensitivity to Backfill Material Stiffness: E_f

Figure 15 plots Δ_{live} as a function of the backfill material (soil) stiffness for pipes made with different materials. Three different backfill material conditions are considered, i.e., soft lightly compacted material (E_f = 10 ksi), stiff compacted material (E_s = 30 ksi), and stiff highly compacted material (E_s = 45 ksi). Lower stiffnesses would correspond to soil that cannot be used as backfill material, while higher stiffnesses would correspond to crushed stone, which is a very expensive high-quality backfill material.

It is observed that Δ_{live} is very sensitive to the stiffness of the backfill material, increasing by a factor up to 90% for E_f decreasing from 45 ksi to 10 ksi. The performance improves less than linearly for increasing soil stiffness. This improvement is almost independent on the pipe material.

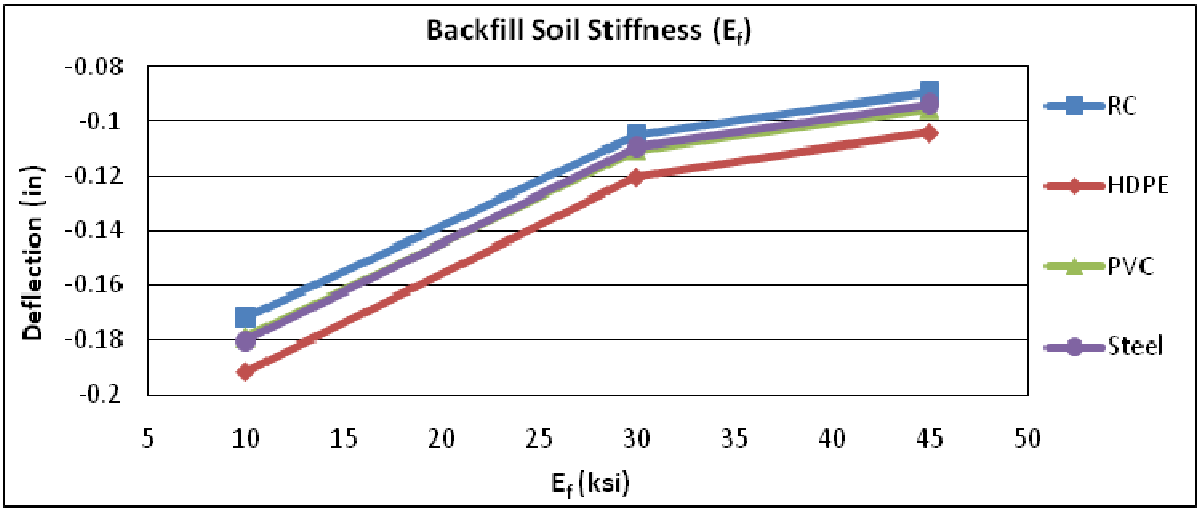

Figure 15
Sensitivity study: effects of initial stiffness of backfill material (i.e., grade of compaction)

Sensitivity to Pipe Geometry: Pipe Diameter, D, and Pipe Thickness, t

Figure 16 plots Δ_{live} as a function of the pipe diameter for pipes made with different materials. Five different diameters are considered, i.e., D = 18 in., 36 in., 42 in., 48 in., and 60 in. These diameters were chosen since they are commonly used for culverts of transportation facilities in Louisiana.

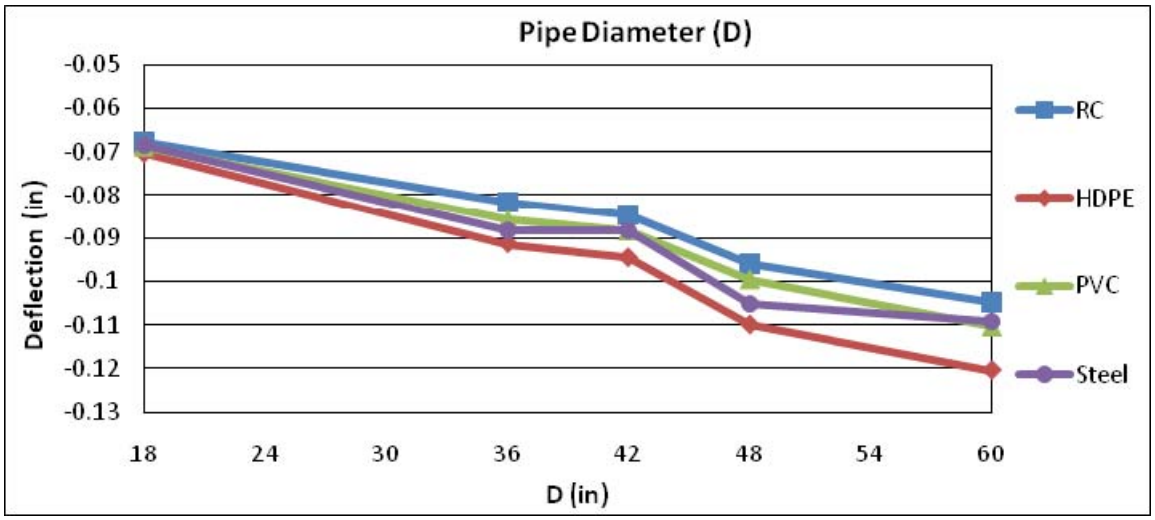

Figure 16
Sensitivity study: effects of pipe diameter

It is observed that Δ_{live} is very sensitive to the pipe diameter, increasing almost proportionally to it when all other geometric and mechanical parameters are maintained the same. Thus, in order to ensure a comparable performance of pipes with different diameters installed in similar soils, the geometric requirements for the trench geometry need to be defined as functions of the pipe diameter.

Figure 17 plots Δ_{live} as a function of the pipe ring stiffness (defined as EI/D^3) for pipes of different materials and diameter D = 60 in. The plot is presented with the pipe ring stiffness in logarithmic scale. For pipes of the same material, the pipe ring stiffness is a function only of the pipe wall thickness. The pipe wall thicknesses considered here are: (1) t = D/10, D/20, and D/30 for RC pipes; (2) t = D/50, D/100, and D/200 for steel pipes; (3) t = D/10 and D/20 for PVC pipes; and (4) t = D/10 and D/20 for HDPE pipes. It is observed that the pipe ring stiffness significantly influences the performance of the pipe, particularly for pipes made of more flexible materials. For the same pipe ring stiffness, pipes made of stiffer materials perform better than pipes made of more flexible materials.

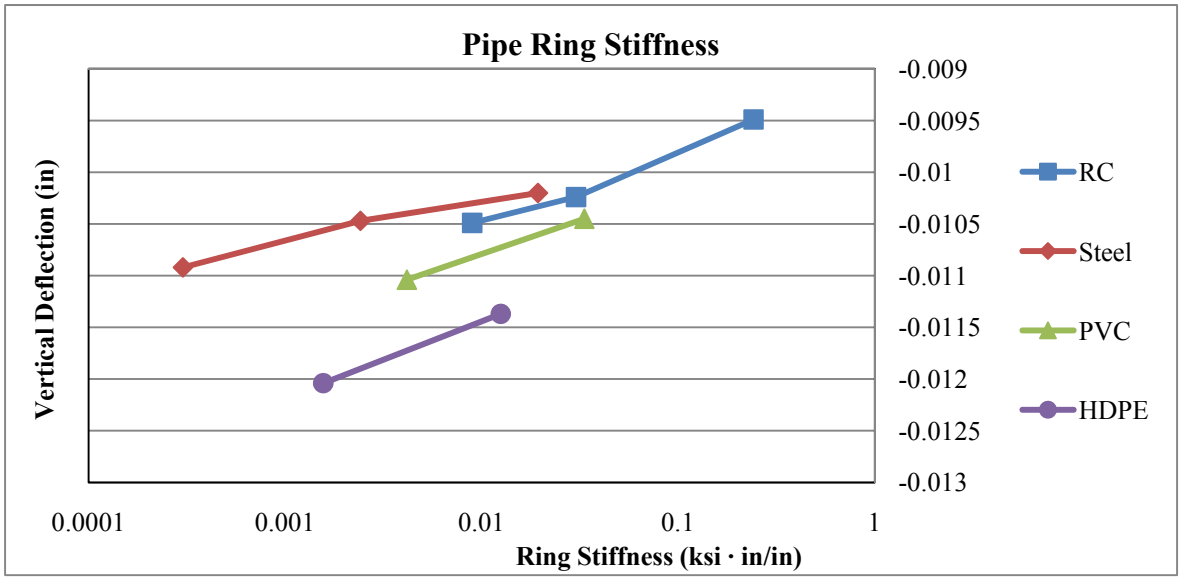

Figure 17
Sensitivity study: effects of pipe ring stiffness (i.e., pipe thickness)

Sensitivity to Road Pavement Type

Figure 18 plots Δ_{live} for pipes made with different materials and different road surface types. The road pavement types considered are: (a) a 4-in. layer of asphalt, (b) a 10-in. layer of asphalt, and (c) an 8-in. concrete pavement. These pavements are typically used for road surfaces in Louisiana.

It is found that the performance of soil-pipe systems in terms of Δ_{live} depends crucially on the type of road surface. In fact, a stiffer road pavement distributes the stresses produced by the live loads more uniformly over a much larger area of soil. Thus, an increase in stiffness of the road pavement significantly decreases the magnitude of the stresses that are transferred to the pipe through the road pavement, the sub-pavement, and the trench cover. As a consequence, Δ_{live} also decreases substantially.

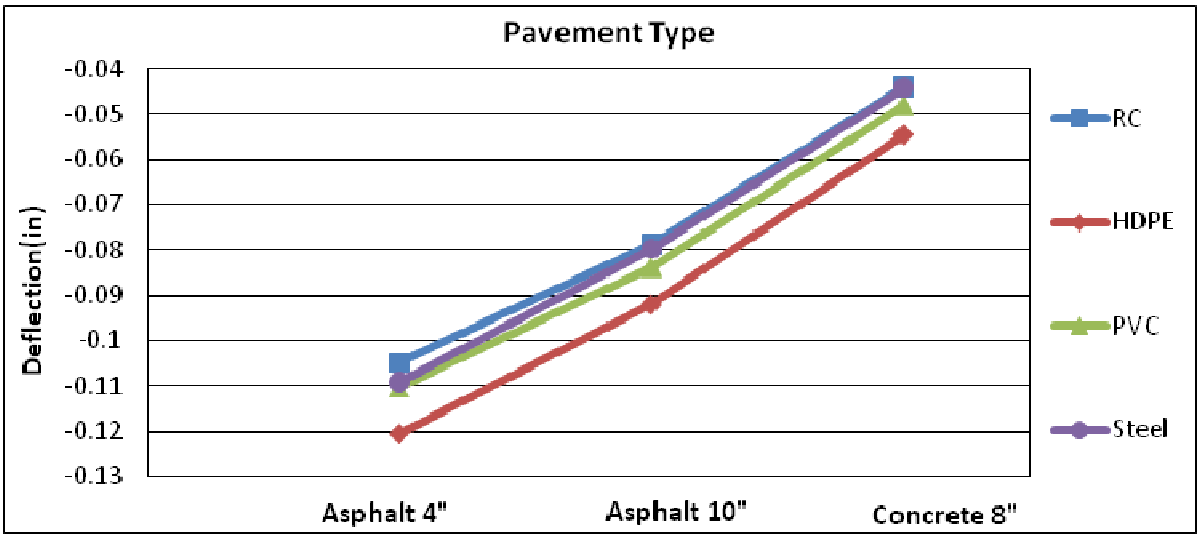

Figure 18
Sensitivity study: effects of different pavement type

Identification of Cases of Possible Insufficient Performance via Linear Elastic FE Analysis

The results of the sensitivity analysis presented above can be used to identify the conditions most likely to produce unsatisfactory performance. It is found that particular attention is needed when large pipes are installed in yielding soils. This situation can be critical if the road pavement is flexible, i.e., asphalt road pavement.

Under the previous conditions, a more advanced (and computationally expensive) nonlinear FE analysis is required to more realistically model the soil-pipe system and accurately estimate its actual response and performance. The nonlinear FE analysis method can also be used to evaluate the appropriate minimum requirements in terms of trench geometry and mechanical properties of the backfill material, which ensure a satisfactory performance of the soil-pipe system even under the critical conditions previously identified.

Model Dimension Sensitivity Analysis Results

The simplified linear elastic FE analysis models used for the sensitivity analysis previously presented are insensitive to the model dimensions, since the natural soil surrounding the trench is modeled only indirectly through the use of equivalent elastic springs. Thus, these FE models use a crude approximation of the soil behavior. A better approximation is obtained by removing the equivalent springs and replacing them with a FE model with the properties of the actual native soil. Upon adding the native soil to the 2-D models, it is necessary to determine the size of the soil region that is needed to ensure that the FE response is independent on the model dimensions.

The results obtained from the 2-D model dimension sensitivity study indicate that the size of the model corresponding to response results independent on the model dimensions is proportional to the trench size. In particular, it is found that the dimensions of the soil surrounding the trench needs to be extended by one trench width in the horizontal direction and by half a trench width in the vertical direction. In terms of thickness of the FE model, small differences in the response are found between models with thicknesses of 24 in. and 48 in. These model dimension sensitivity analysis results obtained from the 2-D models have been used as the starting point for a similar analysis based on the 3-D models.

Several linear elastic 3-D FE models with different dimensions, in both horizontal and vertical directions, of the region of natural soil surrounding the trench were built to study the model dimension sensitivity of the FE results. Vertical deflections at the road surface and maximum stress in the pipe were recorded for all the FE models considered. Typical results in terms of road surface deflection and maximum stress at the pipe are shown in Figure 19 and Figure 20, respectively.

Figure 19 shows the variation of the FE deflection response at the road surface for the 3-D soil-pipe system of an HDPE pipe with a diameter of 60 in. Expansion increments of 2 ft. in the vertical direction and 4 ft. in the horizontal direction are considered. It is observed that an appropriate mesh expansion of 4 ft. in the vertical direction and 8 ft. in the horizontal direction are necessary to ensure that the FE deflection response corresponding to road surface deflection is independent on the model dimensions.

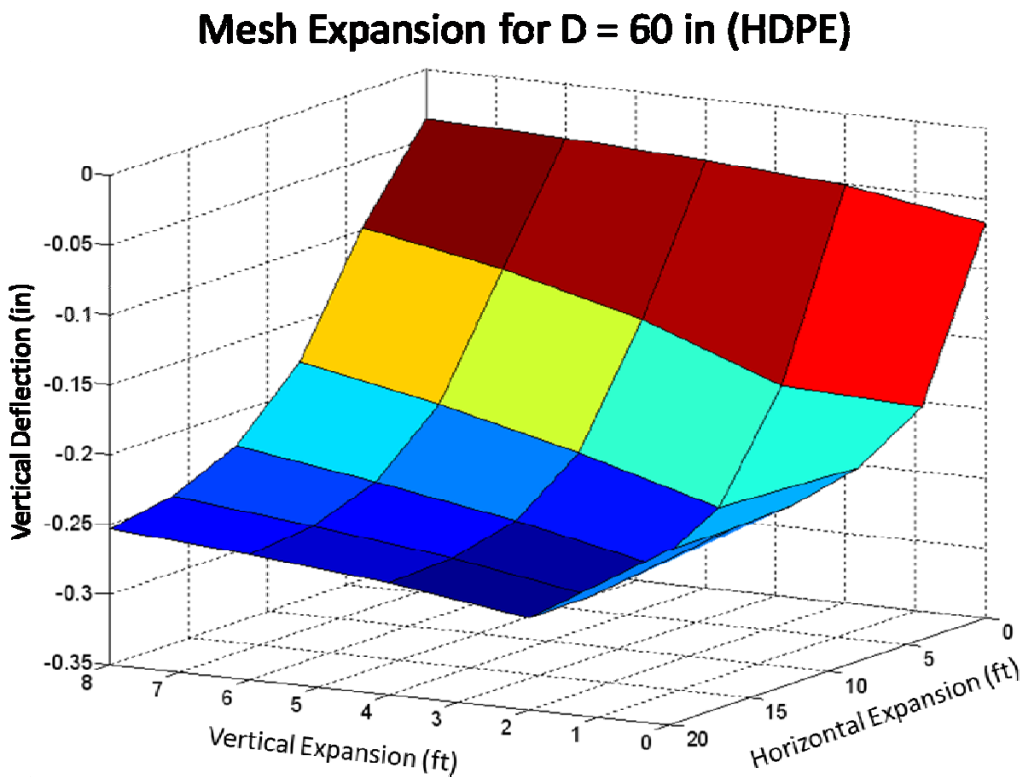

Figure 19

Model dimension sensitivity study: variation of deflection response at the road surface for the 3-D FE of a soil-pipe system with a HDPE pipe of diameter D = 60 in.

Figure 20 shows the variation of the maximum stress response within the pipe for the 3-D soil-pipe system of an HDPE pipe with a diameter of 60 in. Expansion increments of 2 ft. in the vertical direction and 4 ft. in the horizontal direction are also considered. Figure 20 confirms that a mesh expansion of 4 ft. in the vertical direction and 8 ft. in the horizontal direction are also necessary to ensure that the FE response is independent on the model dimensions.

The dimensions of the model were defined based on the data obtained from the FE model dimension sensitivity study and on the need to minimize the dimensions of the model and reduce the computational cost of each FE analysis. It was determined that results practically independent on the model dimensions can be obtained by including in the FE model a region of native soil equal to one trench width in the horizontal direction and to half a trench width in the vertical direction. These results are also consistent with a previous study *[13]*.

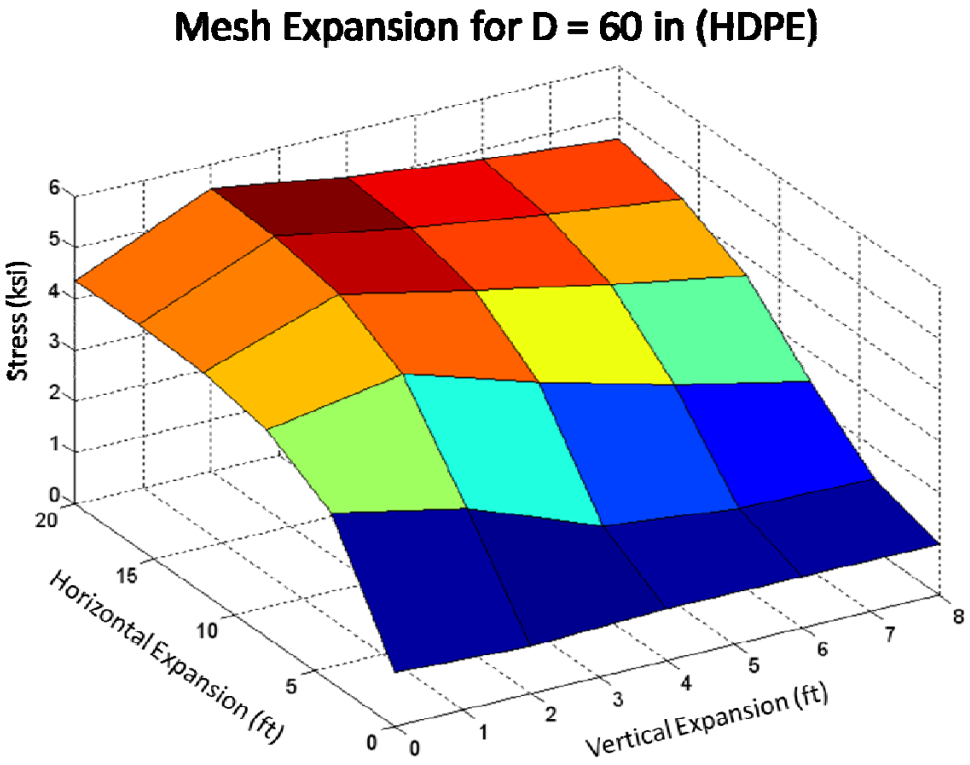

Figure 20
Model dimension sensitivity study: variation of maximum stress in the pipe for the 3-D FE of a soil-pipe system with a HDPE pipe of diameter D = 60 in.

Validation and Verification of Results via Nonlinear Hysteretic FE Analysis

The results obtained from each nonlinear FE model considered are reported in terms of (1) the deflection of the roadway surface in the direction perpendicular to the pipe axis (i.e., along the highlighted thick line shown in Figure 21a), referred to as profile of Δ, and (2) the radial deflection within the pipe ring (expressed as a function of the angular coordinate, see Figure 21b), referred to as profile of Δ_R. The following performance measures are considered: (1) the maximum deflection due to live loads only at the center of the tire print (corresponding to the corner of the FE model where the uniformly distributed live load is applied), referred to as Δ_{live}; (2) the inelastic (residual) deflection at the center of the tire print, referred to as $\Delta_{inelastic}$; (3) the maximum ring deflection due to live loads only, $\Delta_{R,live}$; and (4) the maximum inelastic ring deflection, $\Delta_{R,inelastic}$.

The inelastic deflections are obtained by removing the live loads and correspond to the plastic deformations of the FE model after a vehicle has passed. These deformations are not reversible and can be seen in the form of dips on a roadway surface. Dips on a roadway surface are a concern since they can produce driver discomfort or even failure of the roadway surface. The ring deflection is also important to examine because if a pipe exceeds an allowable performance limit in terms of ring deflection, cracking, buckling, and complete failure can occur.

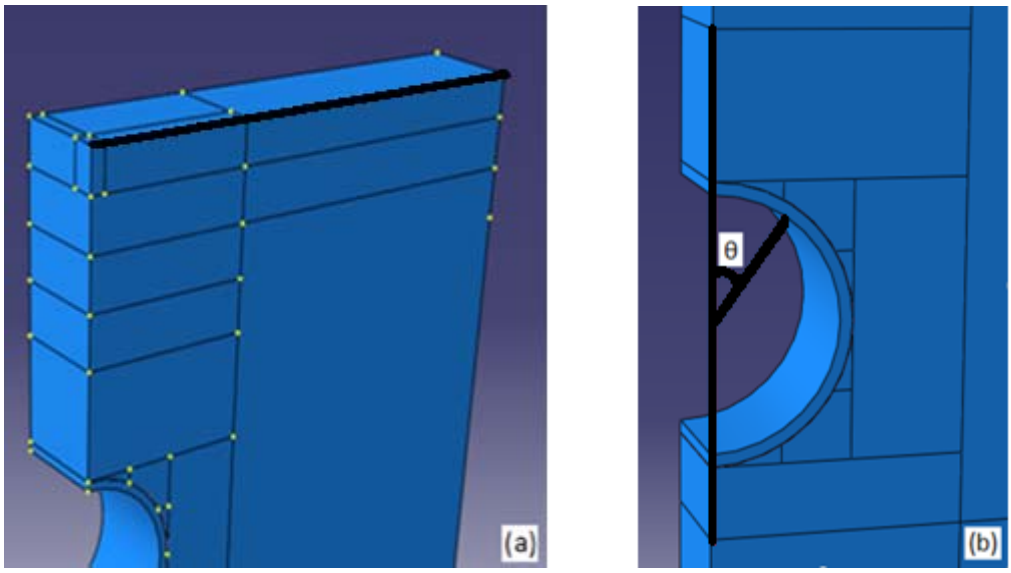

Figure 21
Locations at which the FE response is monitored for computing the performance measures: (a) monitored deflection at the road surface (profile of Δ) and (b) reference system for Δ_R measurement

It is noteworthy that, as the cover height increases, the radial deflection due to live loads only, $\Delta_{R,live}$, always decreases. This phenomenon is due to the fact that a portion of the live loads is supported by the soil located above the pipe and that this portion increases for increasing cover height and increasing stiffness of the road pavement.

Nonlinear FE Analysis Results for RC Pipes

Figure 22 shows the profile of Δ_{live} for a RC pipe with a 42 in. diameter. Figure 23 provides a zoom view of the profile near the region of application of the live loads (i.e., tire print). LADOTD specifies a minimum cover height of 18 in. for any pipe whose pipe stiffness is classified as rigid, such as RC pipes. In Figure 23, it is observed that a cover height of 12 in. produces the smallest absolute value roadway deflection, Δ_{live}, of 0.1318 in. The differences in Δ_{live} among FE models with cover height H_c = 6 in., 12 in., and 18 in. are very small and practically negligible for engineering applications.

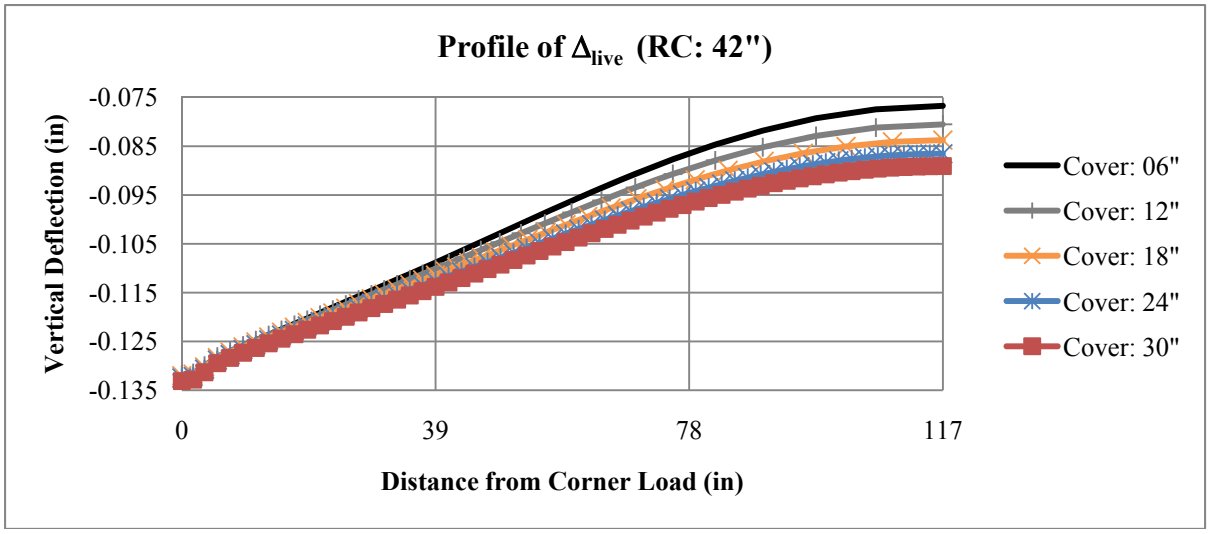

Figure 22

Profile of Δ due to live loads only (Δ_{live}) for RC pipe with D = 42 in.

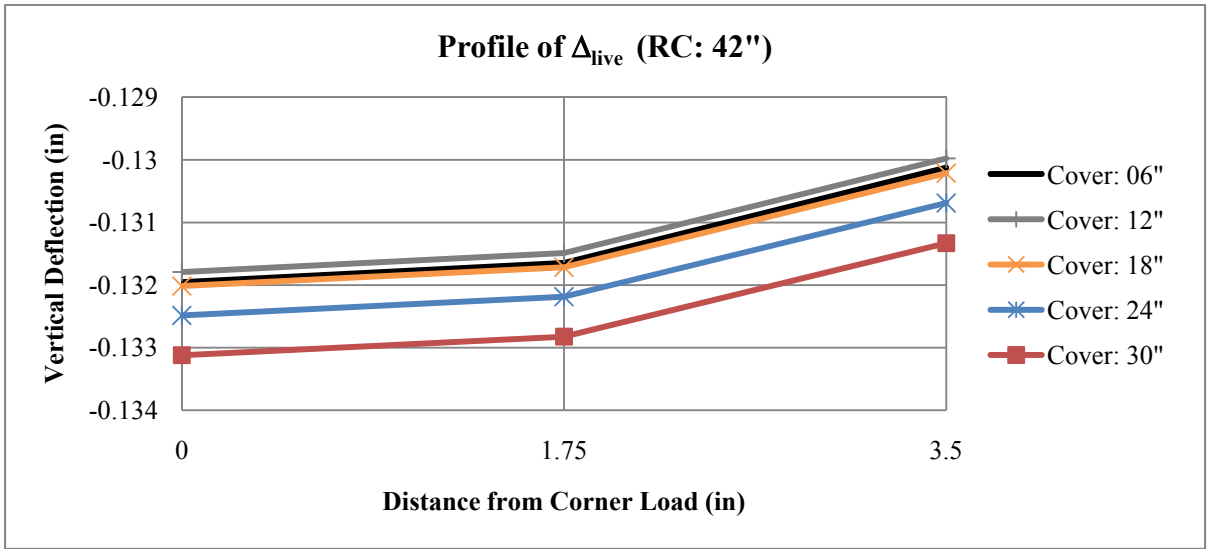

Figure 23

Profile of Δ due to live loads only (Δ_{live}) for RC pipe with D = 42 in.: zoom view

Figure 24 shows the profile of the plastic deformation at the road surface for a 42-in. diameter RC pipe. An optimal cover height of 18 in. is needed for minimum inelastic deflection. The plastic deformations are very small, occur almost exclusively in the soil, and are mainly due to the soil cover self-weight. In Figure 24, it is observed that the data line for the 12-in. cover intersects the data lines for the 18- and 24-in. covers. The reason for this phenomenon is that, at the specific cover of 12-in. for a 42-in. diameter RC pipe, the plastic deformation induced by the live loads is larger than the one produced by the gravity loads.

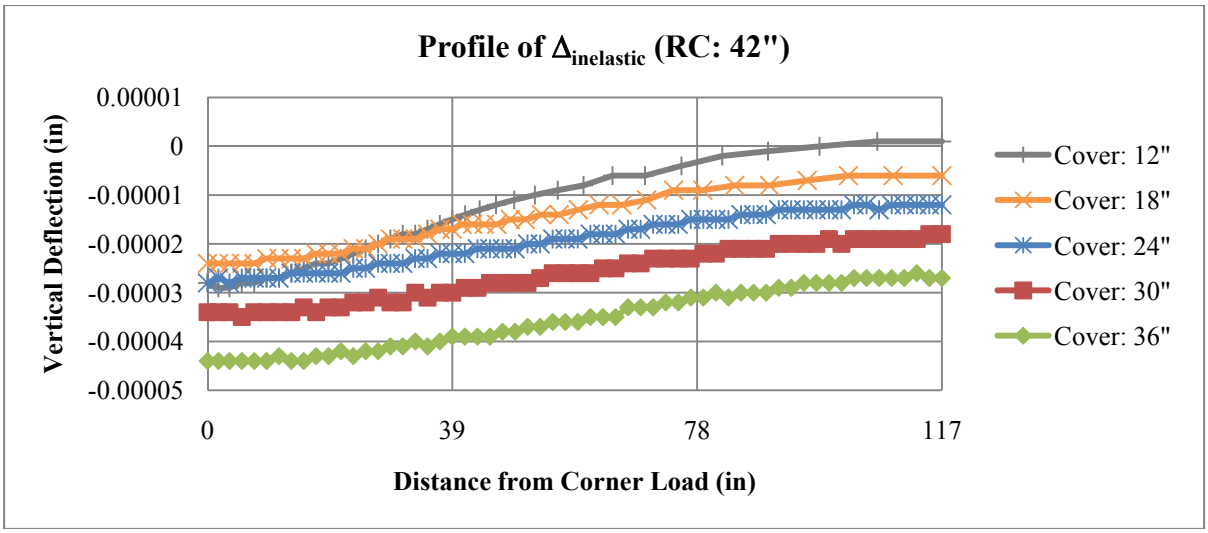

Figure 24

Profile of Δ due to plastic deformation ($\Delta_{inelastic}$) for RC pipe with D = 42 in.

Figure 25 shows the radius change for a RC pipe with a 42 in. diameter due to live loads only. As expected, the radius change due to live loads only decreases for increasing cover height. The observed radius changes are very small for all FE models considered, and the differences in radius change computed for FE models with different cover heights are almost negligible. For the considered soil-pipe FE model, Δ_{live} decreases in absolute value by 0.17%, i.e., from 0.1320 in. for H_c = 18 in. (recommended cover height) to 0.1318 in. for H_c = 12 in. (optimal cover height). This change is practically negligible for application purposes. For the same FE models, $\Delta_{R,live}$ increases by 11.61%.

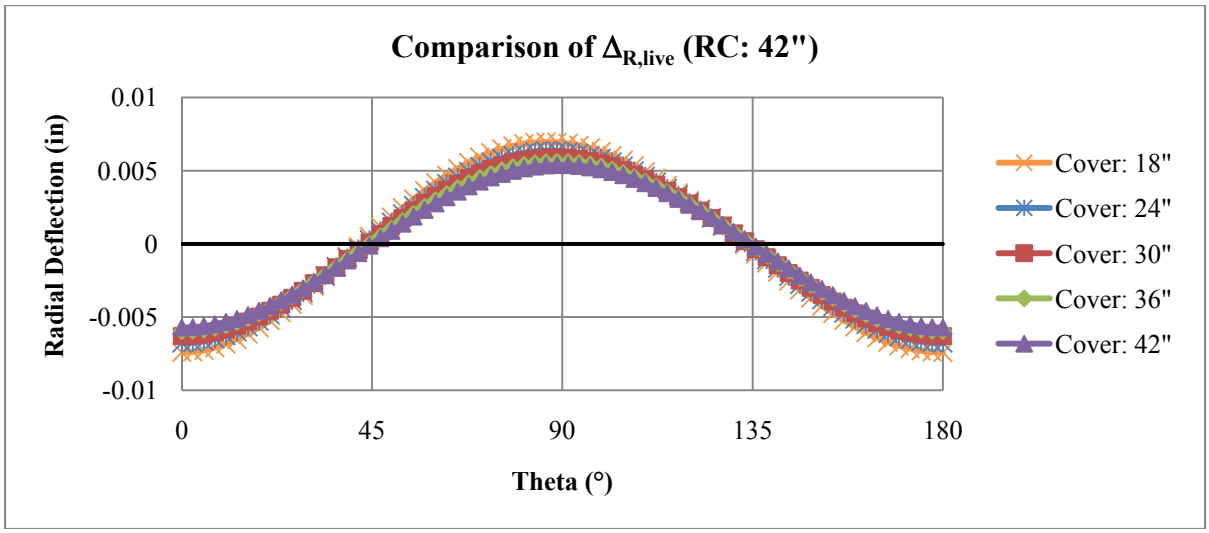

Figure 25

Comparison of Δ_R due to live loads only ($\Delta_{R,live}$) for RC pipe with D = 42 in.

Figure 26 shows the profile of Δ_{live} for a RC pipe with a 60 in. diameter. Figure 27 provides a zoom view of the profile near the region of application of the live loads. Similarly to the case of a 42 in. diameter RC pipe, LADOTD specifies a minimum cover height of 18 in. It is observed that a cover height of 30 in. generates a minimum absolute value roadway deflection of 0.1379 in. In addition, the profile of Δ_{live} for H_c = 24 in. and 30 in. almost coincide.

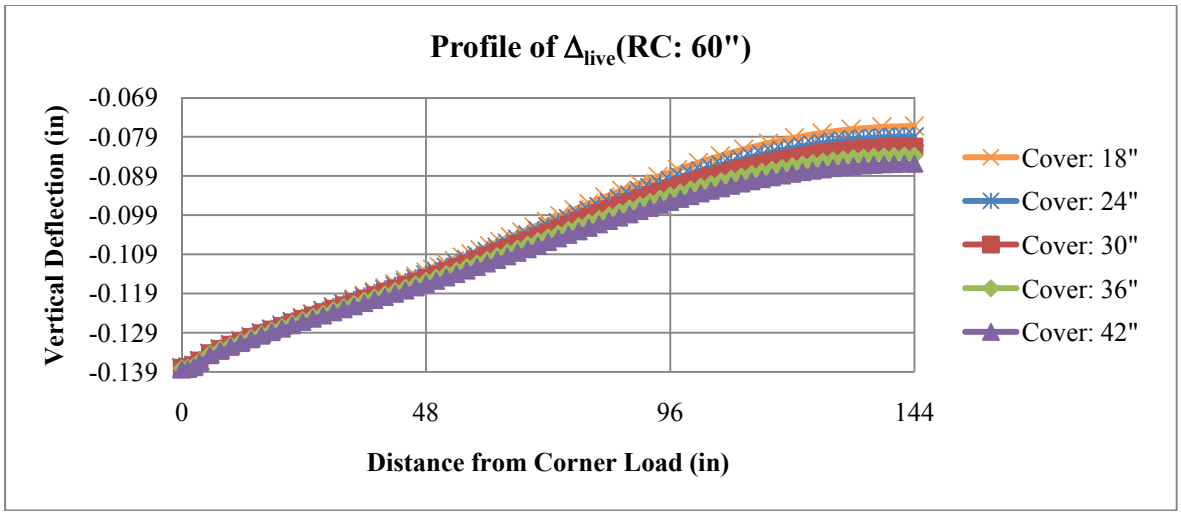

Figure 26

Profile of Δ due to live loads only (Δ_{live}) for RC pipe with D = 60 in.

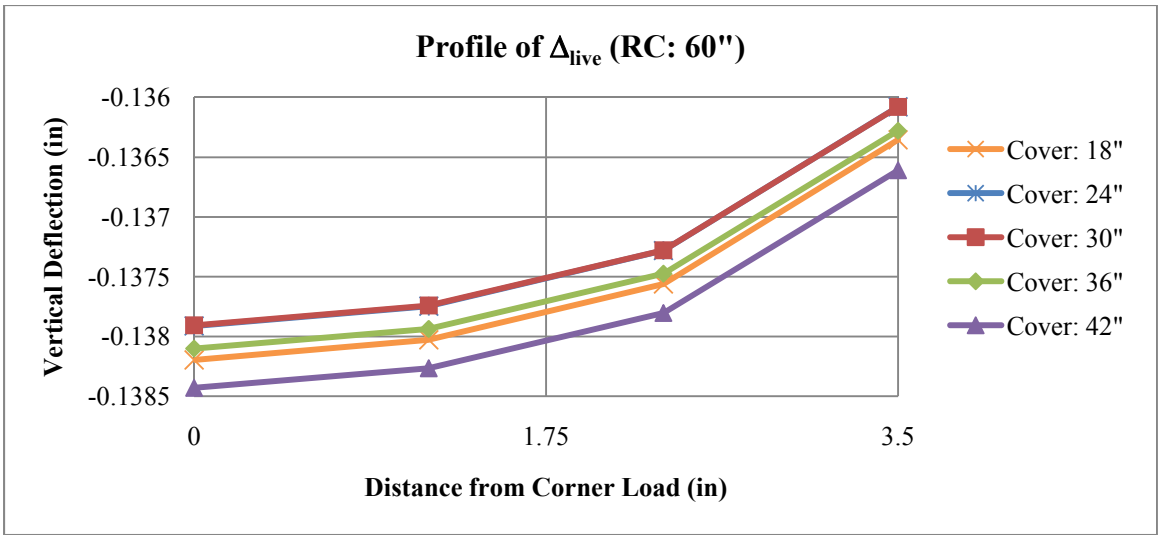

Figure 27

Profile of Δ due to live loads only (Δ_{live}) for RC pipe with D = 60 in.: zoom view

Figure 28 shows the plastic deformation at the road surface, $\Delta_{inelastic}$, for a 60-in. diameter RC pipe. An optimal cover height of 24 in. is needed for minimum plastic deformation. Also in this case, the plastic deformations are very small and affect mainly the soil. Again, the profile of $\Delta_{inelastic}$ corresponding to H_c = 12 in. differs significantly from the profile of $\Delta_{inelastic}$ for larger values of H_c.

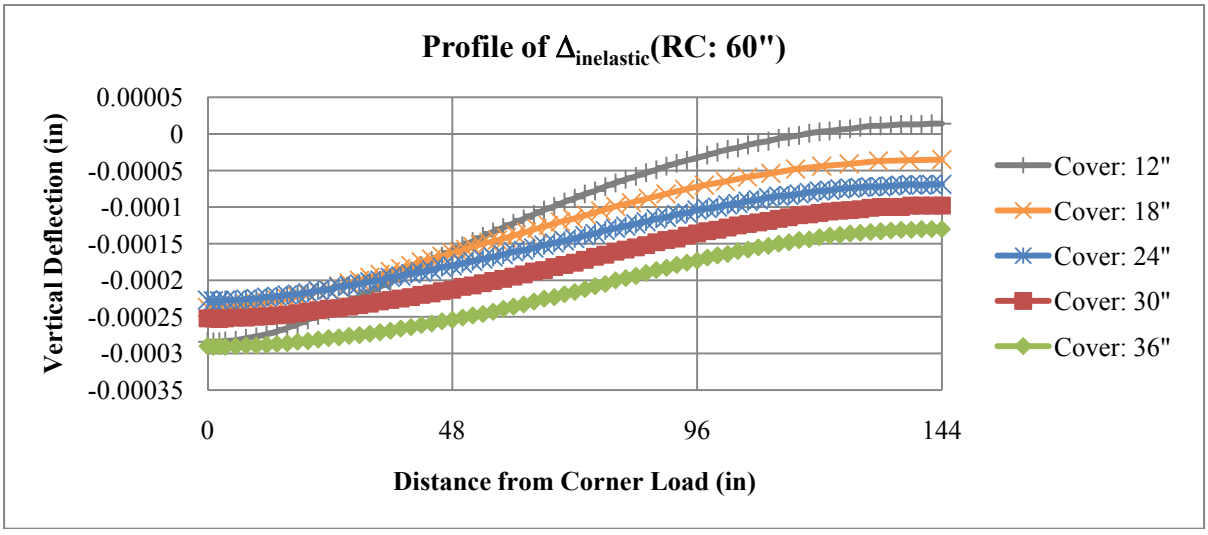

Figure 28

Profile of Δ due to plastic deformation ($\Delta_{inelastic}$) for RC pipe with D = 60 in.

Figure 29 shows the radius change due to live loads only, $\Delta_{R,live}$, for a 60-in. diameter RC pipe. The radius change observed in Figure 29 is very small and slightly decreases for

increasing cover height. For the FE models corresponding to D = 60 in., Δ_{live} decreases in absolute value by 0.21%, i.e., from 0.1382 in. for H_c = 18 in. to 0.1379 in. for H_c = 30 in. This change is practically negligible for application purposes. For the same FE models, $\Delta_{R,live}$ decreases by 15.7%.

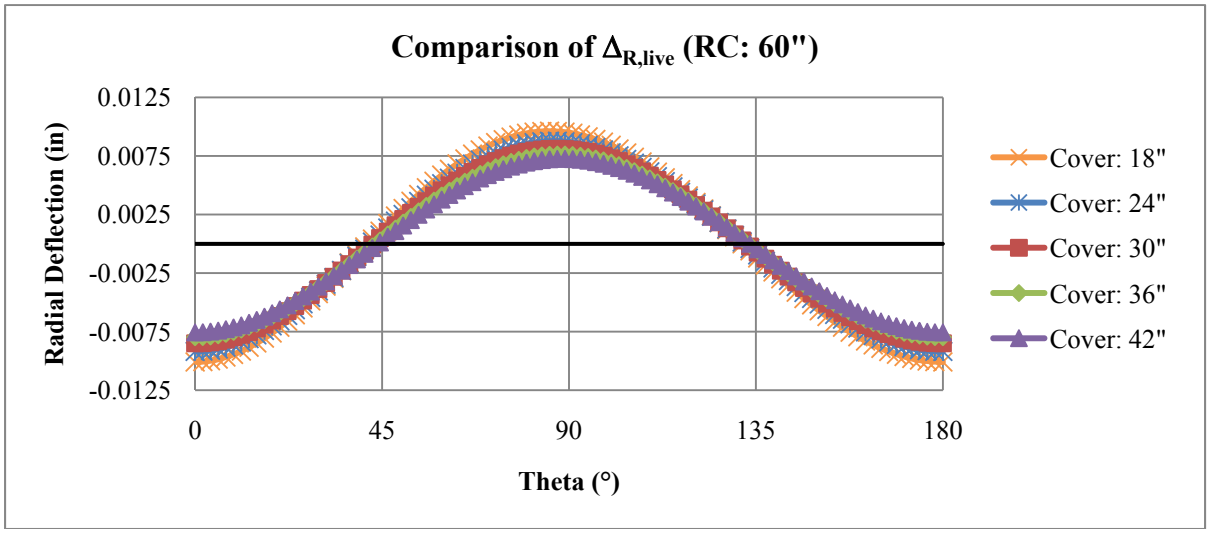

Figure 29

Comparison of Δ_R due to live loads only ($\Delta_{R,live}$) for RC pipe with D = 60 in.

Similar results as the ones presented in detail for the RC pipes were also obtained for the pipes of other materials. For a more concise exposition, only the zoom views of the profile of Δ_{live} are shown in the following sections, while the conclusive discussion of the results is based on all results obtained.

Nonlinear FE Analysis Results for Steel Pipes

Figure 30 shows the profile of Δ_{live} for a 42-in. diameter corrugated steel pipe. For corrugated steel pipes, LADOTD specifies a minimum cover height of 24 in. It is observed that a cover height of 30 in. results in a minimum absolute value surface deflection of 0.1357 in. This deflection is slightly higher than the one observed for an RC pipe of the same diameter. In addition, the difference in Δ_{live} observed between the models with minimum recommended and optimal cover heights is very small.

The profile of Δ_{live} for a 60-in. diameter corrugated steel pipe is shown in Figure 31. A minimum cover height of 24 in. is suggested by LADOTD also for this case. It is observed that a cover height of 60 in. produces a minimum absolute value of Δ_{live} of 0.1427 in. Also in this case, the Δ_{live} corresponding to the optimal cover is slightly higher than for an RC pipe of

the same diameter. It is noteworthy that the difference in Δ_{live} observed here between the models with minimum and optimal cover heights is not negligible.

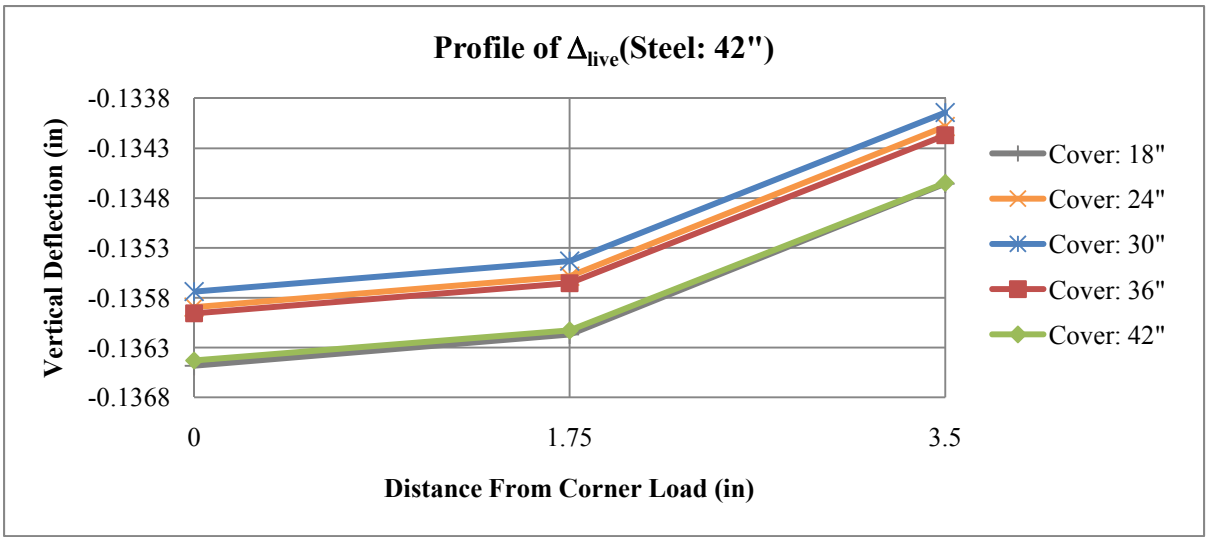

Figure 30

Profile of Δ due to live loads only (Δ_{live}) for steel pipe with D = 42 in.: zoom view

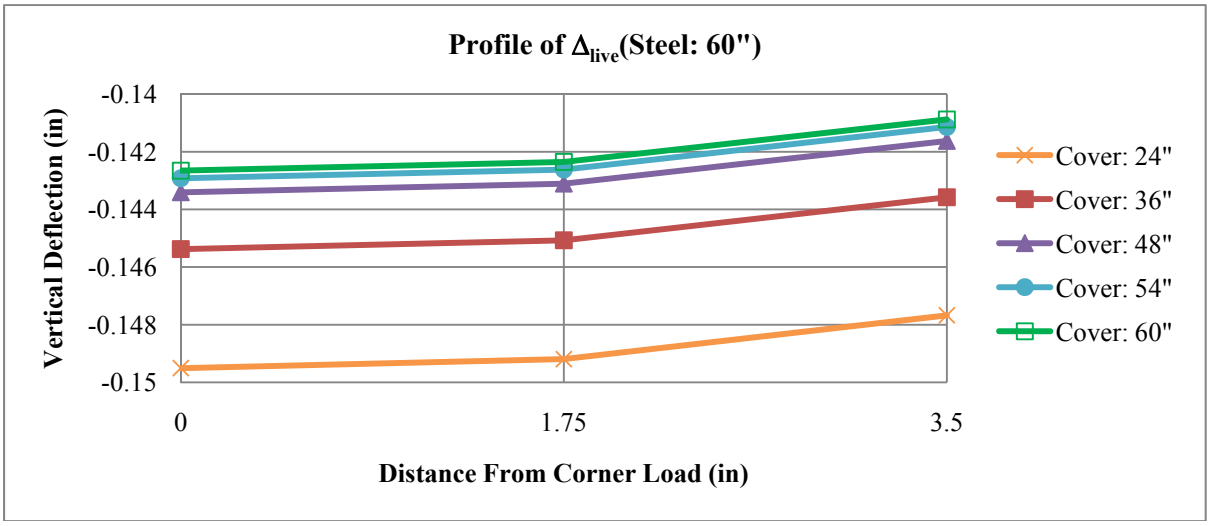

Figure 31

Profile of Δ due to live loads only (Δ_{live}) for steel pipe with D = 60 in.: zoom view

Nonlinear FE Analysis Results for PVC Pipes

The profile of Δ_{live} is illustrated in Figure 32 for a PVC pipe with a 42 in. diameter. LADOTD recommends a minimum cover height of 36 in. for pipes classified as flexible,

such as PVC pipes. Minimum roadway deflection is achieved by using an optimal cover height of 30 in. for a 42-in. PVC pipe. The difference in Δ_{live} observed between the models with minimum recommended and optimal cover heights is practically negligible in this case.

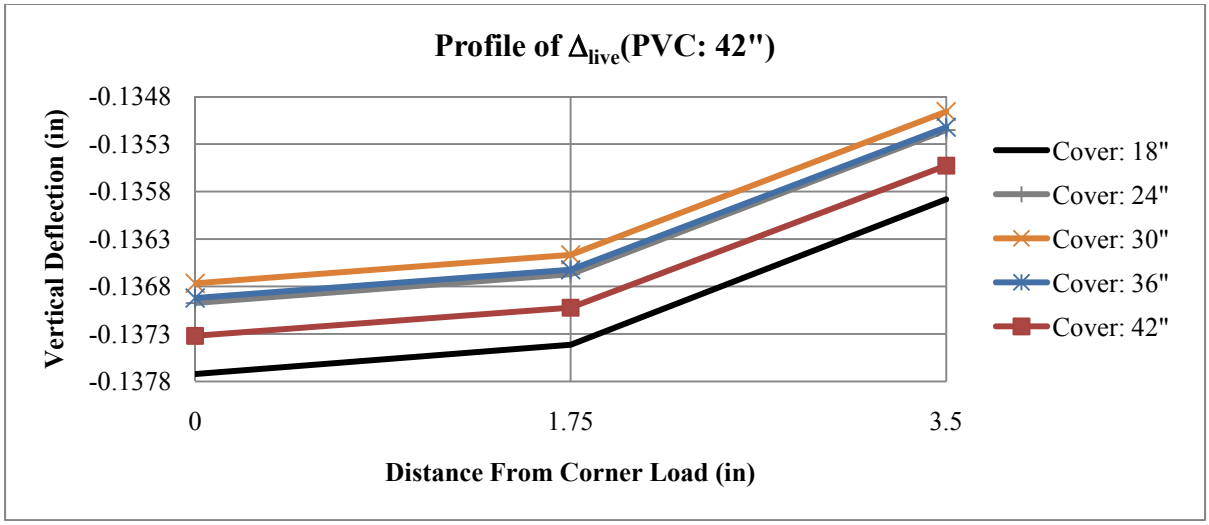

Figure 32

Profile of Δ due to live loads only (Δ_{live}) for PVC pipe with D = 42 in.: zoom view

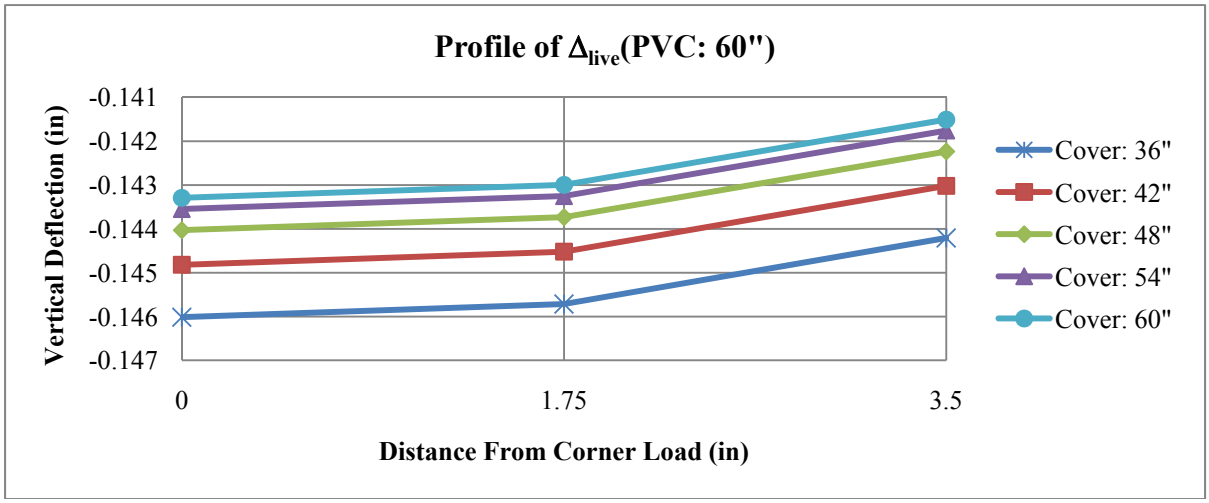

Figure 33

Profile of Δ due to live loads only (Δ_{live}) for PVC pipe with D = 60 in.: zoom view

Figure 33 shows the profile of Δ_{live} for a 60-in. diameter PVC pipe. LADOTD recommends a minimum cover height of 36 in. for all PVC pipes, without differentiation due to the pipe diameter. A cover height of 60 in. produces a minimum absolute road surface deflection of 0.1433 in. Comparing the results presented in Figure 30 and Figure 31 with the results shown

in Figure 32 and Figure 33, respectively, it is observed that the minimum absolute values of Δ_{live} obtained for steel PVC pipes with the same diameter are very similar. At these particular cover heights, both the steel and PVC pipes are performing almost identically.

Nonlinear FE Analysis Results for HDPE Pipes

Figure 34 shows the profile of Δ_{live} for an HPDE pipe with a 42 in. diameter. LADOTD specifies a minimum cover height of 36 in. for any pipe classified as flexible, such as HDPE pipes. It is observed that a cover height of 30 in. produces a minimum absolute value of Δ_{live} equal to 0.1406 in. However, the difference in Δ_{live} observed here between the models with minimum recommended and optimal cover heights is practically negligible.

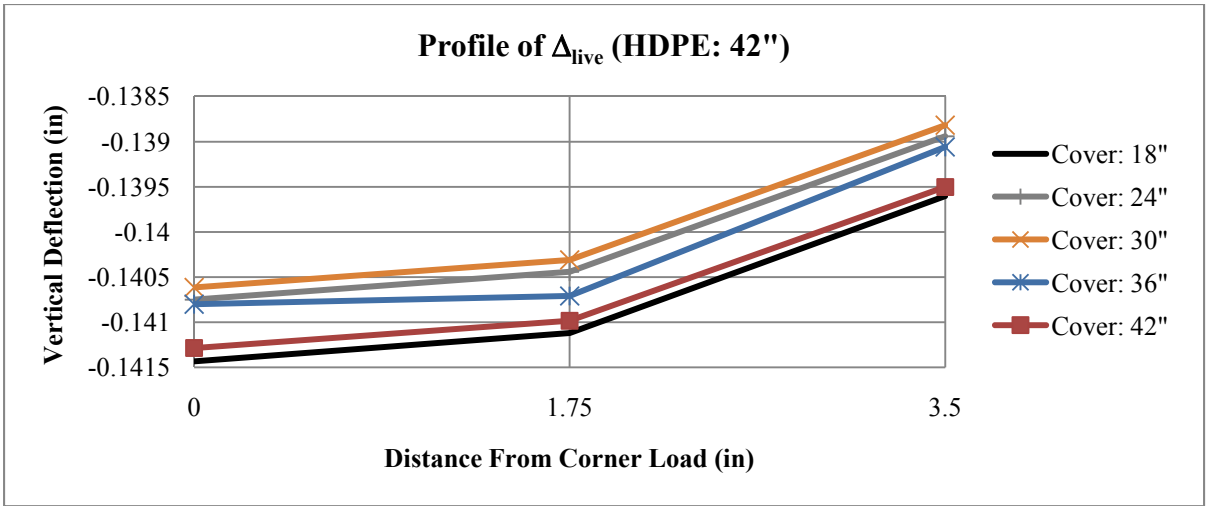

Figure 34

Profile of Δ due to live loads only (Δ_{live}) for HDPE pipe with D = 42 in.: zoom view

The Δ_{live} profile for a 60-in. diameter HDPE pipe is shown in Figure 35. With a pipe stiffness classified as flexible, a minimum cover height of 36 in. is specified by LADOTD. The minimum absolute value of Δ_{live} for a 60-in. HDPE pipe is obtained by using an optimal cover height of 60 in. It is observed that the HDPE pipes are the most flexible pipes among the materials considered, even when the optimal cover heights are used.

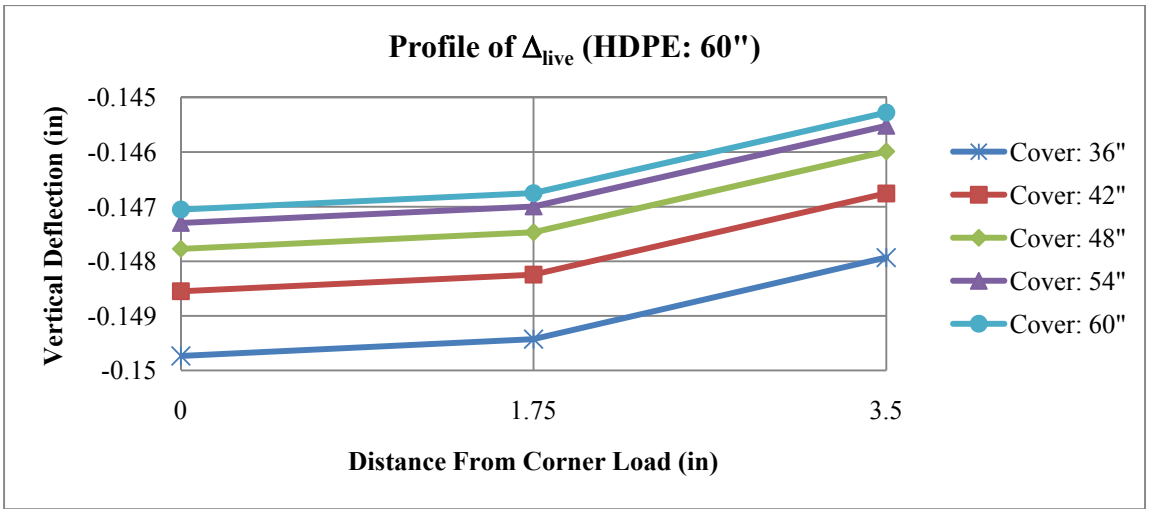

Figure 35

Profile of Δ due to live loads only (Δ_{live}) for HDPE pipe with D = 60 in.: zoom view

Comparison of Deflections for FE Models with Optimal H_c vs. Minimum H_c

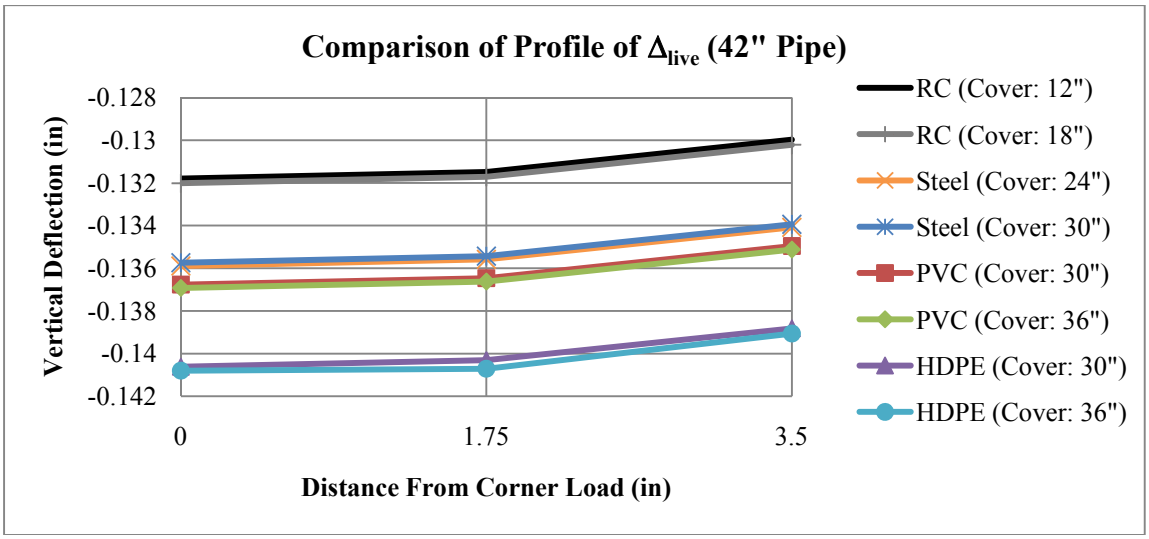

Figure 36

Comparison of profile of Δ due to live loads only (Δ_{live}) for all pipes with D = 42 in.: zoom view

The profiles of Δ_{live} are shown in Figure 36 for all 42-in. diameter pipes of different materials, including the results for both minimum recommended and optimal cover heights. The minimum values of cover heights recommended by LADOTD are as follows: 18 in. for RC, 24 in. for steel, and 36 in. for PVC and HDPE. It is observed than, for all pipes with D = 42 in., the differences in Δ_{live} between the two corresponding models (i.e., with minimum recommended and optimal cover height for the same material) are negligible.

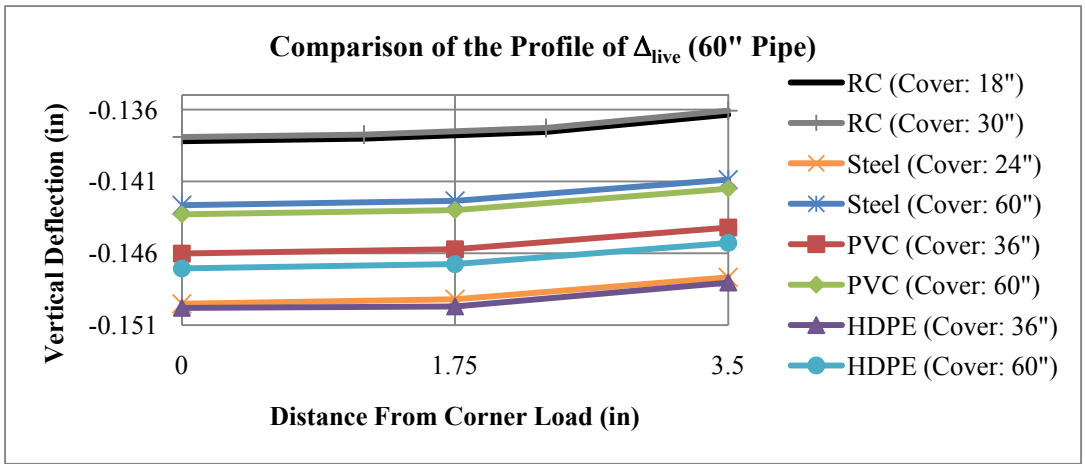

Figure 37
Comparison of profile of Δ due to live loads only (Δ_{live}) for all pipes with D = 60 in.: zoom view

Figure 37 shows the profile of Δ_{live} for all 60-in. diameter pipes of different materials, including the results for both minimum recommended and optimal cover heights. The minimum cover heights recommended by LADOTD are the same as for 42-in. diameter pipes of the same material, i.e., the recommended values of H_c are independent on the pipe diameter. Comparing the results presented in Figure 36 and Figure 37, it is observed that the changes in Δ_{live} due to use of an optimal versus minimum cover height of the 60-in. FE models are much greater for pipes with D = 60 in. than for pipes with D = 42 in.

Table 4
Summary of optimal H_c vs. LADOTD minimum H_c

Pipe Material	D (in.)	LA DOTD Minimum H_c (in.)	Δ_{live} Optimal H_c (in.)	$\Delta_{inelastic}$ Optimal H_c (in.)	$\Delta_{R,live}$ Optimal H_c (in.)	$\Delta_{R,inelastic}$ Optimal H_c (in.)
RC	42	18	12	18	42	24
RC	60	18	30	24	42	24
Steel	42	24	30	42	60	42
Steel	60	24	60	60	60	60
PVC	42	36	30	18	60	18
PVC	60	36	60	48	60	42
HDPE	42	36	30	48	60	18
HDPE	60	36	60	60	60	60

Table 4 summarizes LADOTD suggested minimum cover heights and the optimal cover heights obtained from the results of the nonlinear FE analyses corresponding to the four different performance measures considered in this study, i.e., (1) Δ_{live}, (2) $\Delta_{inelastic}$, (3) $\Delta_{R,live}$, and (4) $\Delta_{R,inelastic}$. Hereinafter, the optimal cover height corresponding to the minimum absolute value of Δ_{live} is considered as the reference value for H_c.

Table 5 compares the performance measures obtained using nonlinear FE models with the optimal cover height and with LADOTD minimum cover height. The same results are presented in terms of percentage changes of the performance measures in Table 6. The optimal cover height is taken as the height of cover, for a particular pipe, corresponding to which Δ_{live} is minimized in absolute value. In some cases, in order to minimize the road surface deflection, the radius change may be negatively impacted. For example, to achieve a minimum absolute Δ_{live} for a 4- in. diameter RC pipe, a cover height of 12 in. is needed instead of the minimum of 18 in. By doing so, the absolute road surface deflection is decreased by approximately 0.17% while $\Delta_{R,live}$ is increased by 11.61%. It is observed that, when the optimal cover height is less than the minimum cover height, $\Delta_{R,live}$ always increases. However, when the optimal cover height is greater than the recommended minimum cover height, the road surface deflection is minimized and the radius change becomes smaller.

Table 5
Comparison of variation in Δ_{live} and $\Delta_{R,live}$ when using optimal H_c vs. LADOTD minimum H_c

Pipe Material	D (in.)	LA DOTD Minimum H_c (in.)	Optimal H_c (in.)	Δ_{live} (in.)		$\Delta_{R,live}$ (in.)	
				Minimum H_c	Optimal H_c	Minimum H_c	Optimal H_c
RC	42	18	12	-0.1320	-0.1318	-0.0074	-0.0083
RC	60	18	30	-0.1382	-0.1379	-0.0101	-0.0085
Steel	42	24	30	-0.1359	-0.1357	-0.0145	-0.0135
Steel	60	24	60	-0.1495	-0.1427	-0.0229	-0.0153
PVC	42	36	30	-0.1369	-0.1368	-0.0136	-0.0143
PVC	60	36	60	-0.1460	-0.1433	-0.0190	-0.0153
HDPE	42	36	30	-0.1408	-0.1406	-0.0204	-0.0210
HDPE	60	36	60	-0.1498	-0.1471	-0.0269	-0.0234

Table 6
Comparison of variation of Δ and Δ_R when using optimal H_c vs. LADOTD minimum H_c

Pipe Material	D (in.)	LA DOTD Minimum H_c (in.)	Optimal H_c (in.)	Δ_{live} Change (%)	$\Delta_{inelastic}$ Change (%)	$\Delta_{R,live}$ Change (%)	$\Delta_{R,inelastic}$ Change (%)
RC	42	18	12	-0.17	16.67	11.61	23.08
RC	60	18	30	-0.21	6.33	-15.70	-21.23
Steel	42	24	30	-0.11	-10.79	-6.97	-4.61
Steel	60	24	60	-4.59	-52.48	-33.40	-35.90
PVC	42	36	30	-0.11	-28.21	5.50	-31.03
PVC	60	36	60	-1.87	-5.62	-19.44	7.71
HDPE	42	36	30	-0.13	0.40	2.79	-3.76
HDPE	60	36	60	-1.83	-17.36	-13.21	-12.59

The reinforced concrete (RC) pipe is very rigid when compared to pipes of other materials and, thus, presents a deflection smaller than pipes with the same diameter and made of other materials. It is observed in Table 5 that the radius change is much smaller for the RC pipes when compared to different material pipes with the same diameter. This smaller deflection is also attributed to the high stiffness of the RC pipe. It is noteworthy that a small deformation is essential when dealing with concrete pipes. If a large deflection were to occur, cracks could then form. According to Watkins, the maximum allowable crack width for concrete pipes is 0.01 in *[4]*. Fractured conduits can become unstable and the cracks can allow for the fluid in the pipes to escape into the surrounding soil.

For the nonlinear FE model of the soil-pipe system corresponding to a 42-in. diameter RC pipe and optimal cover height of 12 in., Δ_{live} decreases in absolute value by 0.17%, when compared to the FE model corresponding to the recommended cover height of 18 in, i.e., from 0.1320 in for H_c = 18 in. to 0.1318 in. for H_c = 12 in. This change is practically negligible for application purposes. For the same FE models, the maximum absolute value of $\Delta_{R,live}$ decreases by 11.61%. Similar observations can be made for all other pipes as well. As expected, the performance of the pipes in terms of deformations and road surface deflections slightly improves when using pipes made of HDPE, PVC, steel, and RC (best performer).

When a buried pipe deflects, the diameter change varies along the circumference of the pipe. The maximum diameter change is usually found along the vertical direction. Figure 38a illustrates the total deflections of the pipe in the loaded FE model compared to the unloaded pipe, while Figure 38b shows the relative deflections of the deformed pipe compared to its undeformed configuration. The pipe diameter change along the vertical direction is obtained

by taking the difference between the deflection at the pipe crest, δ_{top}, and the deflection at the bottom, δ_{bottom}. These deflections are shown in Table 7. The original pipe diameter, deflected pipe diameter, and pipe diameter changes are shown in Table 8.

Table 7
Displacements at the pipe's crest and bottom, δ_{top} and δ_{bottom}, due to both gravity and live loads

Pipe Material	D (in.)	LA DOTD minimum H_c (in.)	δ_{top} (in.)	δ_{bottom} (in.)
RC	42	18	-0.2759	-0.2537
RC	60	18	-0.3359	-0.3038
Steel	42	24	-0.2920	-0.2444
Steel	60	24	-0.3976	-0.3172
PVC	42	36	-0.3178	-0.2631
PVC	60	36	-0.4301	-0.3479
HDPE	42	36	-0.3274	-0.2417
HDPE	60	36	-0.440	-0.3136

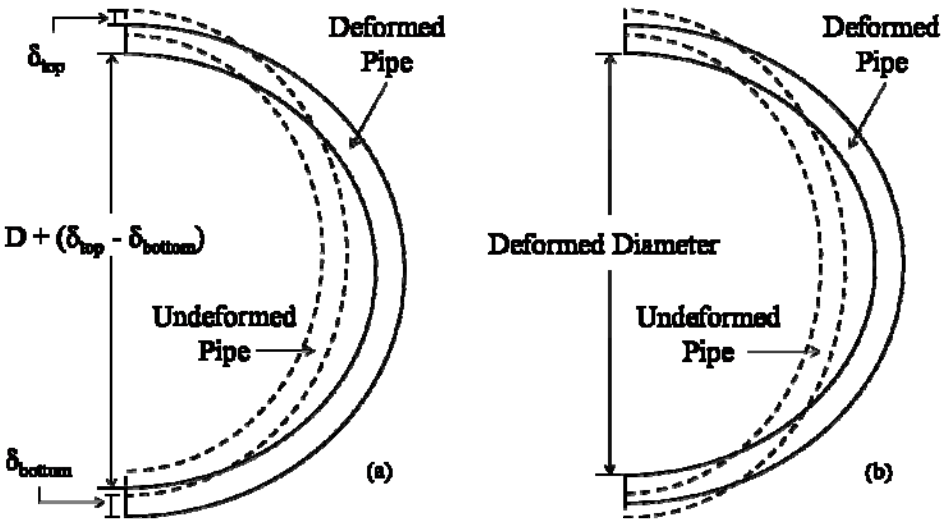

Figure 38
Comparison of undeformed and deformed pipe shape: (a) total deflections of the FE model, and (b) relative deflection of the pipe ring with respect to the undeformed pipe

Table 8
Comparison of diameter changes due to both gravity and live loads

Pipe Material	D (in.)	LADOTD minimum H_c (in.)	Deformed Diameter (in.)	Diameter Change (in.)	Diameter Change (%)	Allowable Diameter Change (%)	Safety Factor
RC	42	18	41.9778	-0.0222	0.0530	0.33	6.23
RC	60	18	59.9680	-0.0320	0.0534	0.20	3.75
Steel	42	24	41.9524	-0.0476	0.1132	5.0	44.17
Steel	60	24	59.9196	-0.0804	0.1340	5.0	37.31
PVC	42	36	41.9453	-0.0547	0.1303	5.0	38.37
PVC	60	36	59.9178	-0.0822	0.1370	5.0	36.50
HDPE	42	36	41.9143	-0.0857	0.2040	5.0	24.51
HDPE	60	36	59.8734	-0.1266	0.2110	5.0	23.70

It is crucial that, for each specific pipe material, the diameter change does not exceed a specified allowable diameter change, usually expressed as a percentage variation of the diameter. Since steel, PVC, and HDPE pipes are extremely flexible when compared to RC pipes, the allowable diameter change for these pipes is much larger than that of RC pipes. Allowable diameter changes are as follows: 0.33% for RC with D = 42 in. and 0.2% for RC with D = 60 in. *[4]*, 5% for steel *[18]*, 5% for PVC *[11]*, and 5% for HDPE *[12]*. The values for the concrete pipes were obtained from the formula presented in Watkins (2000), d = w / t, in which d = allowable ring deflection in percentage, w = maximum allowable crack width that is assumed to equal 0.01 in, and t = pipe wall thickness in inches. It is noteworthy that, for both PVC and HDPE pipes, an allowable diameter change value equal to 7.5% is suggested in *[18]*.

The diameter change can be used to define a performance criterion for the pipe. This performance criterion can be expressed in terms of a safety factor defined as the ratio between the allowable diameter change and the diameter change obtained from the nonlinear FE analysis, all quantities being expressed as percentages. Table 8 compares the diameter change for each nonlinear FE model due to both gravity and live loads with the corresponding allowable diameter change. The FE models considered here for the soil-pipe systems have cover heights equal to the minimum values recommended by LADOTD.

Table 8 also provides the safety factor for diameter change for all considered FE models. It is observed that all pipes are within their individual allowable ranges for diameter change and that the diameter changes obtained from the nonlinear FE analysis are significantly smaller than the allowable diameter changes. The performance of the pipes in terms of diameter changes, due to both gravity and live loads, improves when using pipes made of RC, HDPE, PVC, and steel, which achieve the best performance in terms of diameter change.

CONCLUSIONS

This study analyzed the effects of geometric and mechanical parameters that characterize and affect the soil-pipe interaction system of buried pipe installations located under roads/highways. The analysis focused on the combinations of pipe materials and sizes, natural soil mechanical properties, and road conditions typically encountered in Southern Louisiana. The drainage pipes or culverts installed as part of a roadway project are considered as holistic systems that include not only the pipes and their mechanical properties as determined by materials, geometry, and manufacturing procedures, but also the natural soil and the trench into which the pipe is placed, constructed, and expected to perform.

The first phase of the research employs linear elastic FE analysis to explore a wide range of values for numerous geometric and mechanical parameters. The parameters considered included: (1) excavation (trench) width, (2) fill cover height, (3) bedding height, (4) mechanical properties of the natural soil surrounding the trench, (5) mechanical properties and grade of compaction of the fill material, (6) mechanical properties and grade of compaction of the bedding material, (7) pipe material (RC, steel, PVC, and HDPE), (8) mechanical and geometric properties of the pipe, (9) material (concrete or asphalt) and geometry of the roadway pavement and its sub-pavement, and (10) importance of the road facility. This parametric study consisted of about 25,000 FE analyses and provides pertinent information about the sensitivity of the performance of the buried pipe installations. This information is also used to evaluate the conditions under which pipes made of different materials can perform similarly and, thus, can be used as alternative design solutions.

The sensitivity study based on simplified linear elastic FE analysis showed that the performance of all soil-pipe systems improves for increasing trench excavation width smaller than 2D in which D denotes the pipe diameter. This performance improvement is more significant for flexible pipes and/or yielding natural soil, while this improvement is small for rigid pipes and stiff natural soil. For trench widths larger than 2D, the performance improvement is usually very small. The performance of the soil-pipe system significantly improves for increasing values of H_c for all pipes, even if at a less than linear rate. Thus, for each pipe, it is possible to find an optimal cover height, H_c, beyond which the performance improvement of the soil-pipe system is negligible. It was found that the use of stiff bedding material can cause a significant stress concentration at the bottom of the pipe. The bedding thickness and bedding material stiffness should be decided in order to ensure that the bedding of the pipe is stable. This bedding must be able to redistribute as uniformly as possible the stresses transferred from the pipe and the loading acting above the pipe.

It was found that the natural soil stiffness also significantly influences the performance of soil-pipe systems. The natural soil properties considered in this study were based on typical conditions encountered in Southern Louisiana, where very soft clay is common. In addition, it was found that the performance of soil-pipe systems in terms of Δ_{live} depends crucially on the type of road surface. A stiffer road pavement distributes the stresses produced by the live loads more uniformly over a much larger area of soil. Thus, an increase in stiffness of the road pavement significantly decreases the magnitude of the stresses that are transferred to the pipe through the road pavement, the sub-pavement, and the trench cover. As a consequence, Δ_{live} also decreases substantially.

Linear elastic FE analysis is also used to determine the appropriate dimensions for a 3-D FE model of buried pipe installation. This model dimension sensitivity study suggests that, in order to obtain results insensitive to model dimensions, the FE model needs to include a region of natural soil surrounding the trench with the dimensions of one trench width in the horizontal direction and half a trench width in the vertical direction. In the direction of the pipe axis, a thickness of 24 in. sufficiently models 3-D effects.

The second phase of the research, based on advanced nonlinear FE analysis, evaluates four different performance measures for buried pipe installations with pipes of different materials (RC, steel, PVC, and HDPE) and different internal diameters (42 in. and 60 in.), i.e., (1) road surface deflection due to live loads only, Δ_{live}, (2) plastic road surface deflection, $\Delta_{inelastic}$, (3) radial deformation due to live loads only, $\Delta_{R,live}$, and (4) plastic radial deformation, $\Delta_{R,inelastic}$. The main results of this research phase are the optimal values of the cover height for the trench fill material corresponding to each performance measure considered. It was found that the optimal cover heights are very close to the minimum cover heights recommended by LADOTD for 42-in. diameter pipes. In addition, the observed differences in the performance measures are practically negligible for application purposes. However, for pipes with diameters equal to 60 in., the differences in performance between optimal and minimum recommended cover heights are significant. This observation suggests that the value of the minimum recommended cover height should be expressed as a function of the pipe diameter in order to ensure a homogeneous level of performance. When considering the optimal cover height, the performance of the pipes in terms of road surface deflections, Δ_{live}, slightly improves when using pipes made of HDPE, PVC, steel, and RC (best performer) when the same natural soil conditions and road pavement type are considered. When considering the minimum recommended cover height, the performance of the pipes in terms of diameter changes, due to both gravity and live loads, improves when using pipes made of RC, HDPE, PVC, and steel (best performer).

The research results confirm that the performance of the soil-structure interaction system constituted by the pipe, the trench backfill, and the natural soil surrounding the trench depends significantly not only on the pipe material and stiffness, but also on geometric parameters defining the trench in which the pipe is installed. Minimum requirements for these geometric parameters can be established to obtain equivalent performance of different pipe systems under similar design conditions.

RECOMMENDATIONS

This research focused on soil conditions typical of Southern Louisiana. The results of this research, when integrated with appropriate experimental data and field experience, can be used as guidance in establishing guidelines for the alternate selection and application of typical highway drainage products, such as pipes and culverts.

Based on the results obtained in this research, the following specific recommendations are made for implementation:

1) The minimum cover height should be expressed as a function of the pipe diameter.
2) For flexible and semi-flexible pipes, the minimum trench width should be equal to twice the pipe diameter, while for rigid pipes, a minimum trench width equal to the pipe diameter + 3 ft. is sufficient.
3) Different minimum requirements can be made for yielding and stiff soils. In the absence of specific data from in-situ tests, the more demanding requirements for yielding soil should be followed in favor of safety.
4) Different minimum requirements can be made for different road pavements with more demanding requirements for more flexible road pavements.

Further research is also recommended in order to determine the effects on the performance of buried pipe installation of (1) the removal of trench installation walls, (2) the long-term behavior and the fatigue behavior of soil-pipe systems, (3) the fluctuation of the water level in the soil near the buried pipes, and (4) uncertainty in pipes, trench filling material, and natural soil.

ACRONYMS, ABBREVIATIONS, & SYMBOLS

2-D	Two Dimensional
3-D	Three Dimensional
AASHTO	American Association of State Highway and Transportation Officials
ADS	Advanced Drainage Systems Inc.
AISC	American Institute of Steel Construction
AutoCAD	Auto Computer Aided Design
C3D4	4-noded linear tetrahedron
C3D6	6-noded triangular prism
C3D8I	8-noded linear brick with incompatible modes
CANDE	Culvert Analysis and Design
CDP	Concrete Damaged Plasticity
DOF	Degrees of Freedom
DOT	Department of Transportation
FE	Finite Element
FEA	Finite Element Analysis
FHWA	Federal Highway Administration
H20	AASHTO Standard H-type 20 Ton Vehicle
HDPE	High Density Polyethylene
LADOTD	Louisiana Department of Transportation
LE	Linear Elastic
LRFD	Load Resistance Factor Design
LTRC	Louisiana Transportation Research Center
PVC	Polyvinyl Chloride
RC	Reinforced Concrete
SPIDA	Soil-Pipe Interaction and Design Analysis
SSI	Soil-Structure Interaction
ft.	feet
hrs	hours
in.	inch(es)
kips	kilo pounds
ksi	kilo pounds per square inch
lb/ft^3	pounds per cubic foot
mins	minutes
c_b	bedding material cohesion

c_f	fill material cohesion
c_s	natural soil cohesion
d	allowable diameter change percentage
D	pipe diameter
Δ	deflection
$\Delta_{inelastic}$	maximum dip depth at road surface due to plastic deformation
Δ_{live}	maximum dip depth at road surface due to live loads only
Δ_{max}	maximum elastic deformation at road surface due to both gravity and live loads
$\Delta_{R,inelastic}$	maximum radial deformation due to plastic deformation
$\Delta_{R,live}$	maximum radial deformation due to live loads only
$\Delta\sigma$	maximum stress increment
δ_{top}	deflection at the pipe crest
δ_{bottom}	deflection at the pipe bottom
E	Young's modulus
E_b	bedding material stiffness
E_f	fill material stiffness
E_s	natural soil stiffness
E_{sp}	sub-pavement stiffness
H_b	bedding height
H_c	fill cover height
H_p	road pavement thickness
H_{sp}	sub-pavement thickness
I	moment of inertia
%	percentage
ϕ	friction angle
ϕ_b	bedding material friction angle
ϕ_f	fill material friction angle
ϕ_s	natural soil friction angle
θ	reference angle for radial deformation
t	pipe thickness
w	allowable crack width
W	trench excavation width
σ_{max}	maximum stress reached in the pipe due to both gravity and live loads
σ_y	yield strength
$\sum$	summation

REFERENCES

1. Jeyapalan, J. K. and Hamida, H. B. "Comparison of German to Marston Design Methods." *ASCE Journal of Transportation Engineering*, Vol. 114, No. 4, 1988, pp. 420-434.

2. Burns, J. C. "Experimental Investigation of Shear Capacity of Precast Reinforced Concrete Box Culverts." *M.S. Thesis*. The University of Texas at Arlington, Arlington, TX, 2009.

3. Katona, M. G., Smith, J. M., Odello, R. S., and Allgood, J. R. "CANDE - A Modern Approach for the Structural Design and Analysis of Buried Culverts." *Report No. FHWA-RD-77-5*, U.S. Naval Civil Engineering Lab, Port Hueneme, CA, 1976.

4. Watkins, R. K., and Anderson L. R. *Structural Mechanics of Buried Pipes.* CRC Press LLC, Boca Raton, FL, 2000.

5. Slatter, G. "Suggested Bedding Factors of Controlled Low-Strength Material for Concrete Pipe." *Proceedings*, ASCE International Conference on Pipeline Engineering and Construction, July 13-16, 2003, Baltimore, MD. Editor: Najafi M., Publisher: American Society of Civil Engineering, New York, NY, 2003, pp. 1086–1095.

6. CSI. *SAP2000 Application Programming Interface Documentation*. Version 11. Computers & Structure, Inc., Berkeley, CA, 2007.

7. AASHTO. *LRFD Bridge Design Specifications*. American Association of State and Highway Transportation Officials. Washington, D.C., 2007.

8. ABAQUS. *Version 6.8 Documentation*. Dassault Systemes Simulia Corp., Providence, RI, 2008.

9. AASHTO M 170. *Standard Specification for Reinforced Concrete Culvert, Storm Drain, and Sewer Pipe.* American Association of State and Highway Transportation Officials. Washington, D.C., 2007.

10. AASHTO M 36. *Standard Specification for Corrugated Steel Pipe, Metallic-Coated for Sewers and Drains*. American Association of State and Highway Transportation Officials. Washington, D.C., 2007.

11. AASHTO M 278. *Standard Specification for Class PS46 Poly (Vinyl Chloride) (PVC) Pipe.* American Association of State and Highway Transportation Officials. Washington, D.C., 2007.

12. AASHTO M 294. *Standard Specification for Corrugated Polyethylene Pipe, 300 to 1500 mm Diameter.* American Association of State and Highway Transportation Officials. Washington, D.C., 2007.

13. Kararam, A. "Nonlinear Finite Element-Based Investigation of the Effect of Bedding Thickness on Underground Pipe." *M.S. Thesis*. The University of Texas at Arlington, Arlington, TX, 2006.

14. Ibrahimbegovic, A. (2009). *Nonlinear Solid Mechanics: Theoretical Formulations and Finite Element Solution Methods.* Series: *Solid Mechanics and Its Applications*, Vol. 160, Springer-Verlag, New York, NY, 2009.

15. Jankowiak, T., and Lodygowski, T. "Identification of Parameters of Concrete Damage Plasticity Constitutive Model." *Foundations of Civil and Environmental Engineering*, Vol. 6, 2005, pp. 53-69.

16. Budhu, M. *Soil Mechanics and Foundations*. 1st Edition. John Wiley and Sons, Inc., Hoboken, NJ, 2000.

17. AISC. *Steel Construction Manual*. 13th Edition. American Institute of Steel Construction, Inc., Chicago, IL, 2005.

18. Moser, A. P. *Buried Pipe Design*. 2nd Edition. McGraw-Hill, New York, NY, 2001.

APPENDIX A

Nonlinear FE Results for Overall Comparisons

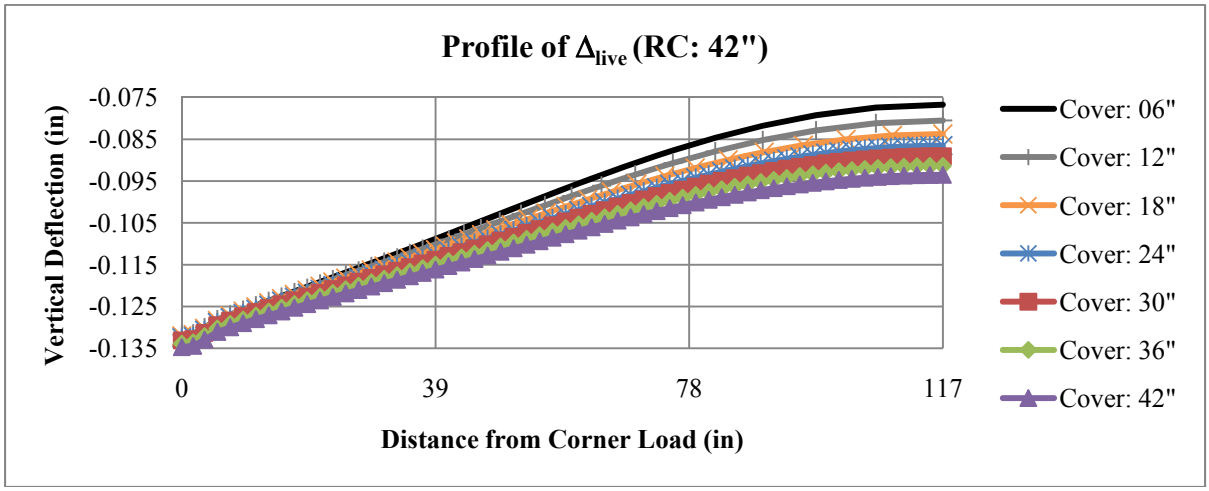

Figure 39
Profile of Δ_{live} for RC pipe with D = 42 in.

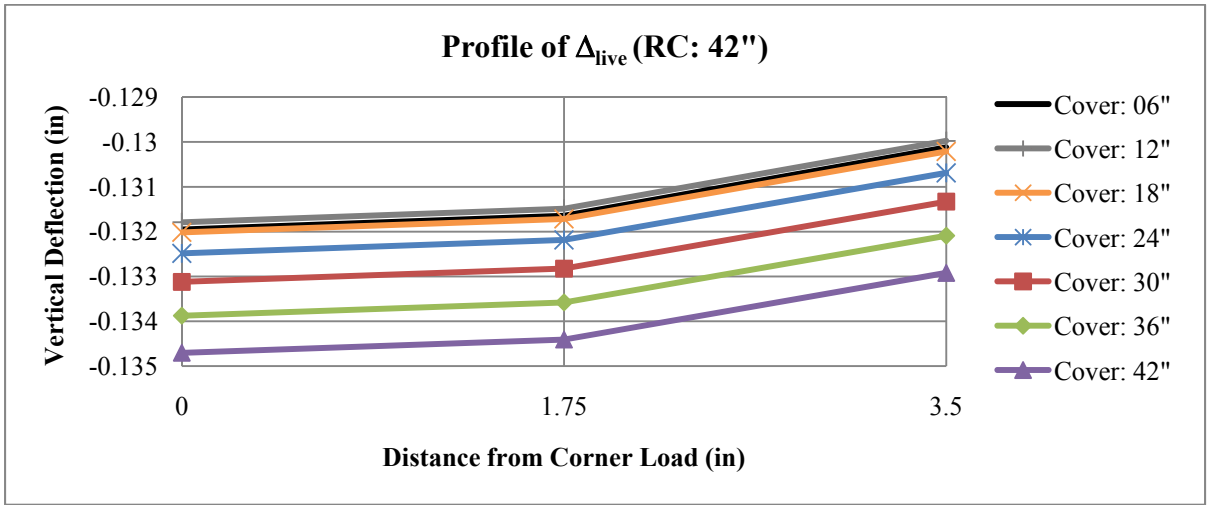

Figure 40
Profile of Δ_{live} for RC pipe with D = 42 in.: zoom view

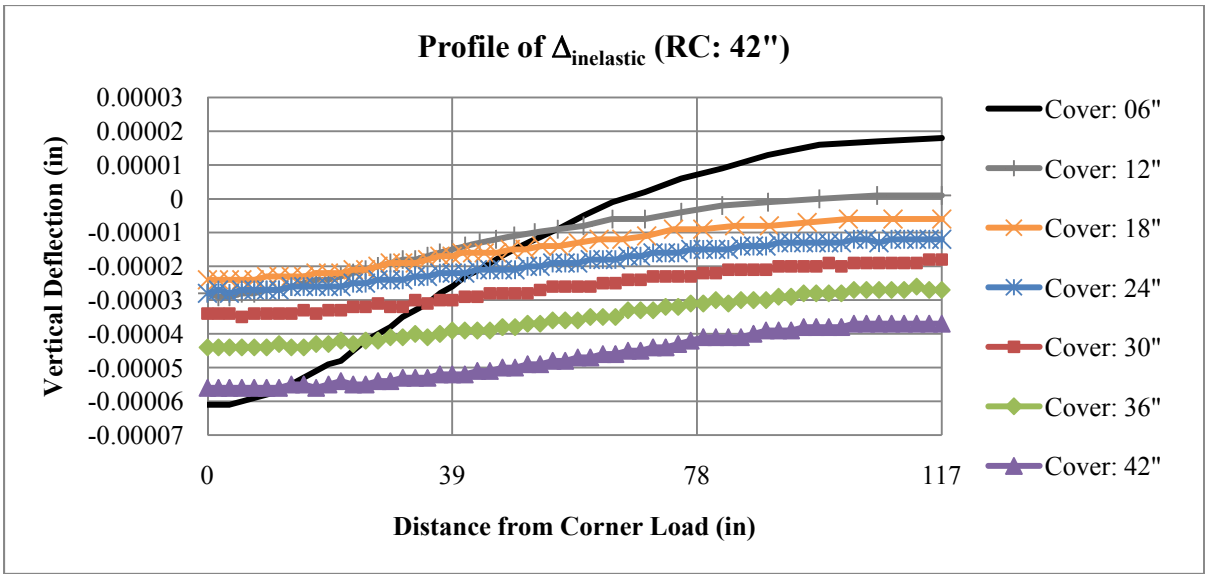

Figure 41
Profile of $\Delta_{inelastic}$ for RC pipe with D = 42 in.

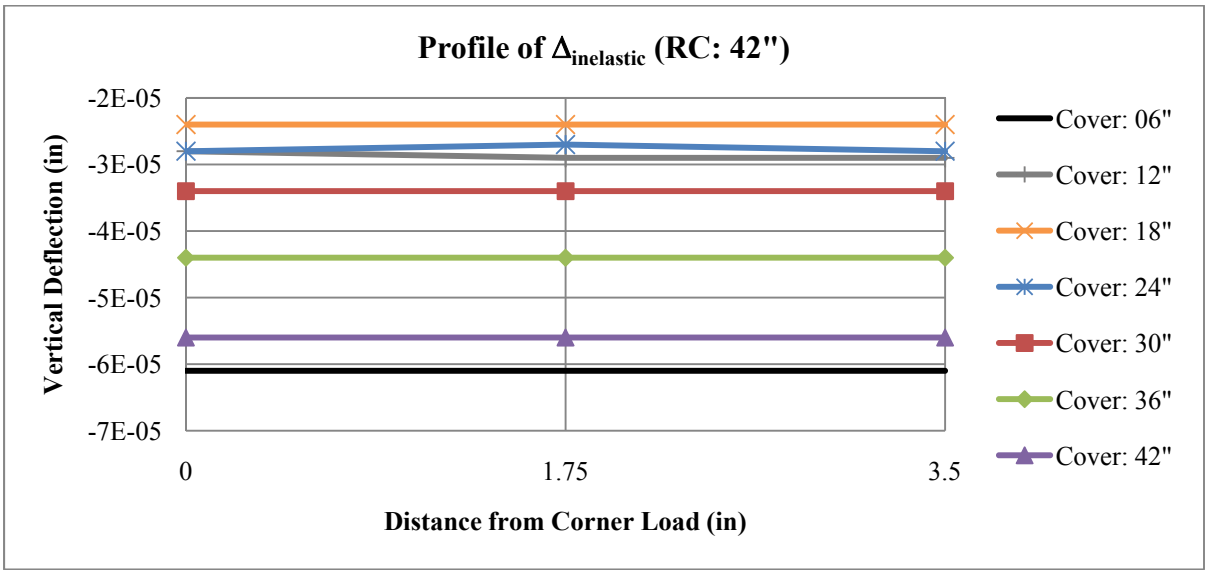

Figure 42
Profile of $\Delta_{inelastic}$ for RC pipe with D = 42 in.: zoom view

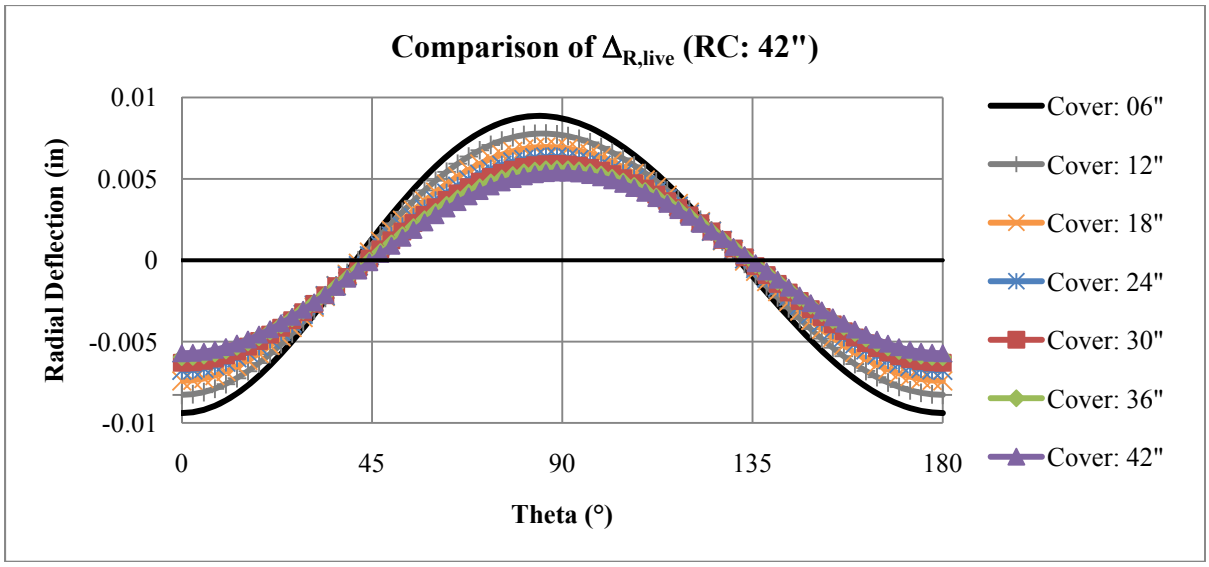

Figure 43
Comparison of $\Delta_{R,live}$ for RC pipe with D = 42 in.

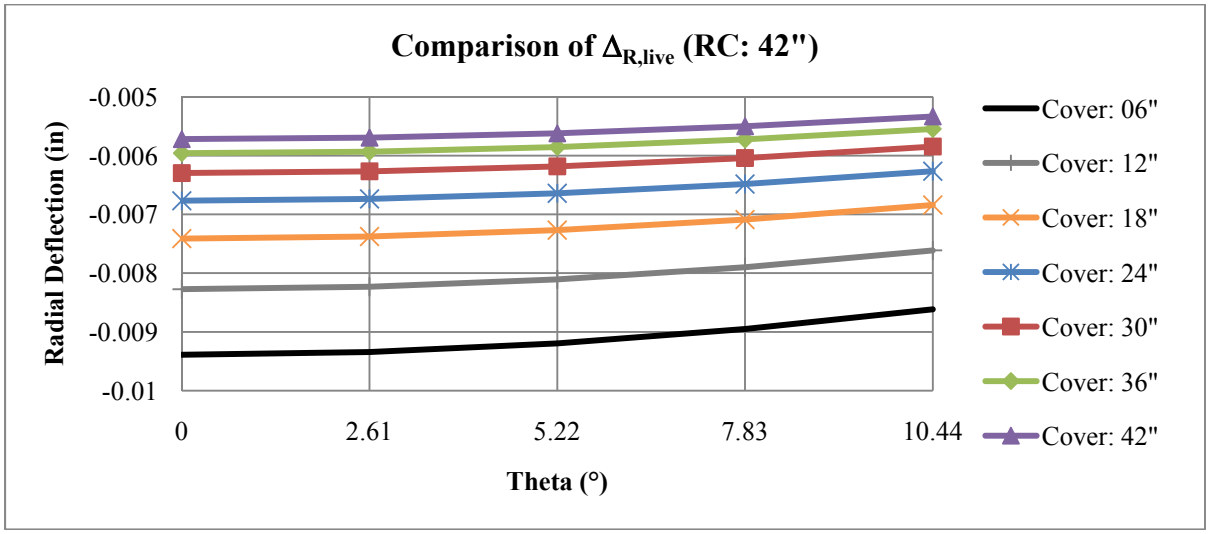

Figure 44
Comparison of $\Delta_{R,live}$ for RC pipe with D = 42 in.: zoom view

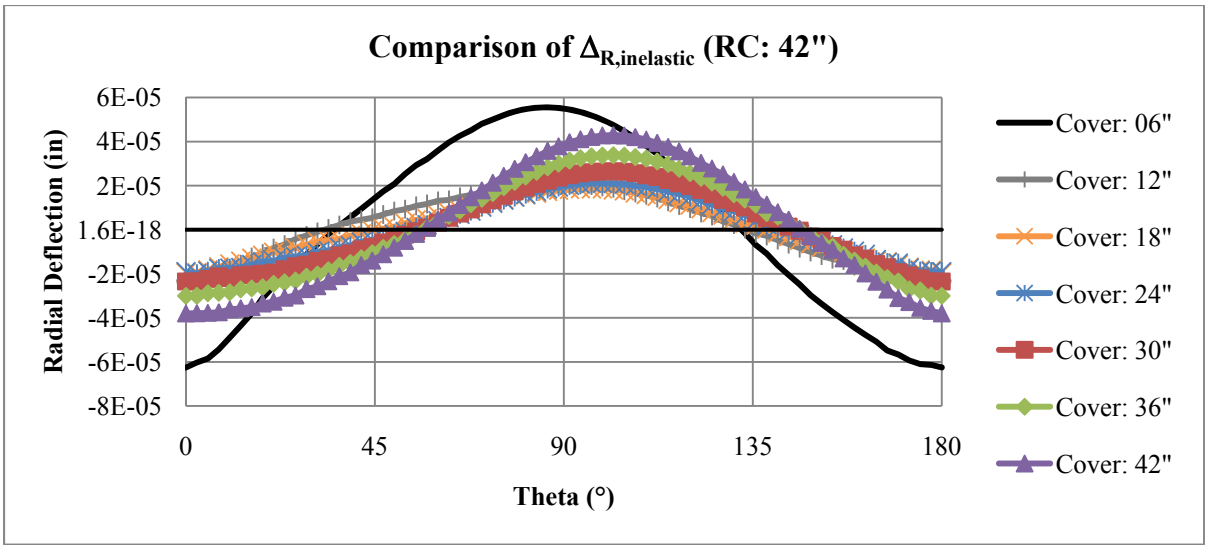

Figure 45
Comparison of $\Delta_{R,inelastic}$ for RC pipe with D = 42 in.

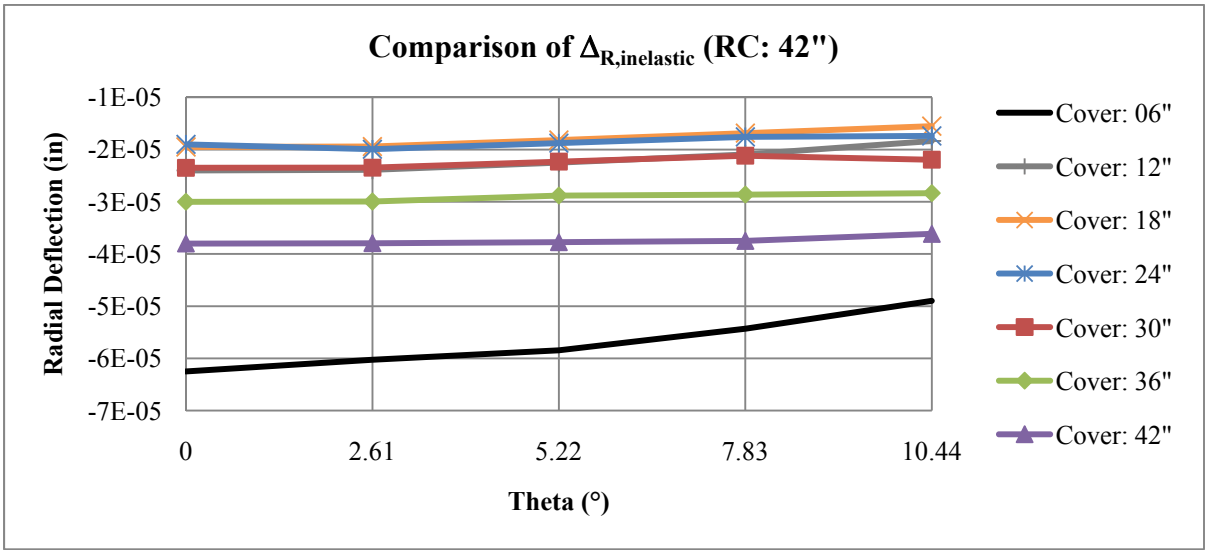

Figure 46
Comparison of $\Delta_{R,inelastic}$ for RC pipe with D = 42 in.: zoom view

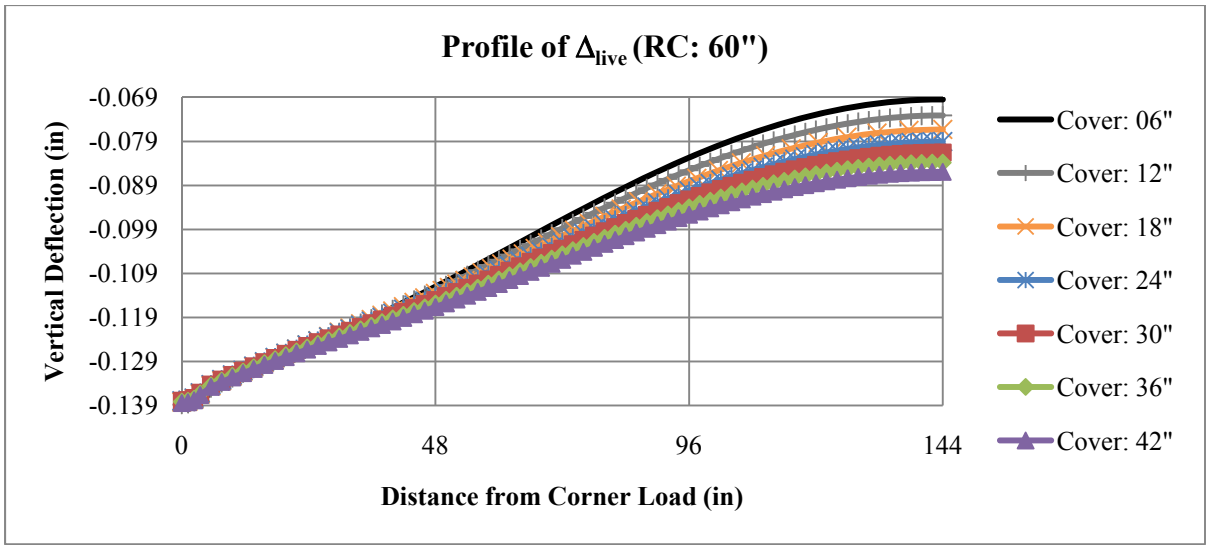

Figure 47
Profile of Δ_{live} for RC pipe with D = 60 in.

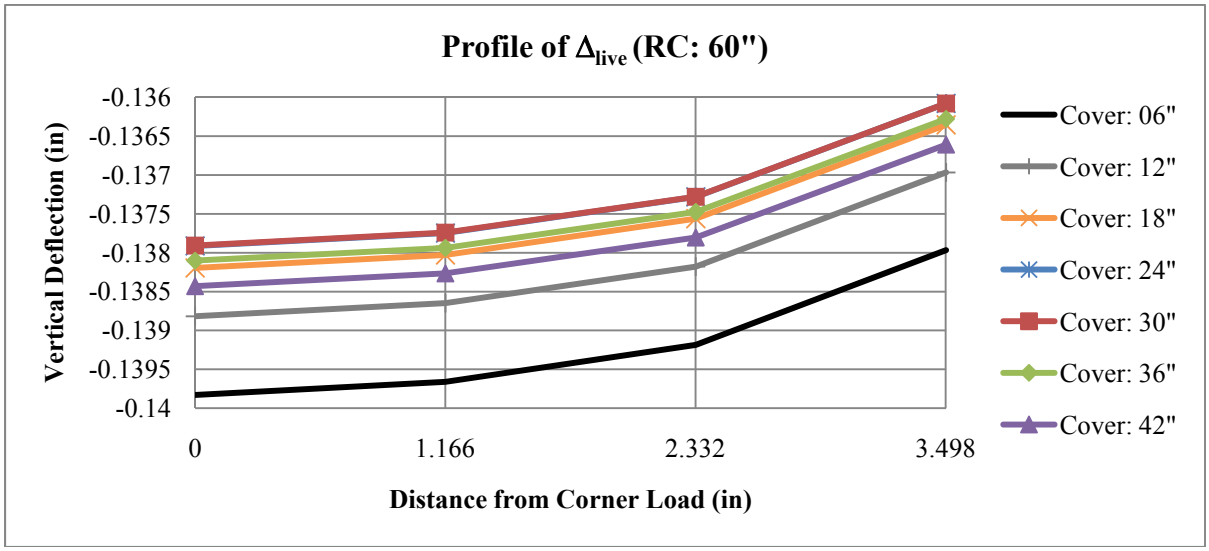

Figure 48
Profile of Δ_{live} for RC pipe with D = 60 in.: zoom view

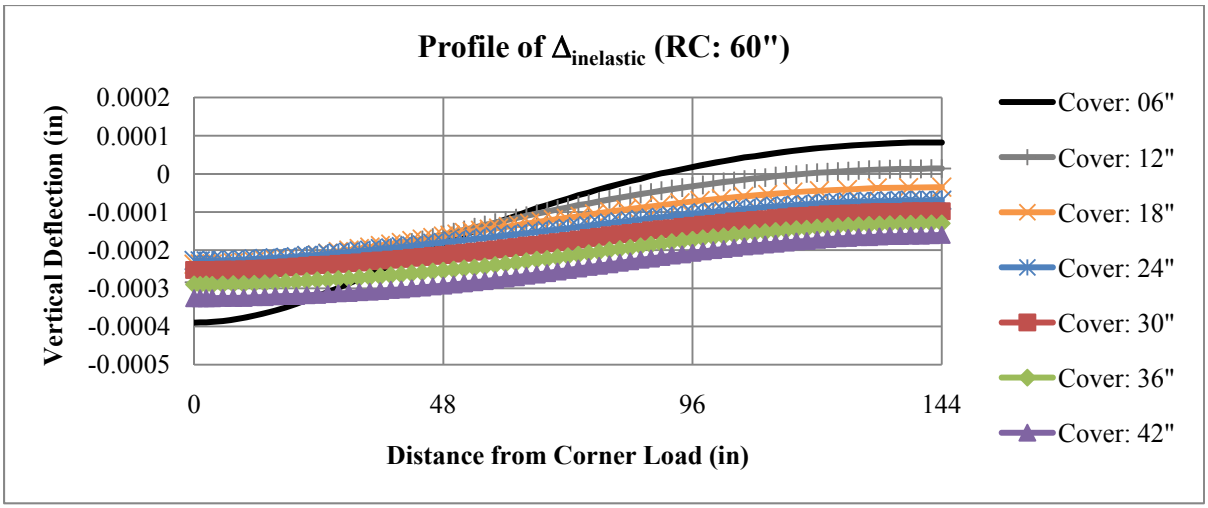

Figure 49
Profile of $\Delta_{inelastic}$ for RC pipe with D = 60 in.

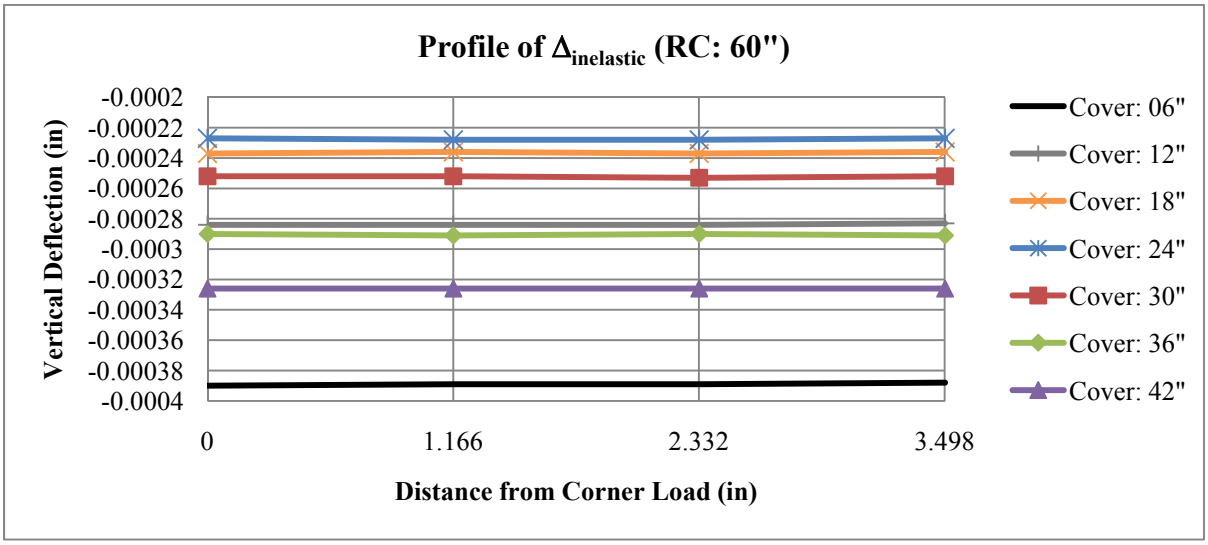

Figure 50
Profile of $\Delta_{inelastic}$ for RC pipe with D = 60 in.: zoom view

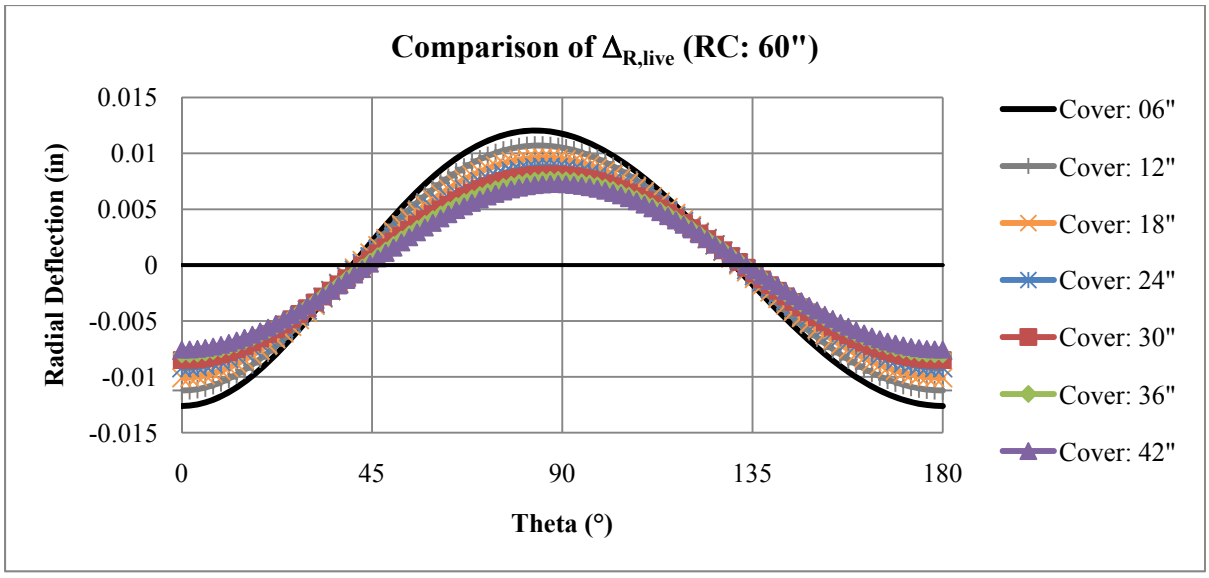

Figure 51
Comparison of $\Delta_{R,live}$ for RC pipe with D = 60 in.

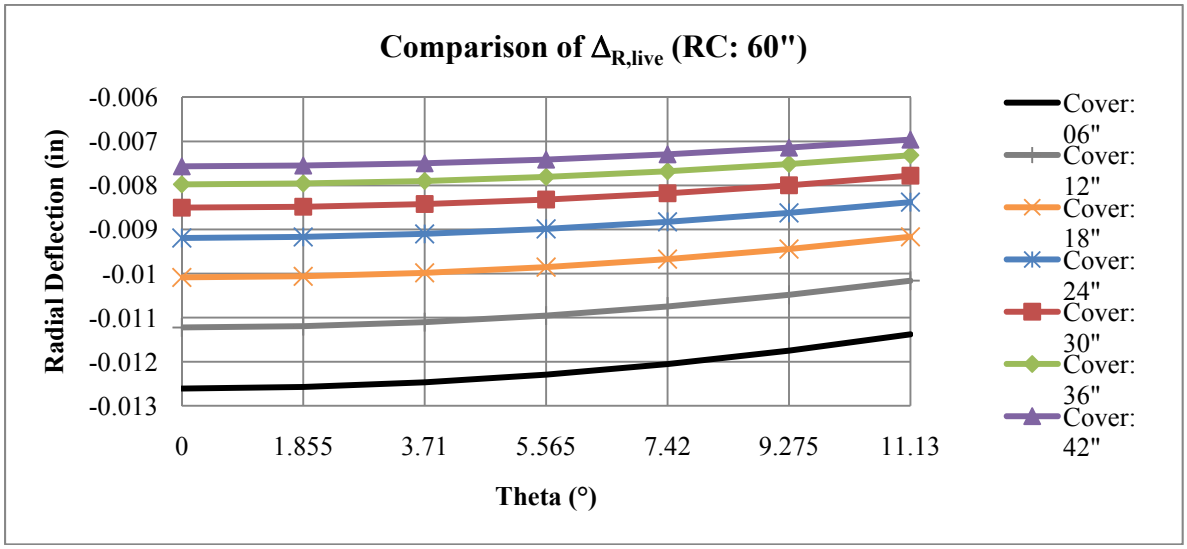

Figure 52
Comparison of $\Delta_{R,live}$ for RC pipe with D = 60 in.: zoom view

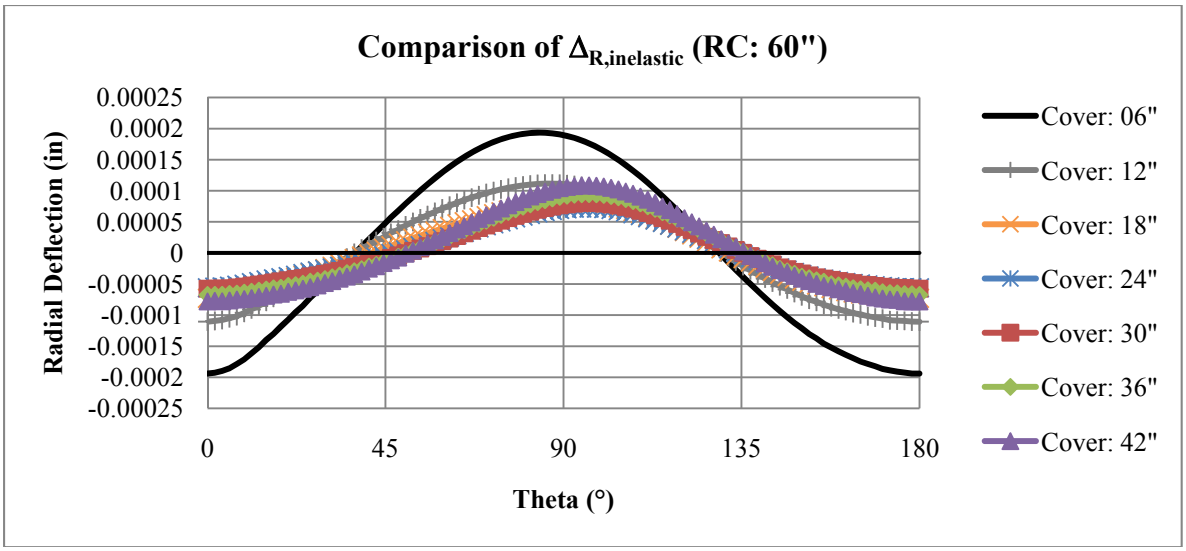

Figure 53
Comparison of $\Delta_{R,inelastic}$ for RC pipe with D = 60 in.

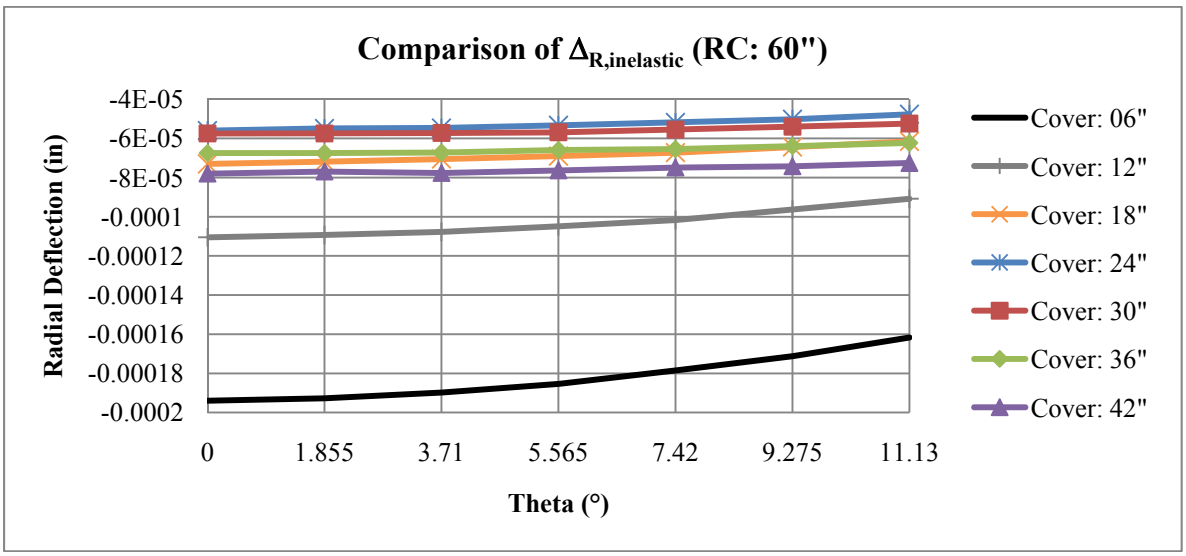

Figure 54
Comparison of $\Delta_{R,inelastic}$ for RC pipe with D = 60 in.: zoom view

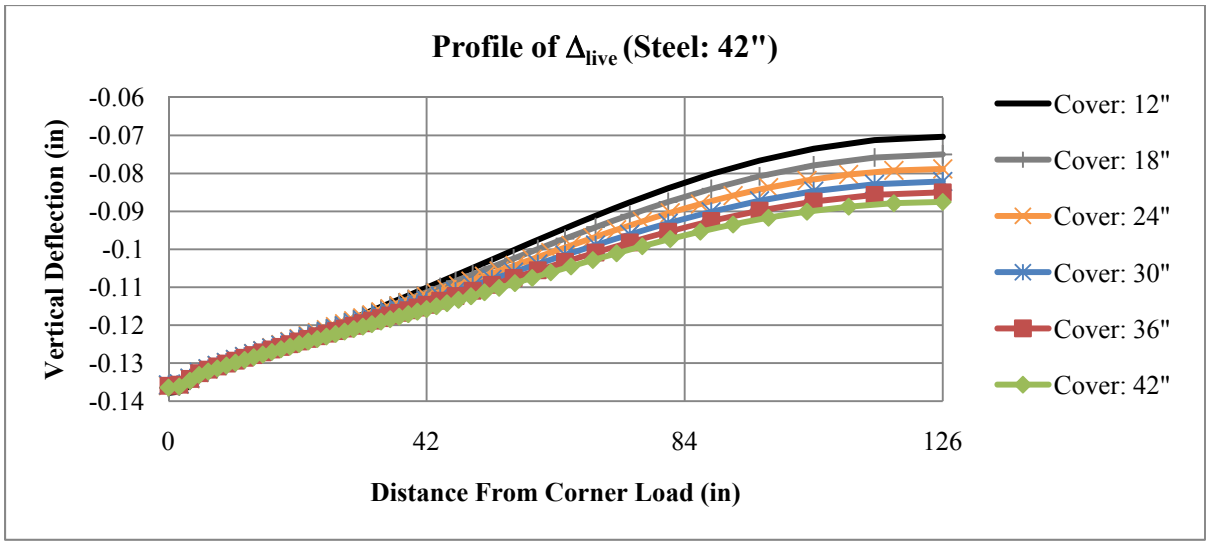

Figure 55
Profile of Δ_{live} for steel pipe with D = 42 in.

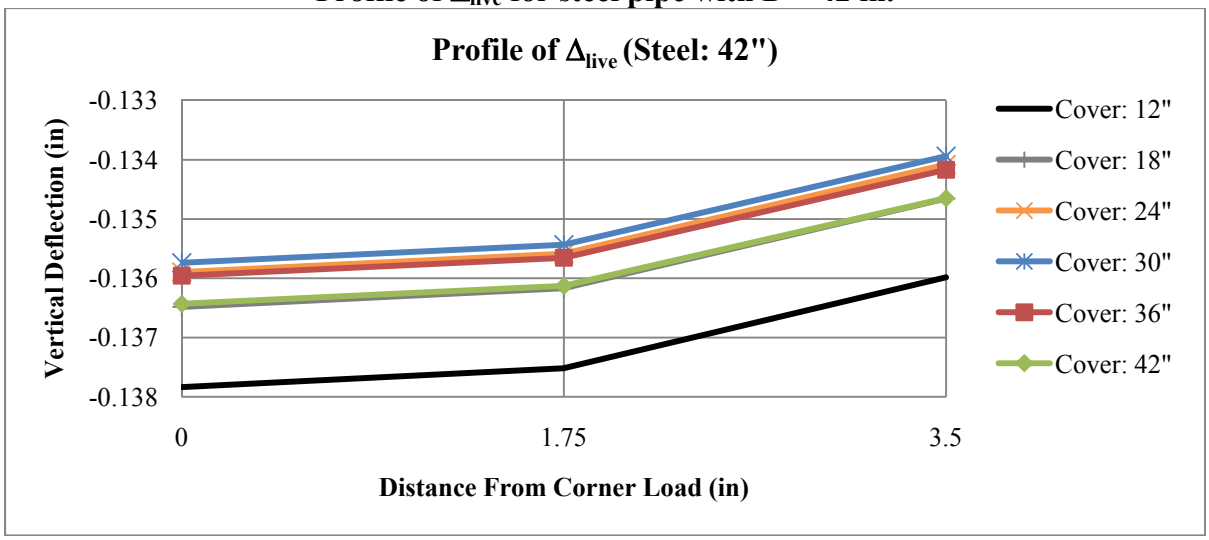

Figure 56
Profile of Δ_{live} for steel pipe with D = 42 in.: zoom view

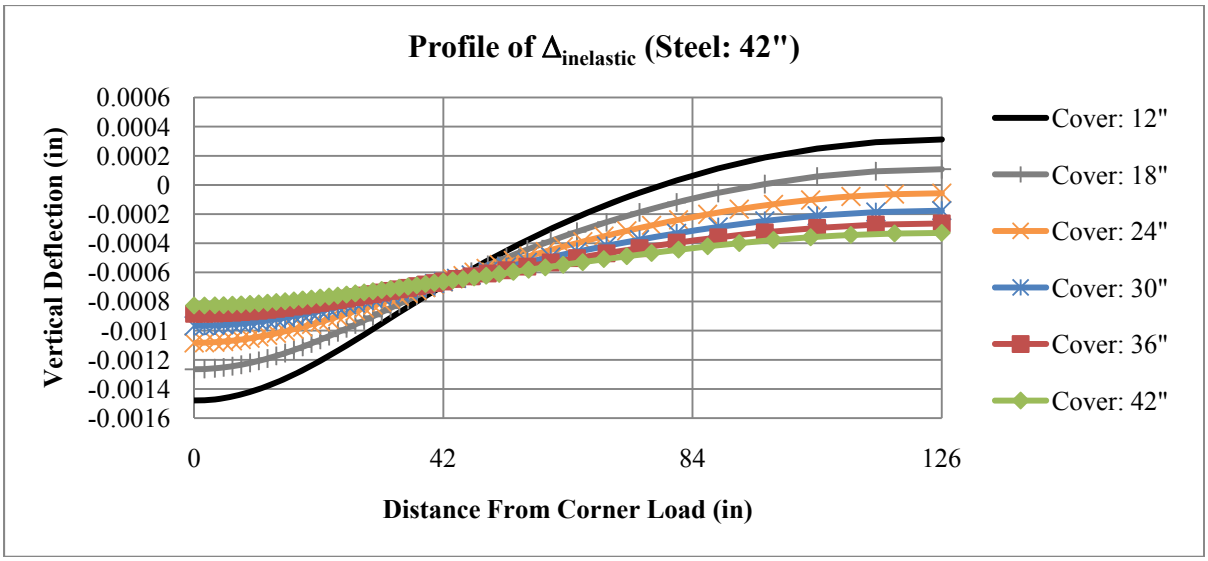

Figure 57
Profile of $\Delta_{inelastic}$ for steel pipe with D = 42 in.

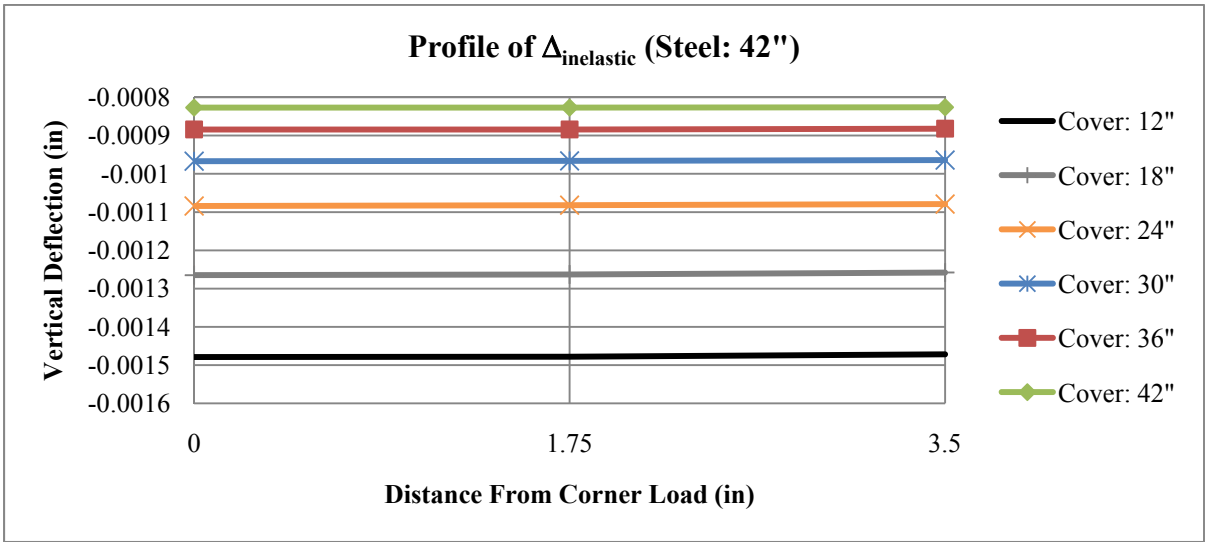

Figure 58
Profile of $\Delta_{inelastic}$ for steel pipe with D = 42 in.: zoom view

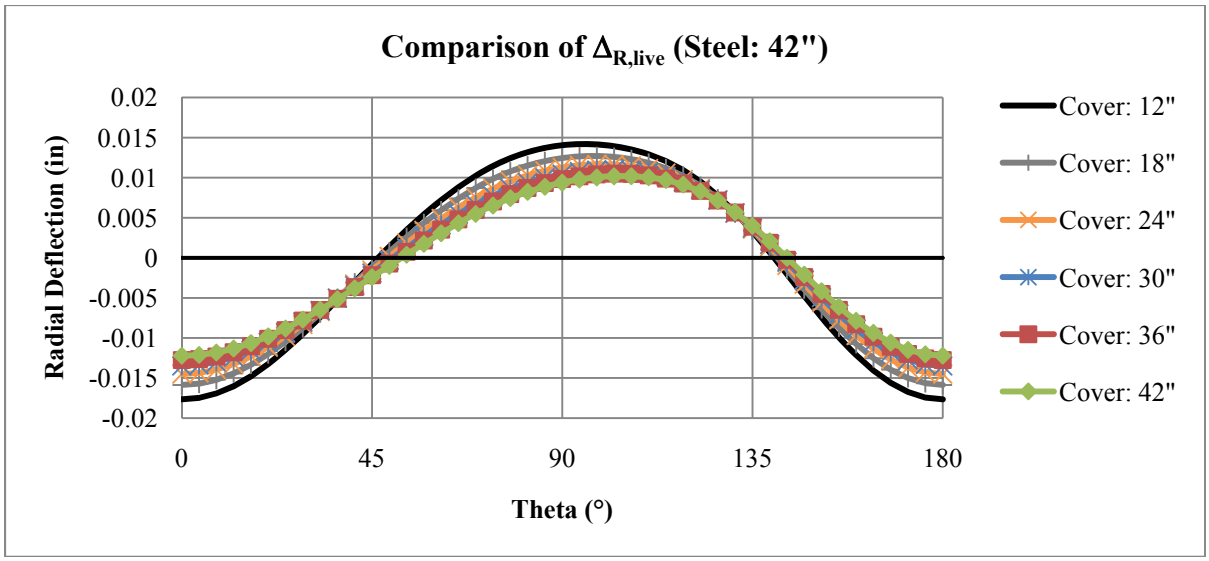

Figure 59
Comparison of $\Delta_{R,live}$ for steel pipe with D = 42 in.

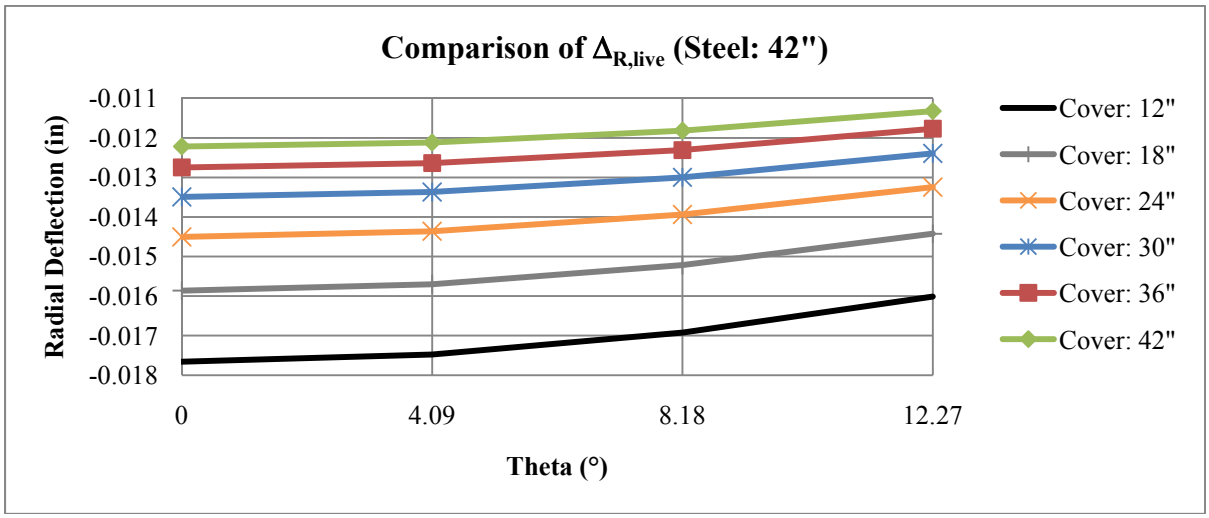

Figure 60
Comparison of $\Delta_{R,live}$ for steel pipe with D = 42 in.: zoom view

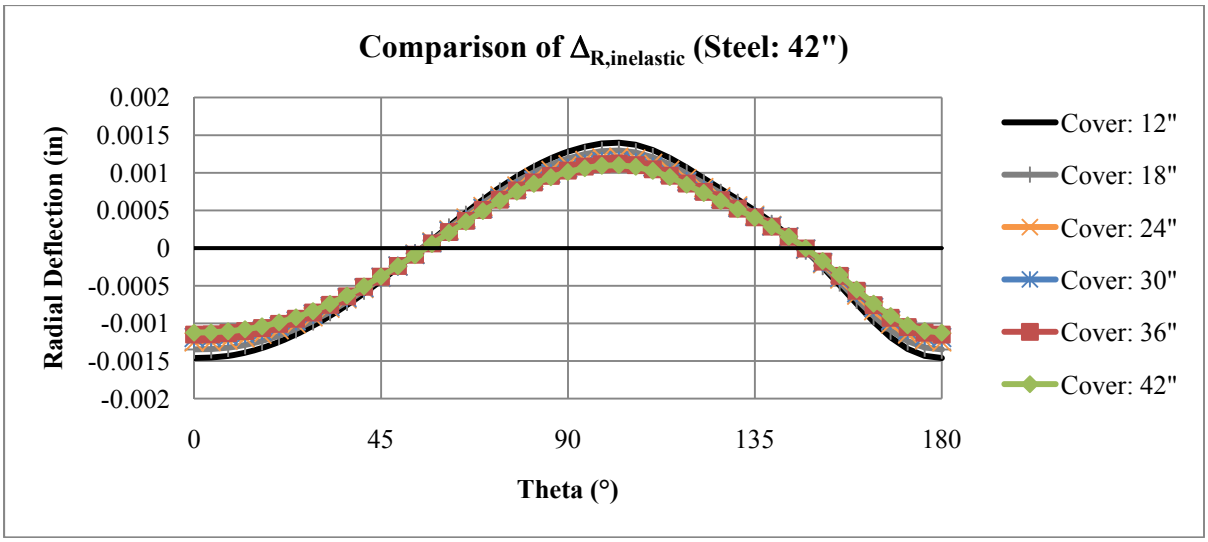

Figure 61
Comparison of $\Delta_{R,inelastic}$ for steel pipe with D = 42 in.

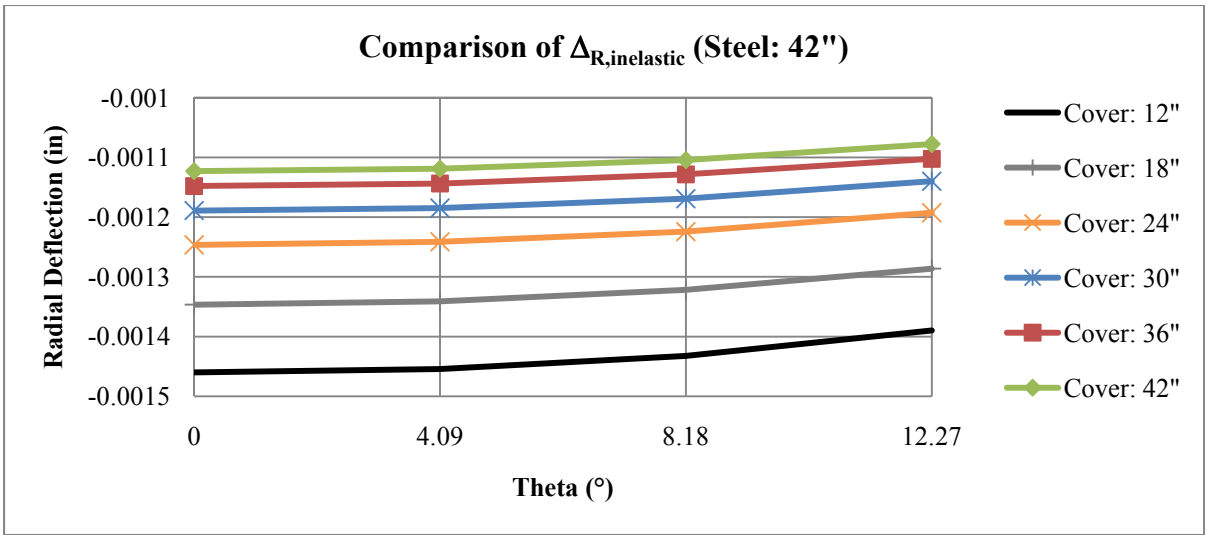

Figure 62
Comparison of $\Delta_{R,inelastic}$ for steel pipe with D = 42 in.: zoom view

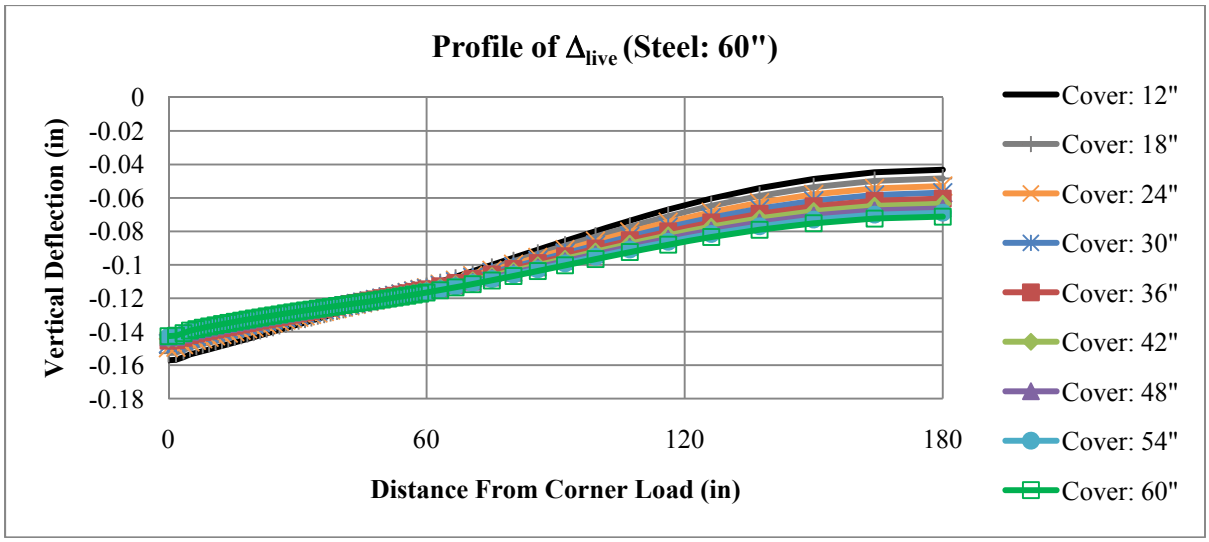

Figure 63
Profile of Δ_{live} for steel pipe with D = 60 in.

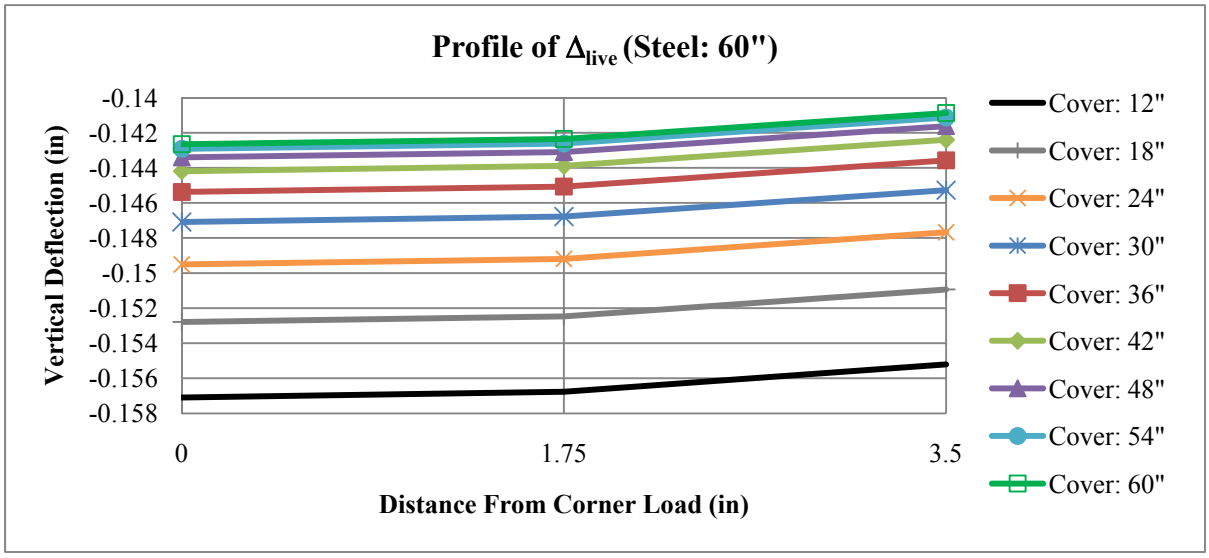

Figure 64
Profile of Δ_{live} for steel pipe with D = 60 in.: zoom view

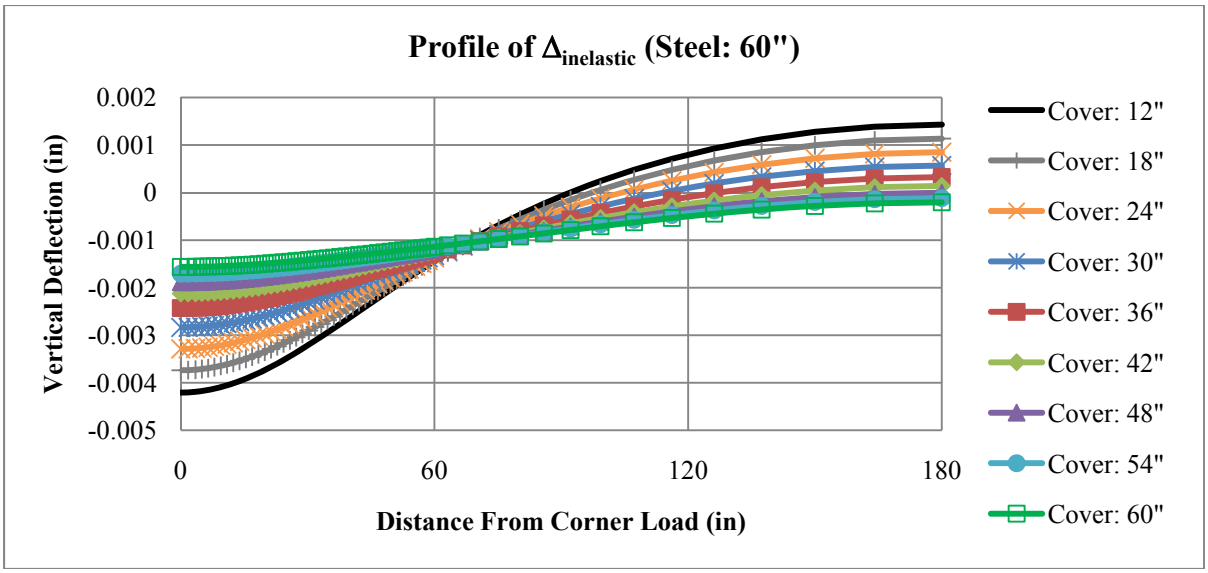

Figure 65
Profile of $\Delta_{inelastic}$ for steel pipe with D = 60 in.

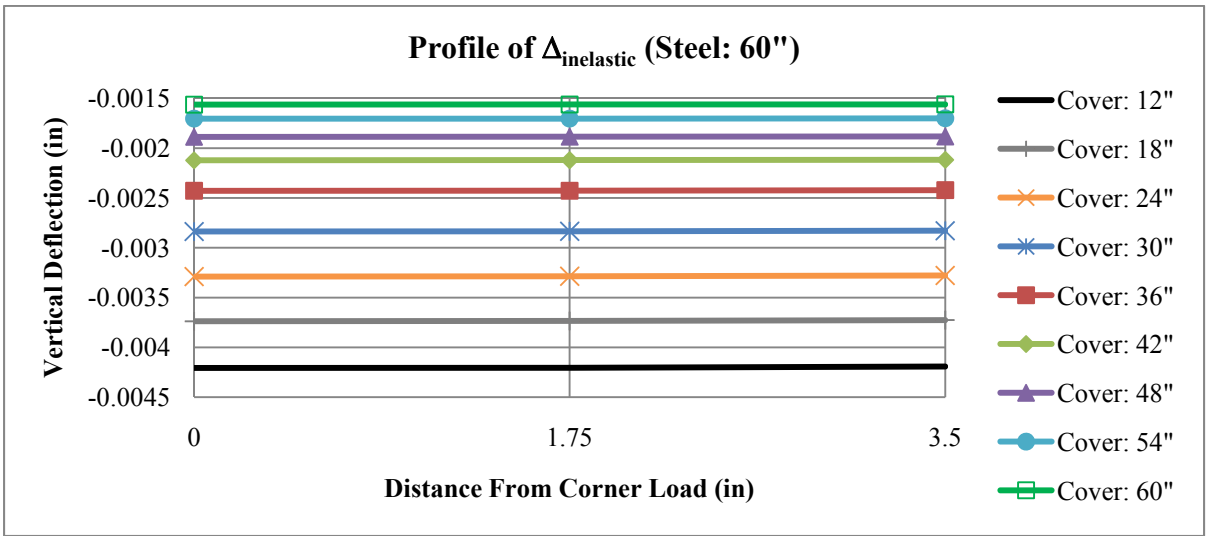

Figure 66
Profile of $\Delta_{inelastic}$ for steel pipe with D = 60 in.: zoom view

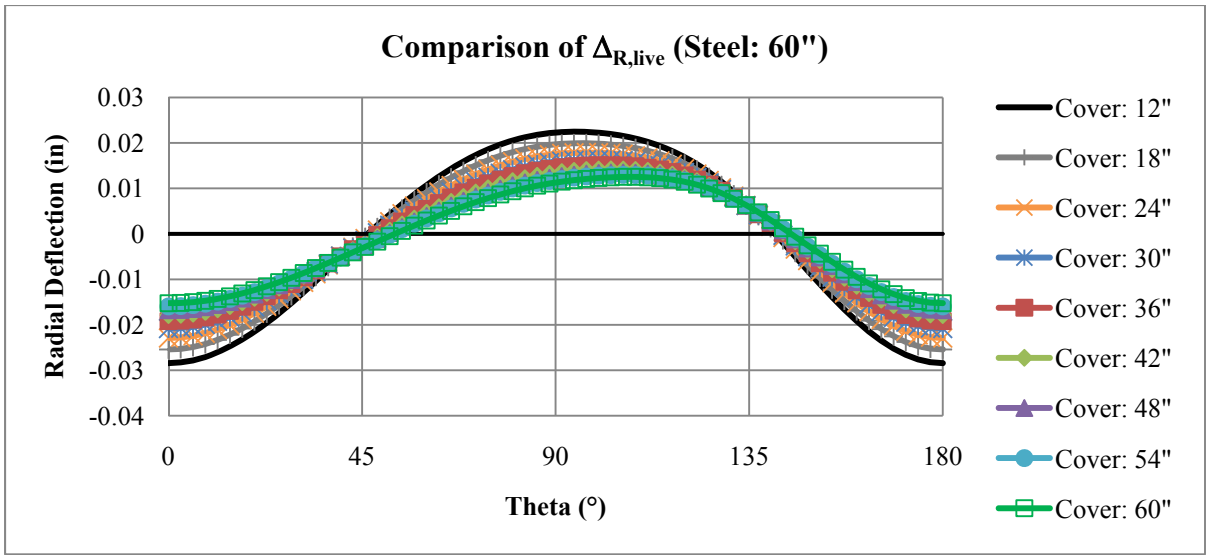

Figure 67
Comparison of $\Delta_{R,live}$ for steel pipe with D = 60 in.

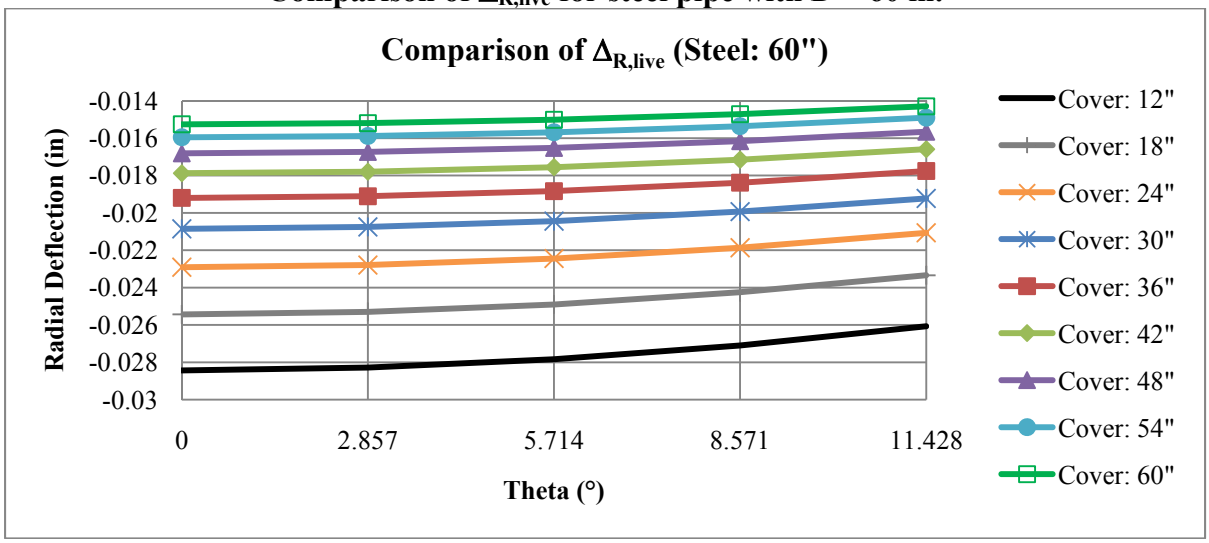

Figure 68
Comparison of $\Delta_{R,live}$ for steel pipe with D = 60 in.: zoom view

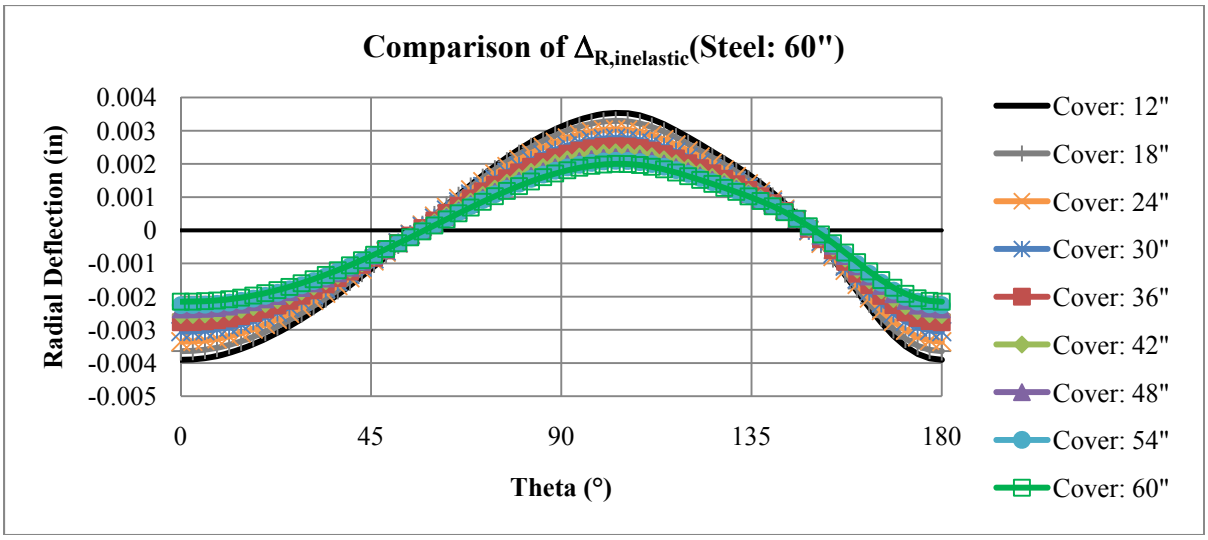

Figure 69
Comparison of $\Delta_{R,inelastic}$ for steel pipe with D = 60 in.

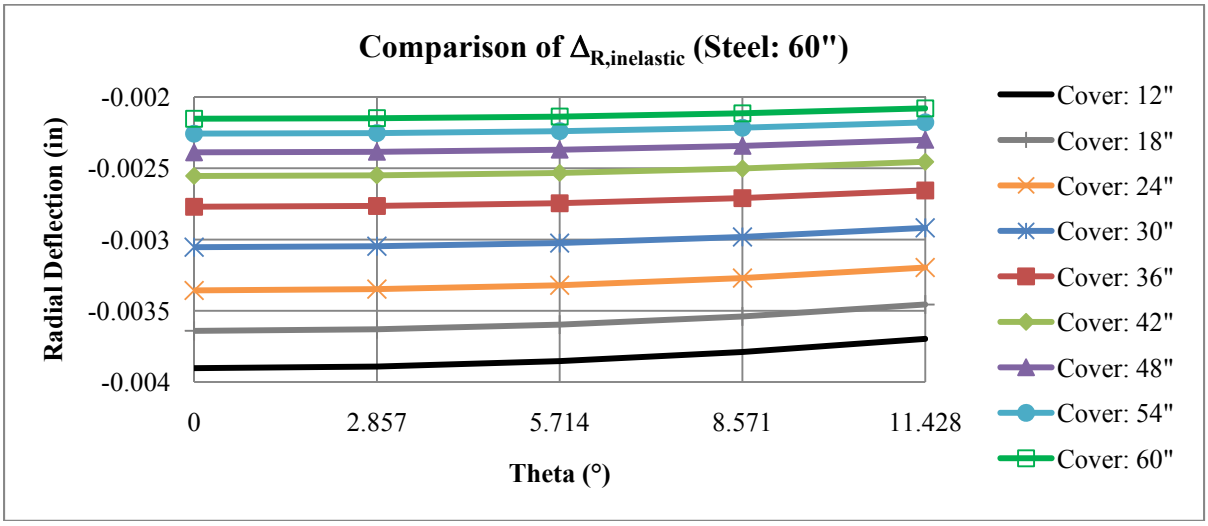

Figure 70
Comparison of $\Delta_{R,inelastic}$ for steel pipe with D = 60 in.: zoom view

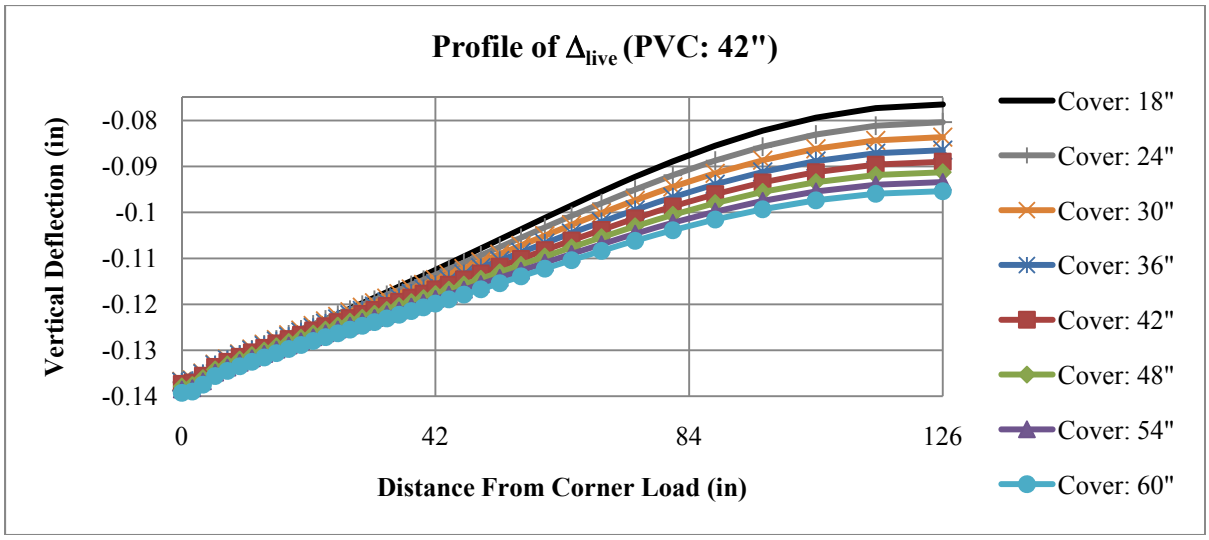

Figure 71
Profile of Δ_{live} for PVC pipe with D = 42 in.

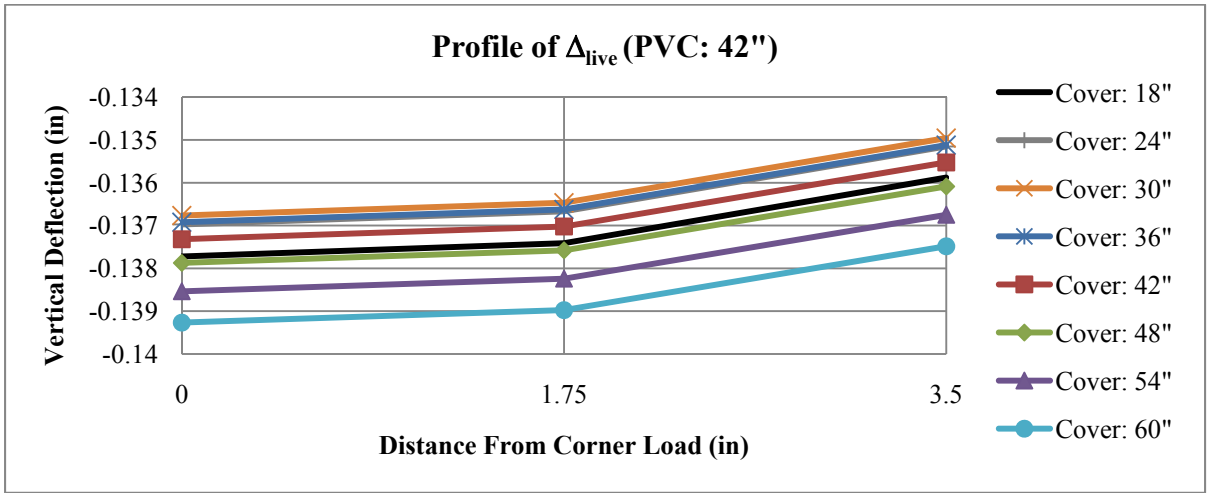

Figure 72
Profile of Δ_{live} for PVC pipe with D = 42 in.: zoom view

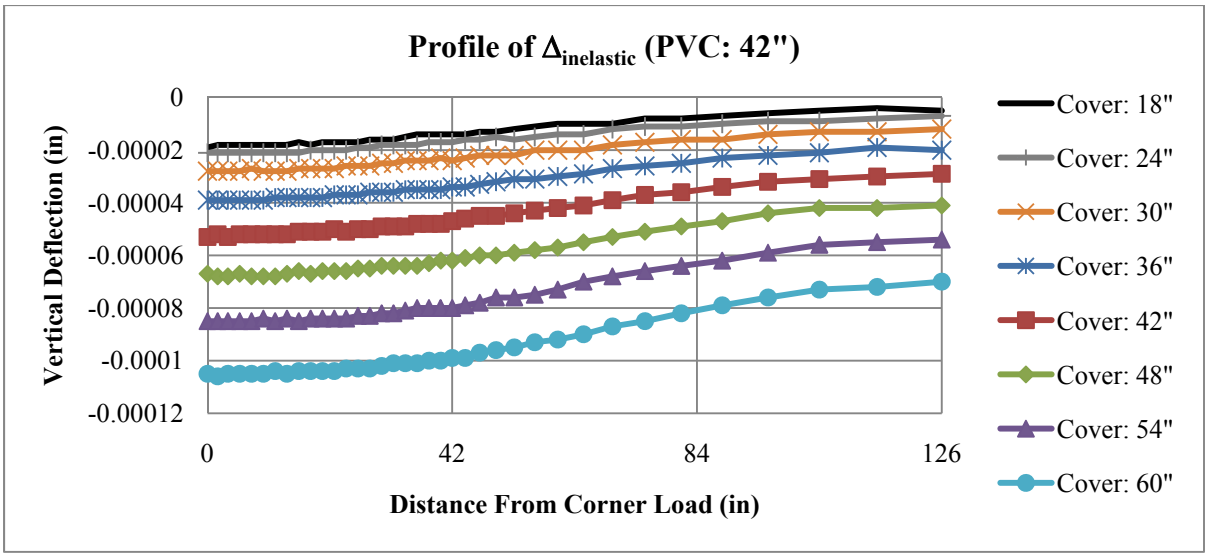

Figure 73
Profile of $\Delta_{inelastic}$ for PVC pipe with D = 42 in.

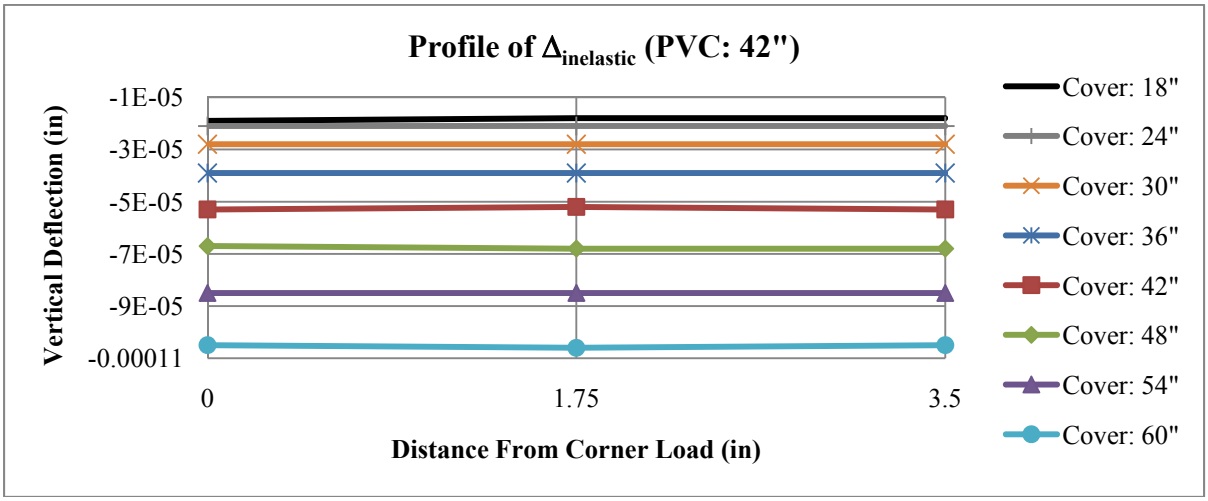

Figure 74
Profile of $\Delta_{inelastic}$ for PVC pipe with D = 42 in.: zoom view

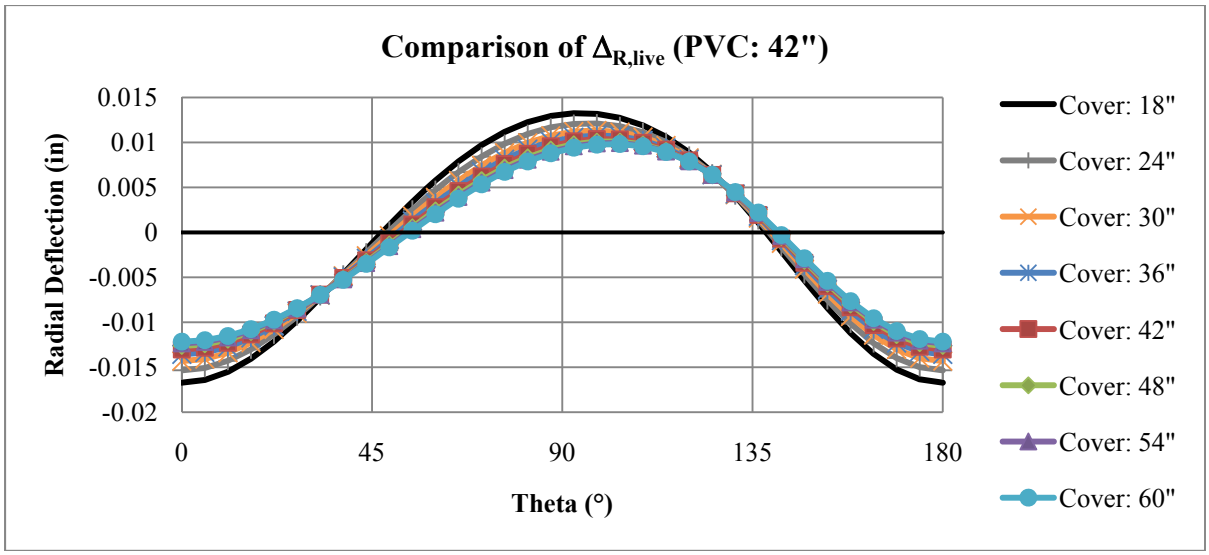

Figure 75
Comparison of $\Delta_{R,live}$ for PVC pipe with D = 42 in.

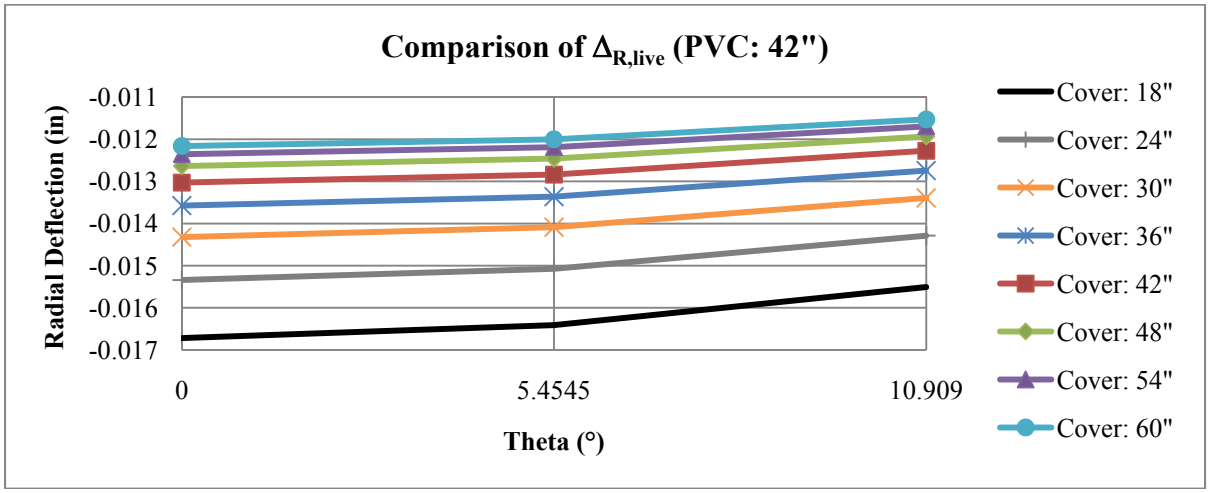

Figure 76
Comparison of $\Delta_{R,live}$ for PVC pipe with D = 42 in.: zoom view

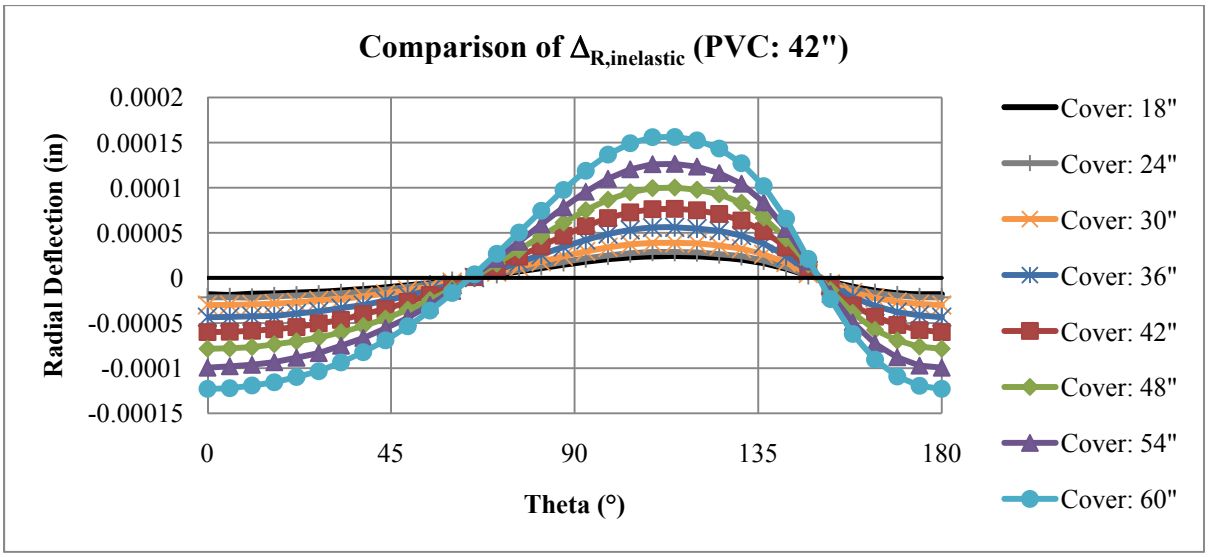

Figure 77
Comparison of $\Delta_{R,inelastic}$ for PVC pipe with D = 42 in.

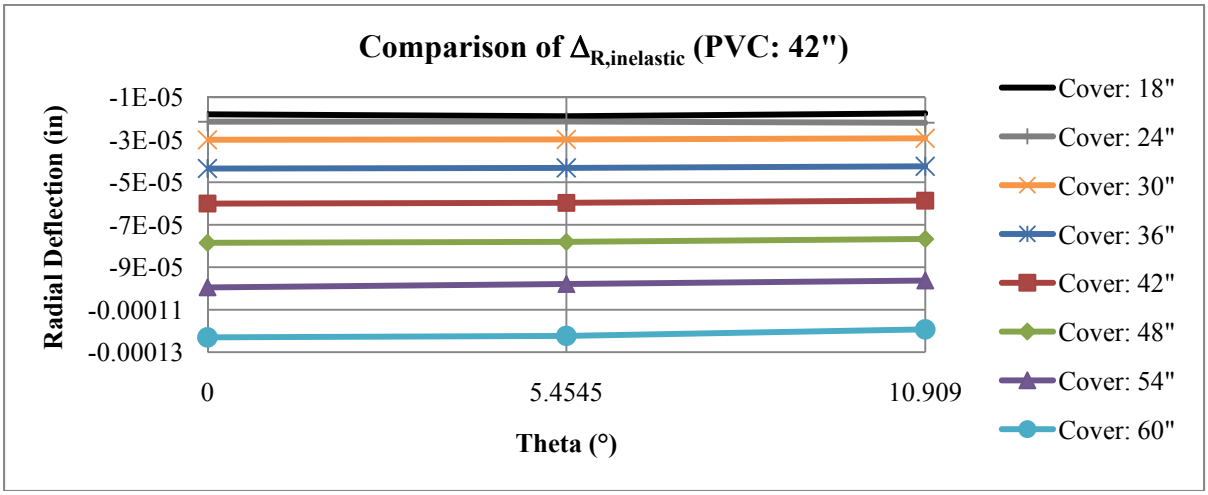

Figure 78
Comparison of $\Delta_{R,inelastic}$ for PVC pipe with D = 42 in.: zoom view

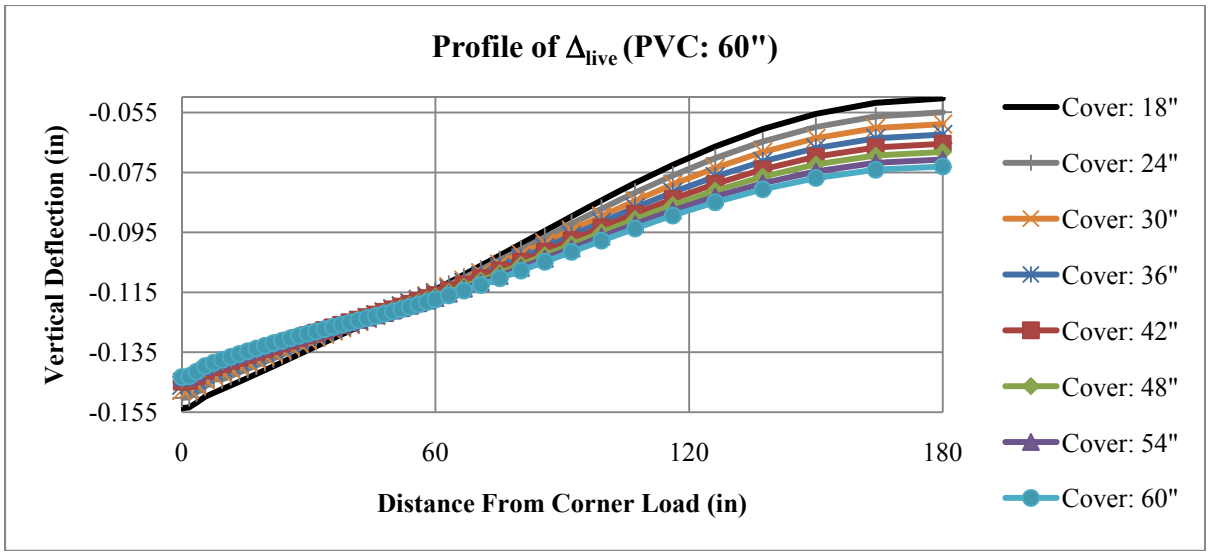

Figure 79
Profile of Δ_{live} for PVC pipe with D = 60 in.

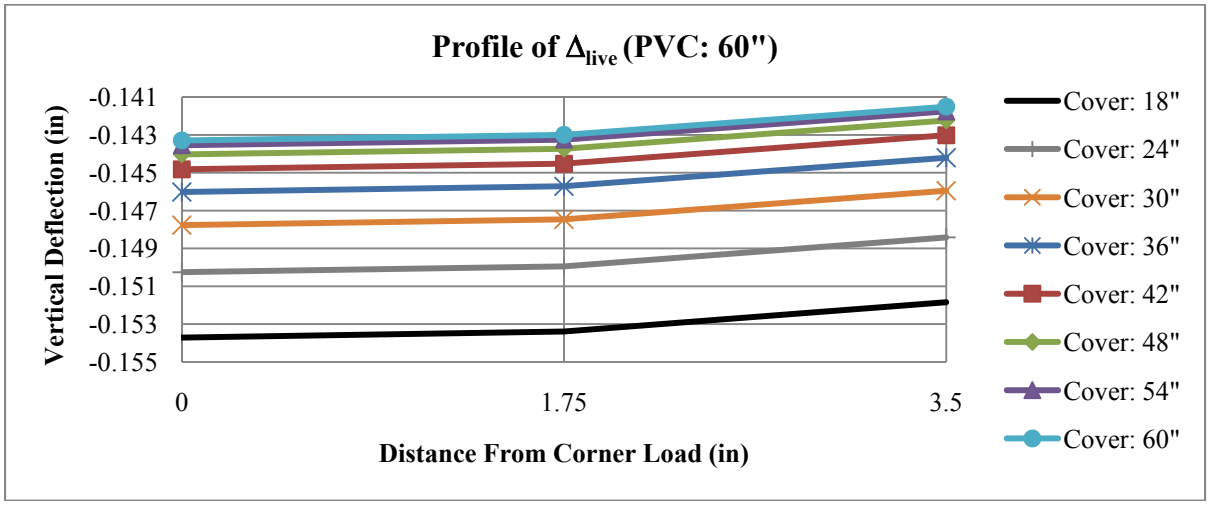

Figure 80
Profile of Δ_{live} for PVC pipe with D = 60 in.: zoom view

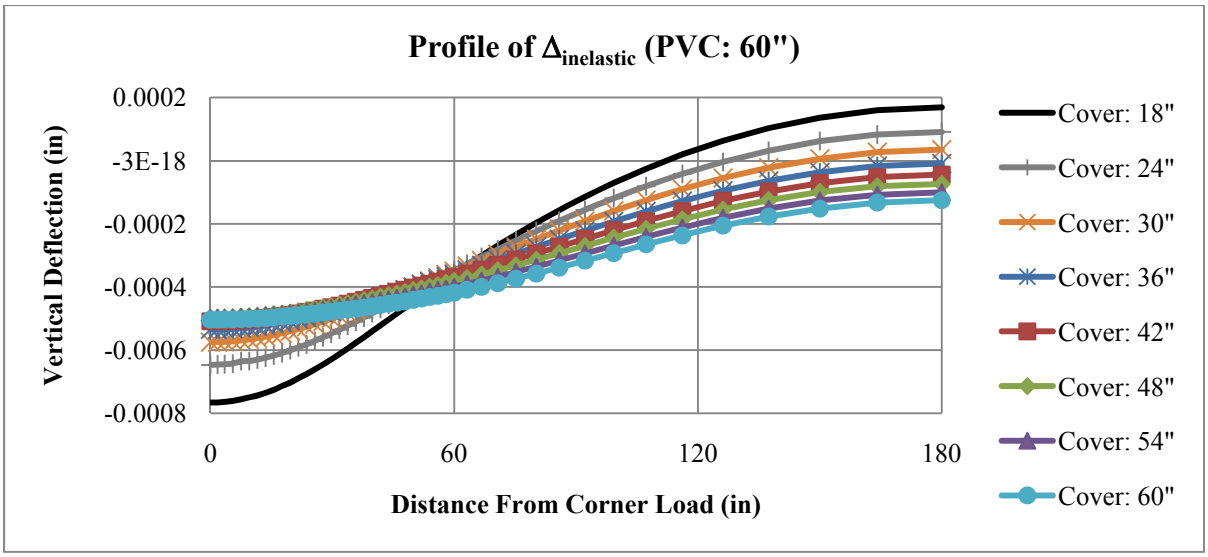

Figure 81
Profile of $\Delta_{inelastic}$ for PVC pipe with D = 60 in.

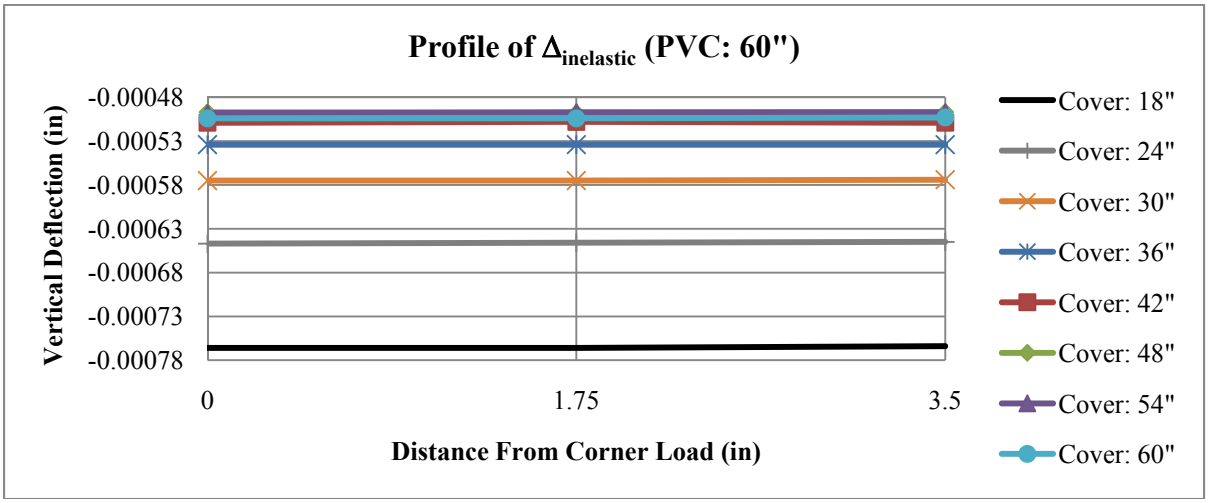

Figure 82
Profile of $\Delta_{inelastic}$ for PVC pipe with D = 60 in.: zoom view

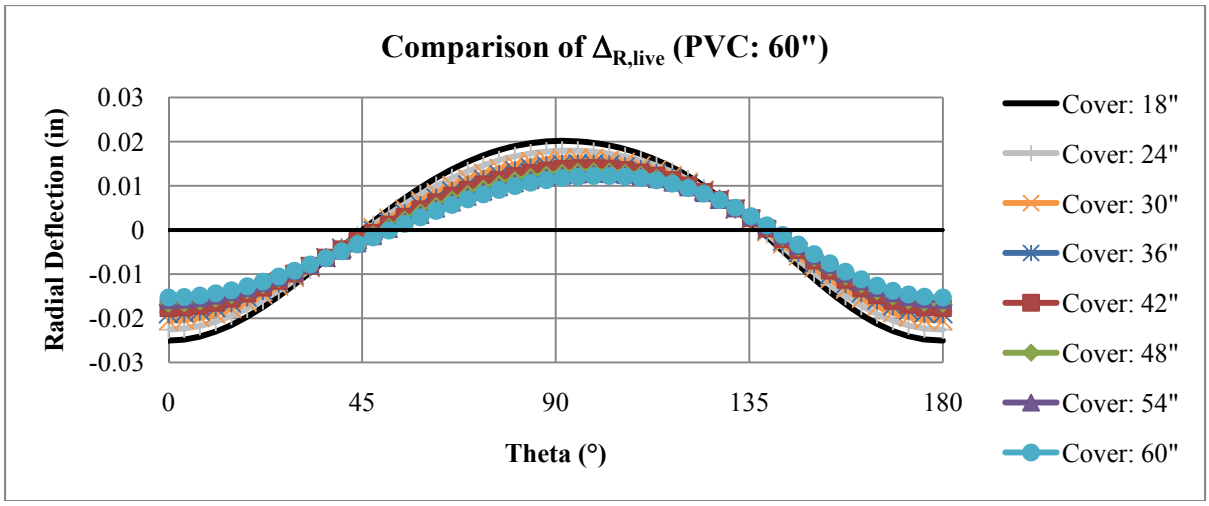

Figure 83
Comparison of $\Delta_{R,live}$ for PVC pipe with D = 60 in.

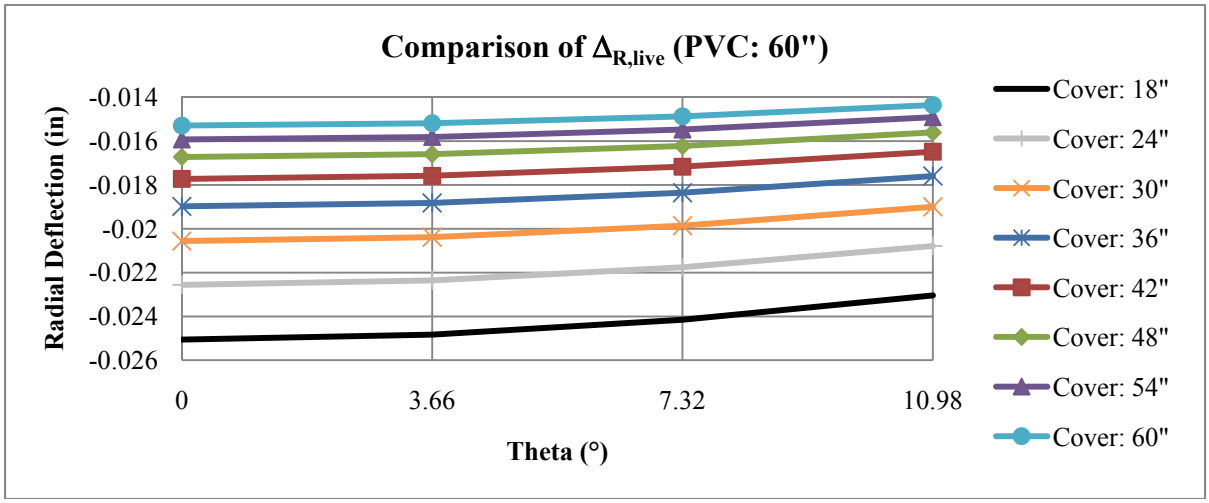

Figure 84
Comparison of $\Delta_{R,live}$ for PVC pipe with D = 60 in.: zoom view

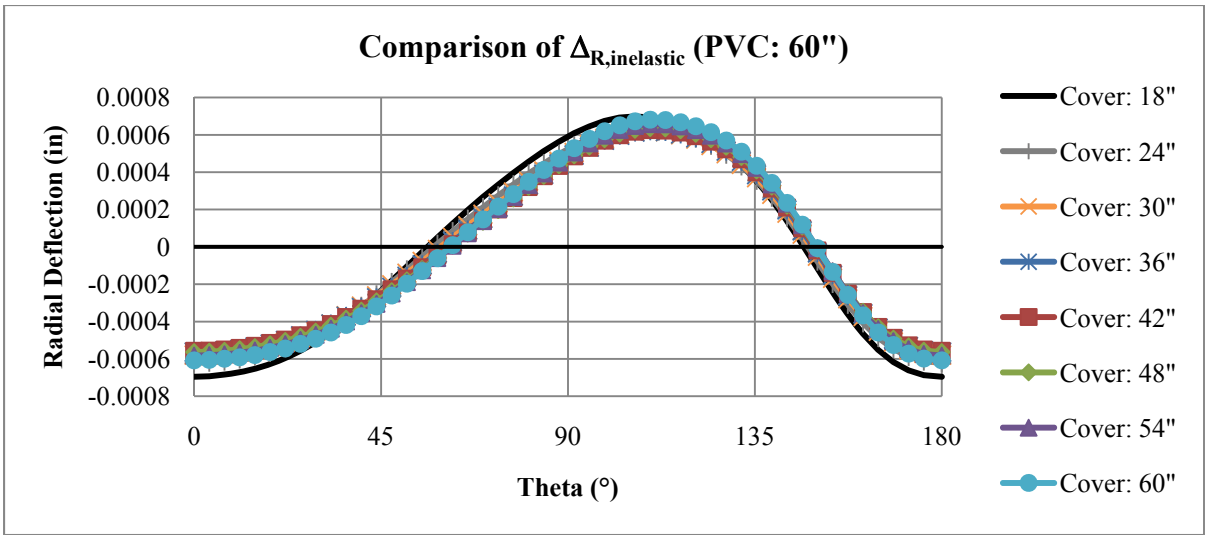

Figure 85
Comparison of $\Delta_{R,inelastic}$ for PVC pipe with D = 60 in.

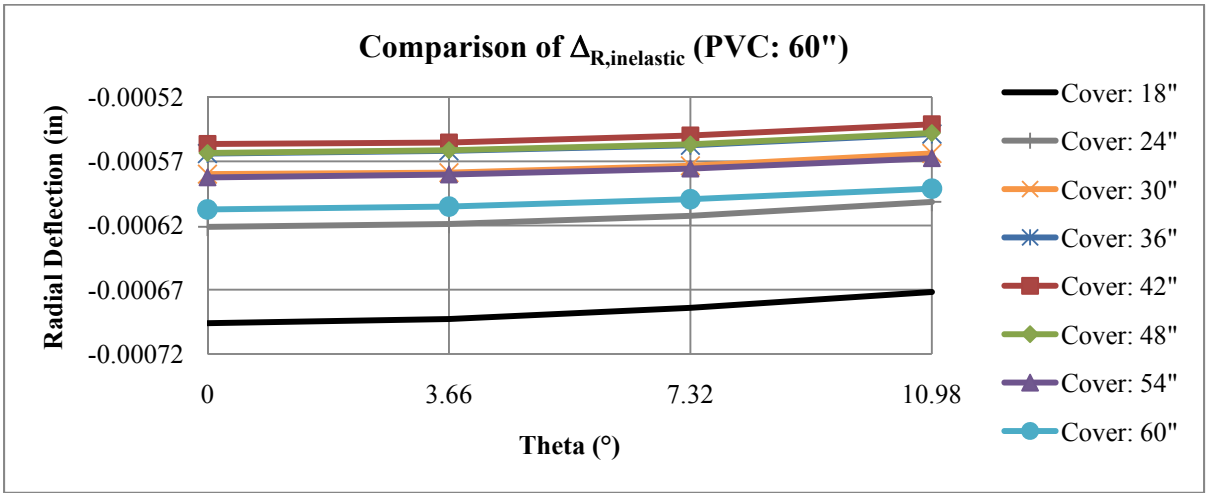

Figure 86
Comparison of $\Delta_{R,inelastic}$ for PVC pipe with D = 60 in.: zoom view

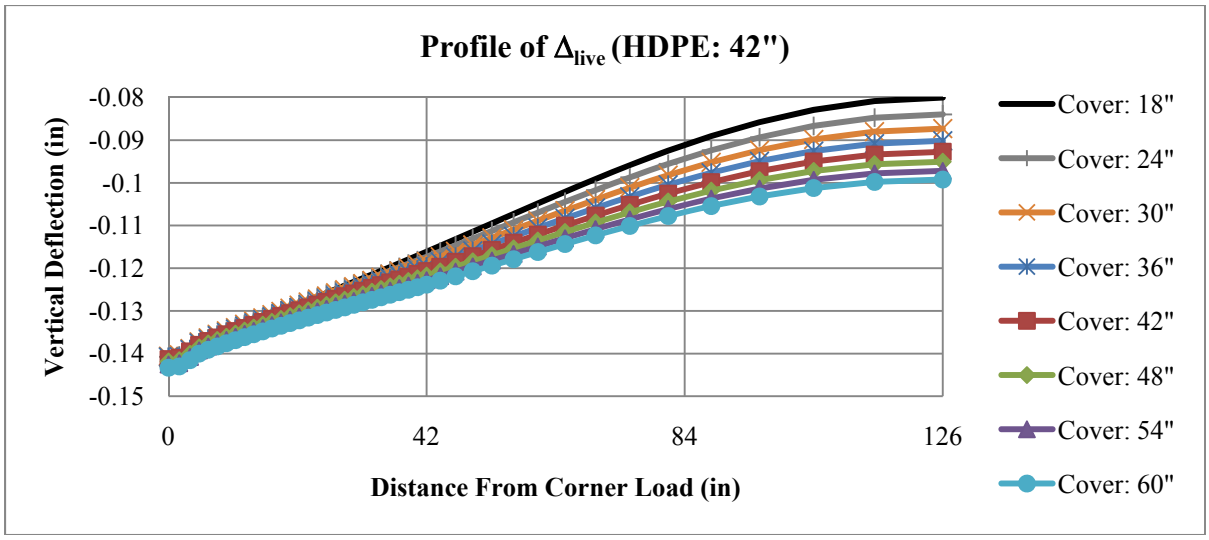

Figure 87
Profile of Δ_{live} for HDPE pipe with D = 42 in.

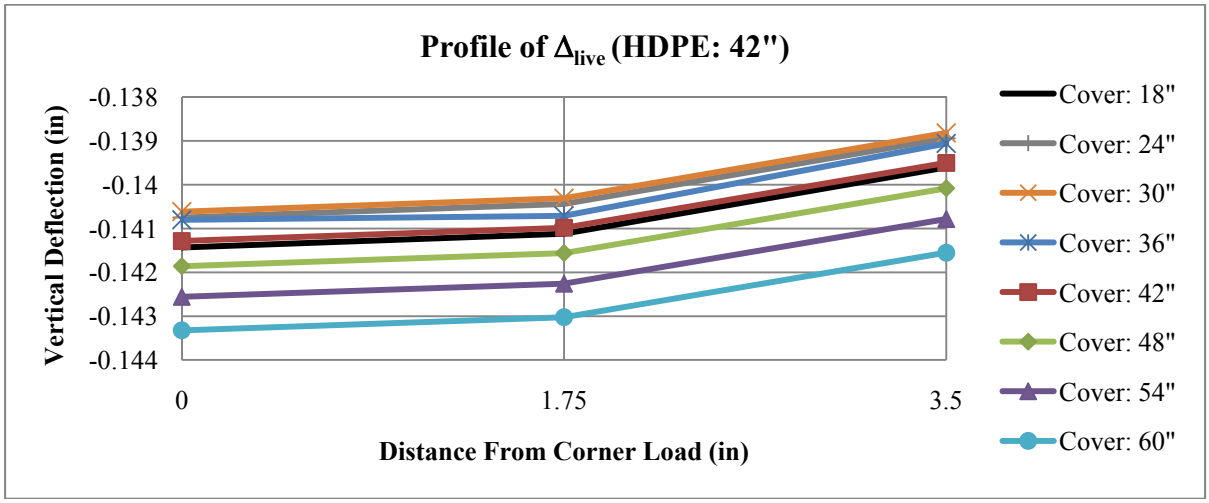

Figure 88
Profile of Δ_{live} for HDPE pipe with D = 42 in.: zoom view

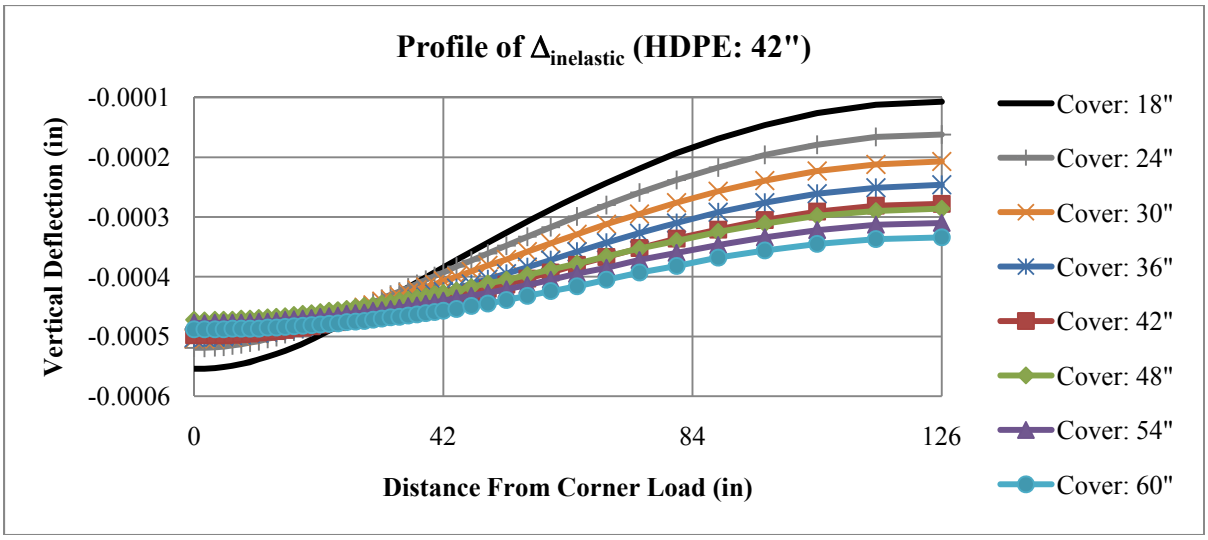

Figure 89
Profile of $\Delta_{inelastic}$ for HDPE pipe with D = 42 in.

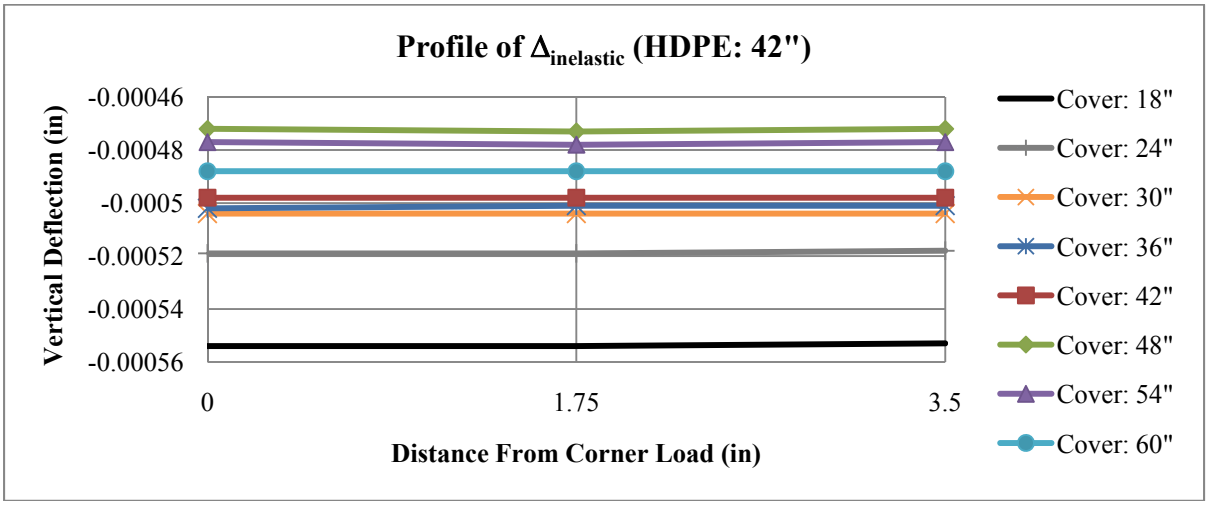

Figure 90
Profile of $\Delta_{inelastic}$ for HDPE pipe with D = 42 in.: zoom view

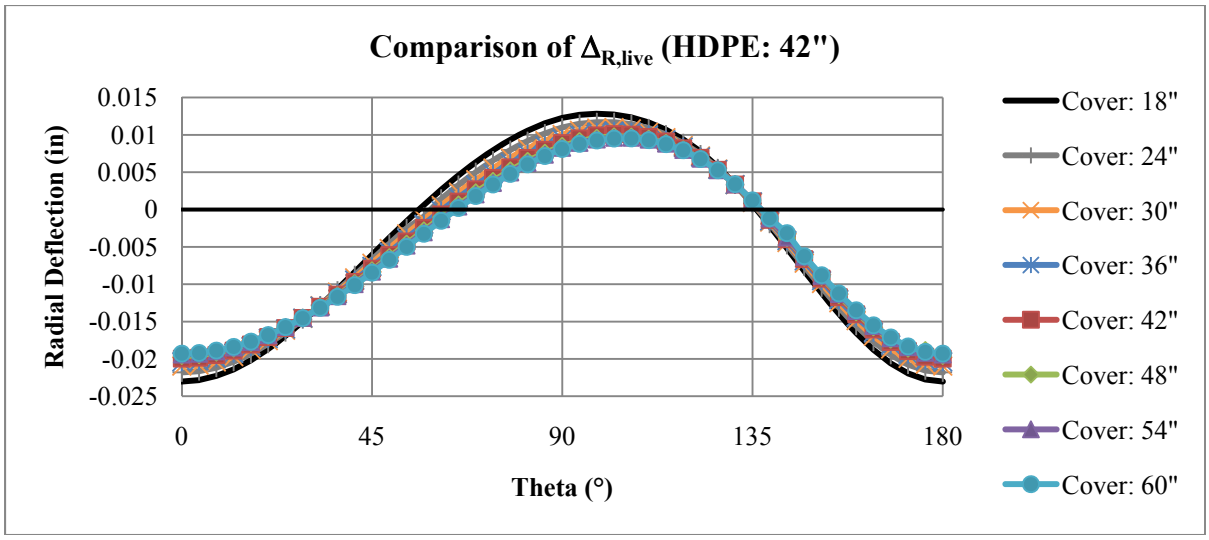

Figure 91
Comparison of $\Delta_{R,live}$ for HDPE pipe with D = 42 in.

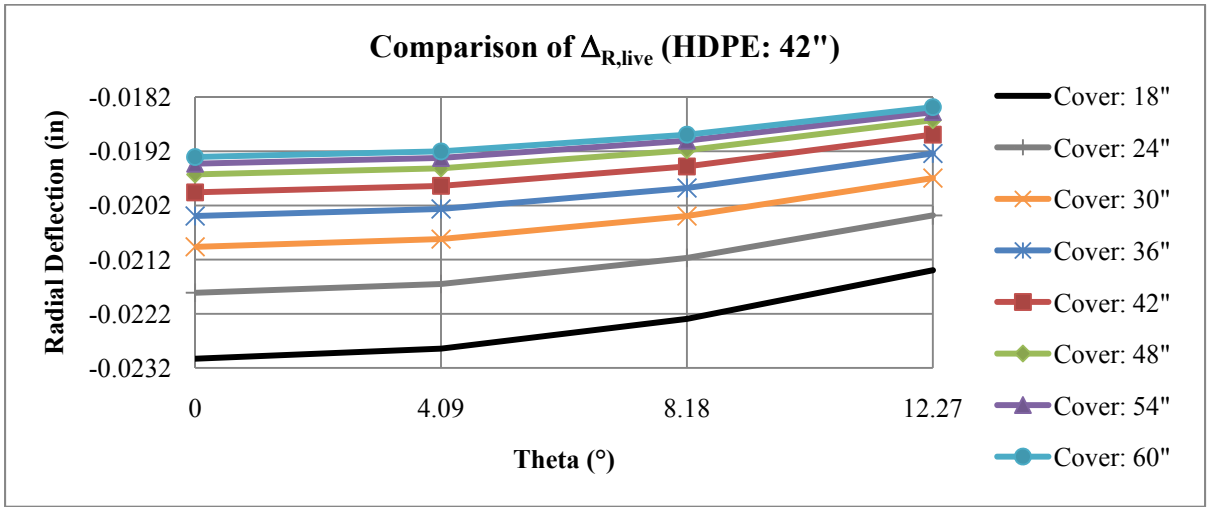

Figure 92
Comparison of $\Delta_{R,live}$ for HDPE pipe with D = 42 in.: zoom view

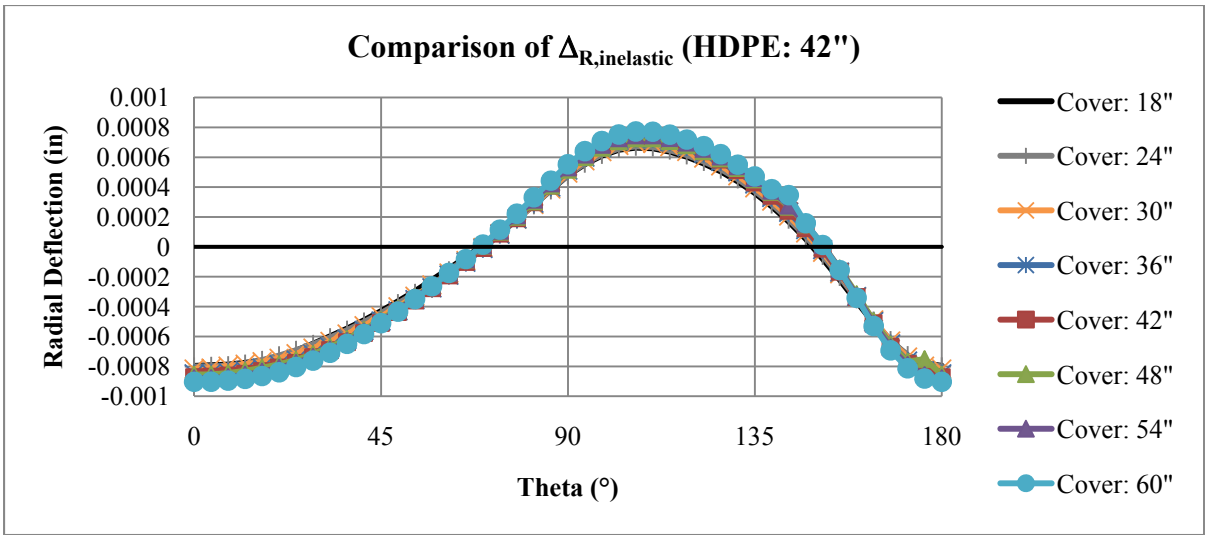

Figure 93
Comparison of $\Delta_{R,inelastic}$ for HDPE pipe with D = 42 in.

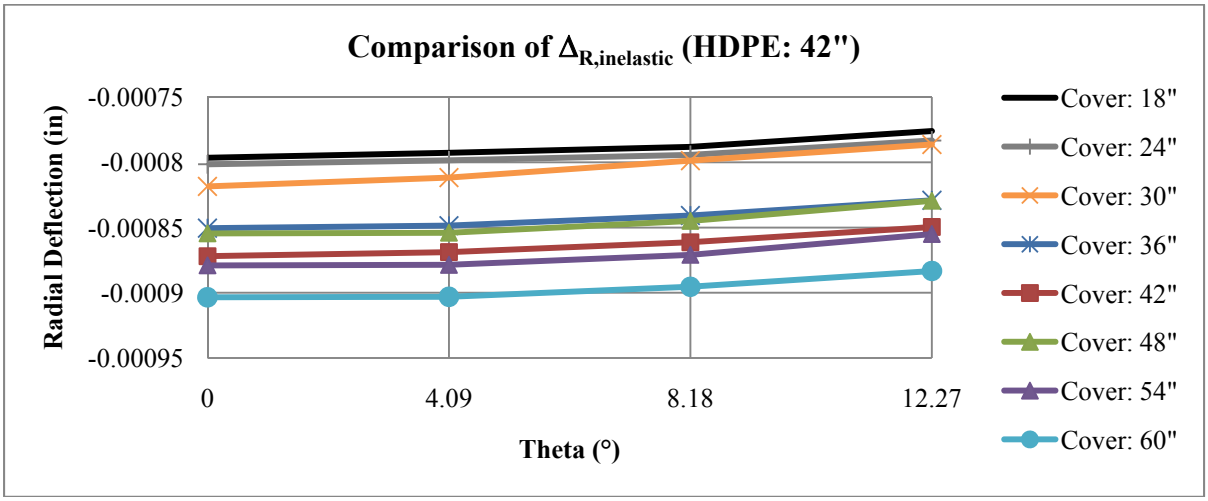

Figure 94
Comparison of $\Delta_{R,inelastic}$ for HDPE pipe with D = 42 in.: zoom view

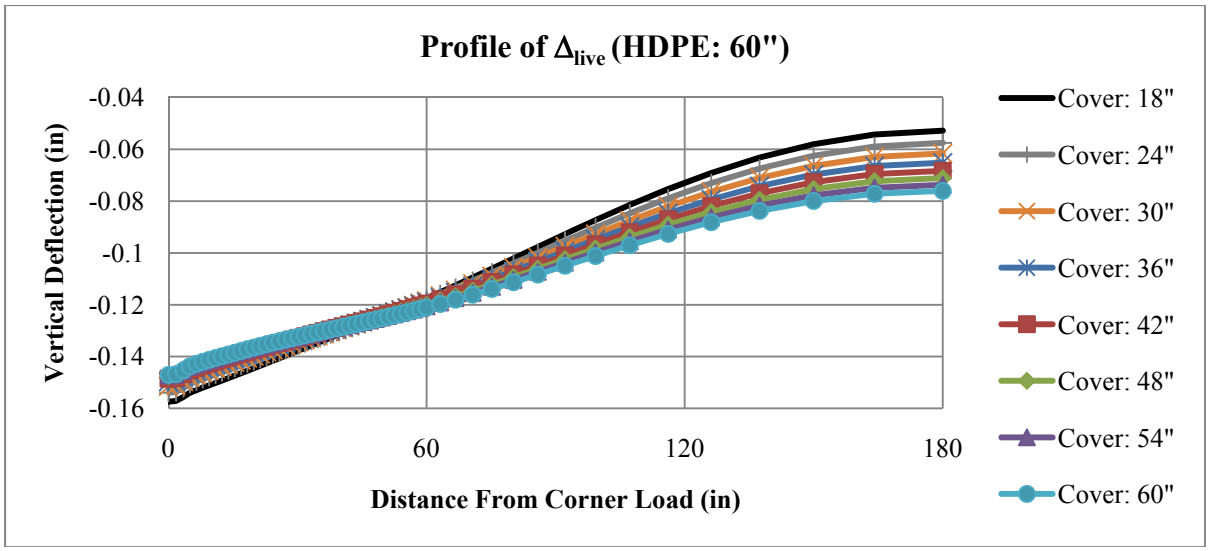

Figure 95
Profile of Δ_{live} for HDPE pipe with D = 60 in.

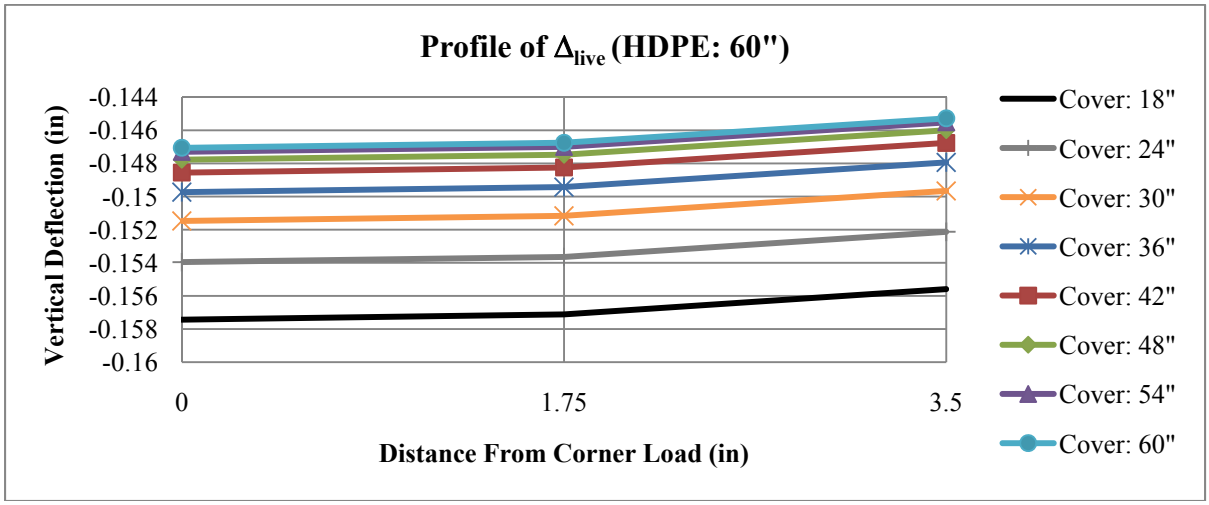

Figure 96
Profile of Δ_{live} for HDPE pipe with D = 60 in.: zoom view

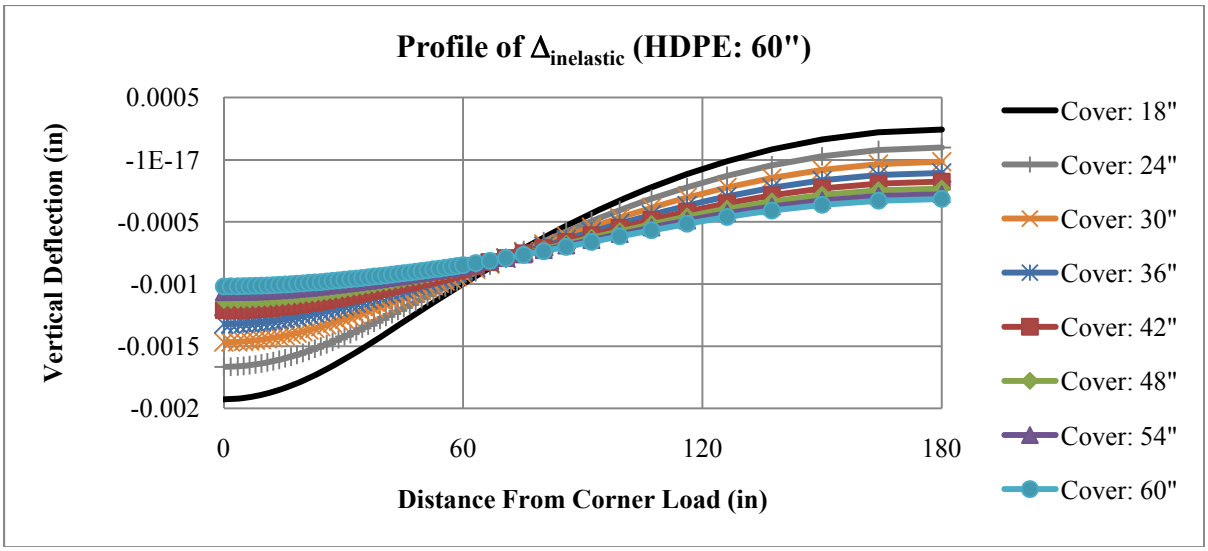

Figure 97
Profile of $\Delta_{inelastic}$ for HDPE pipe with D = 60 in.

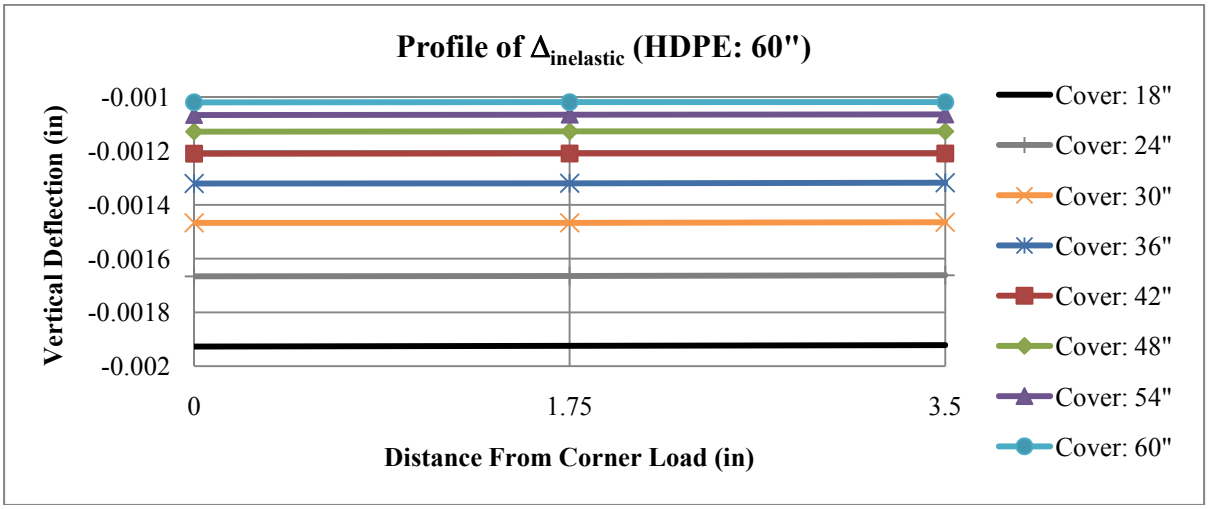

Figure 98
Profile of $\Delta_{inelastic}$ for HDPE pipe with D = 60 in.: zoom view

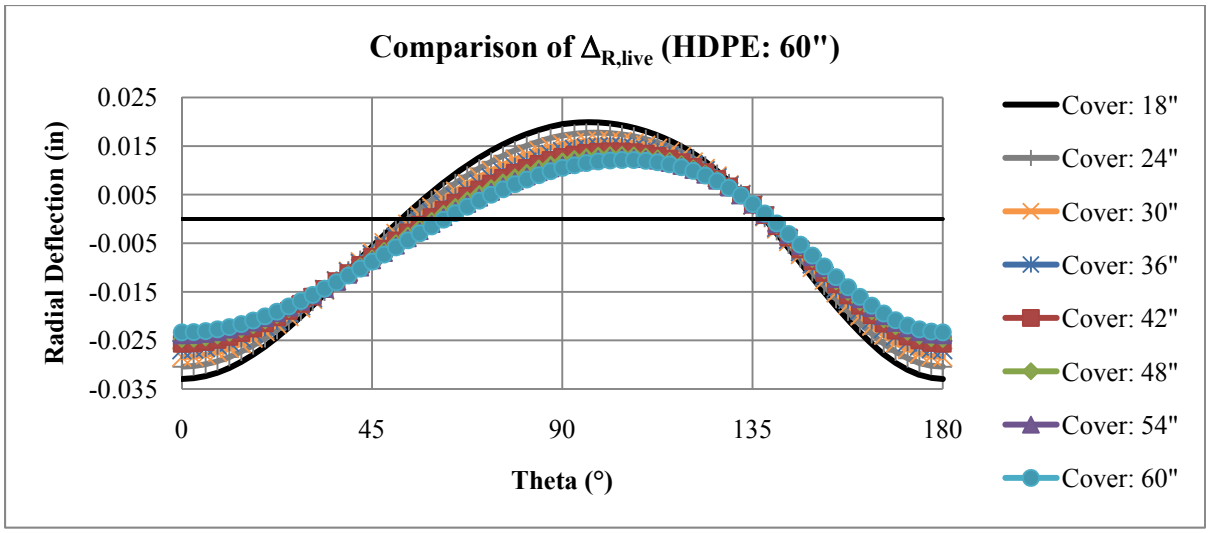

Figure 99
Comparison of $\Delta_{R,live}$ for HDPE pipe with D = 60 in.

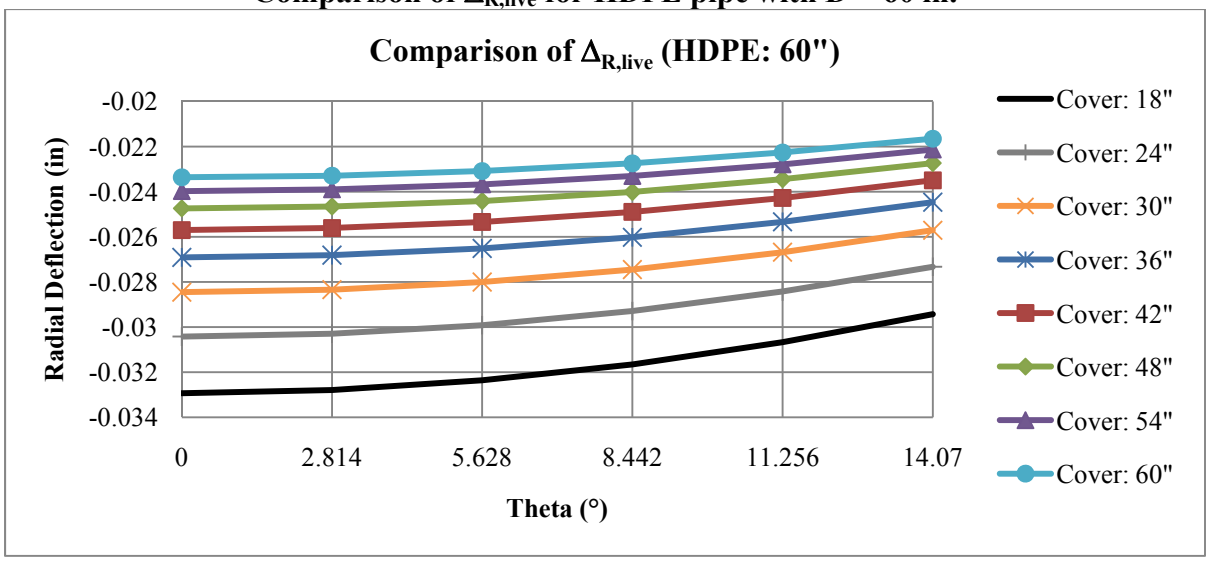

Figure 100
Comparison of $\Delta_{R,live}$ for HDPE pipe with D = 60 in.: zoom view

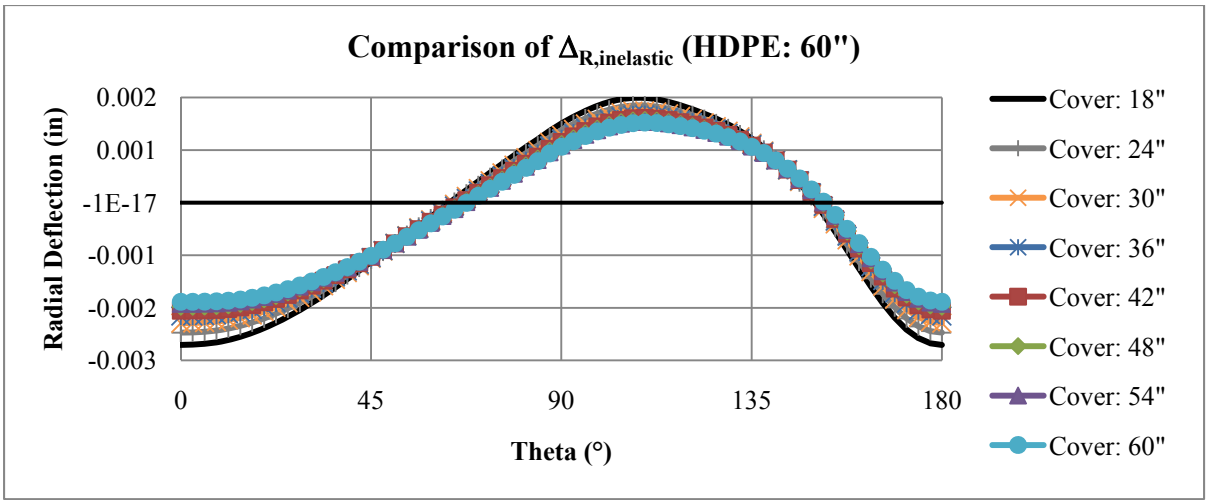

Figure 101
Comparison of $\Delta_{R,inelastic}$ for HDPE pipe with D = 60 in.

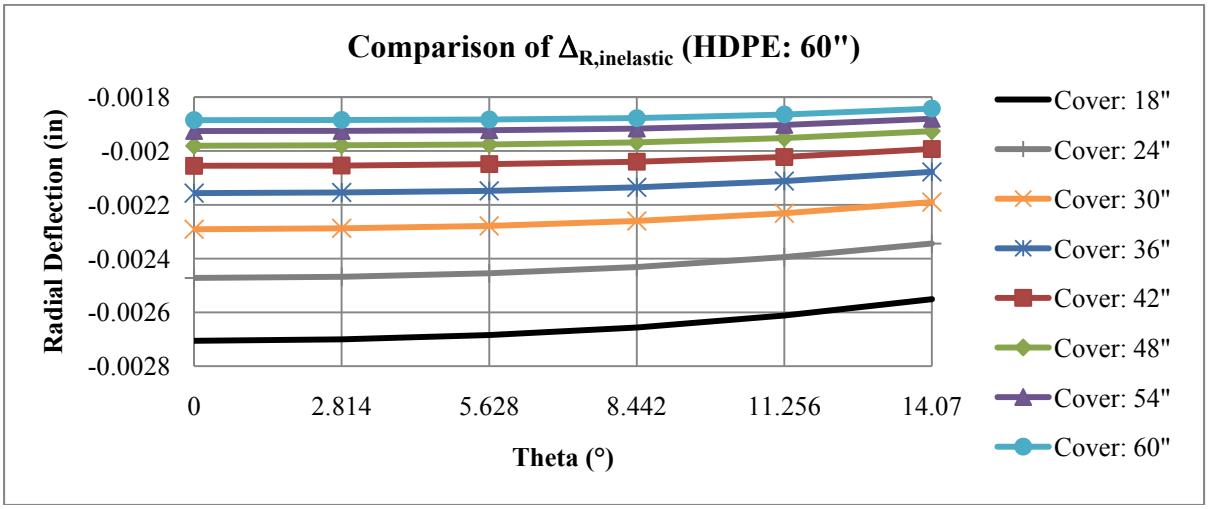

Figure 102
Comparison of $\Delta_{R,inelastic}$ for HDPE pipe with D = 60 in.: zoom view

APPENDIX B

Comparison of Results from Optimal Cover vs. Minimal Cover

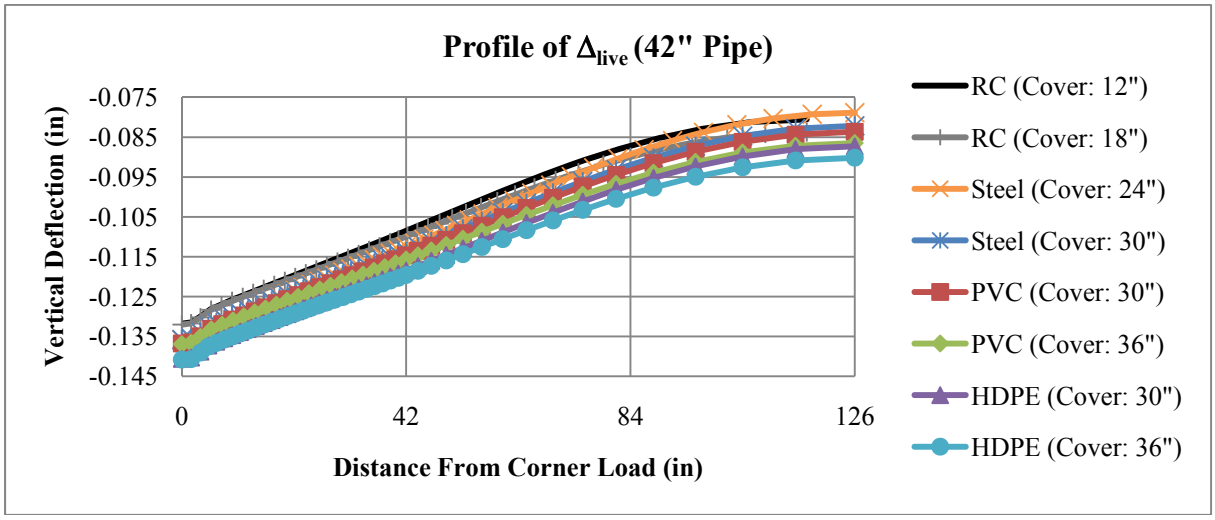

Figure 103

Profile of Δ_{live} for pipes with D = 42 in.

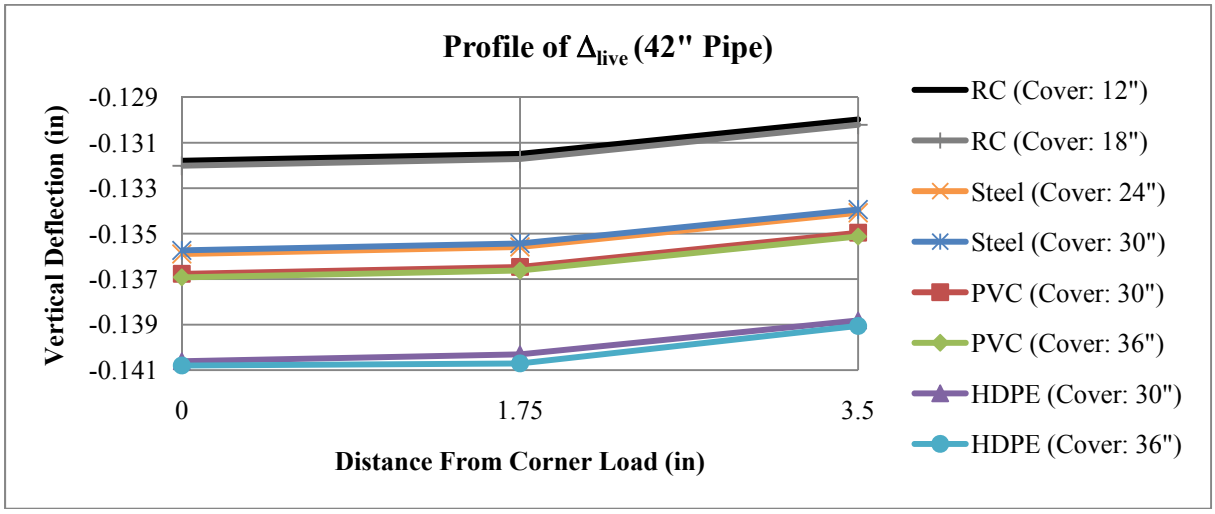

Figure 104

Profile of Δ_{live} for pipes with D = 42 in.: zoom view

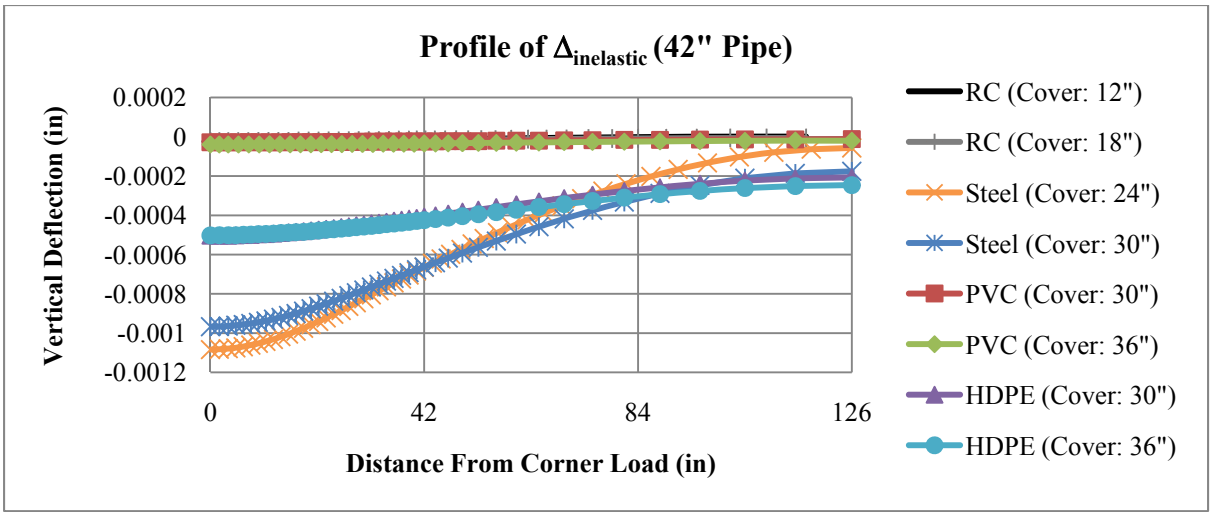

Figure 105
Profile of $\Delta_{inelastic}$ for pipes with D = 42 in.

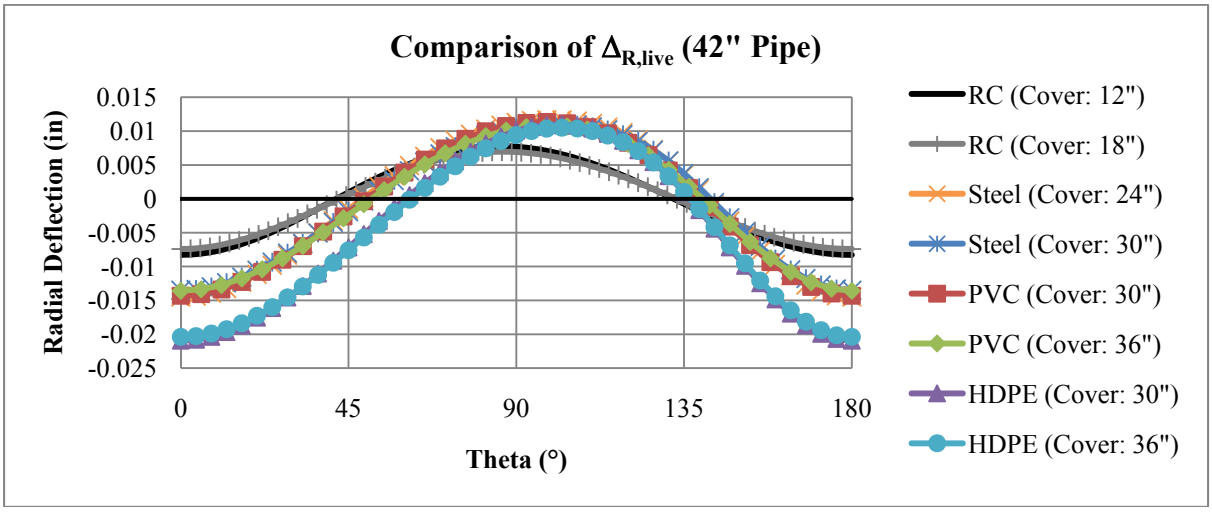

Figure 106
Comparison of $\Delta_{R,live}$ for pipes with D = 42 in.

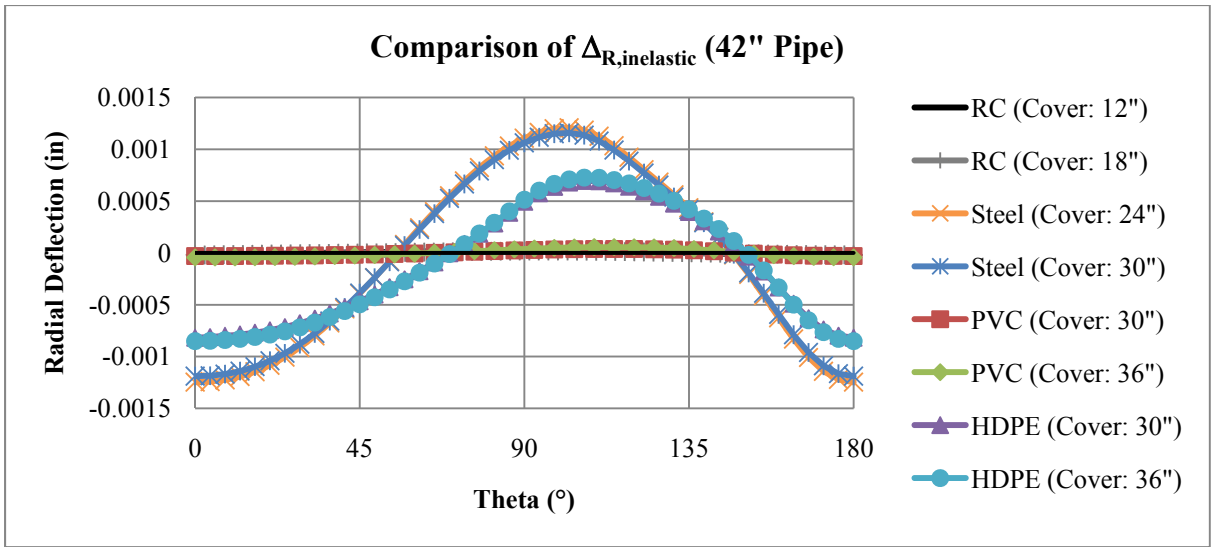

Figure 107
Comparison of $\Delta_{R,inelastic}$ for pipes with D = 42 in.

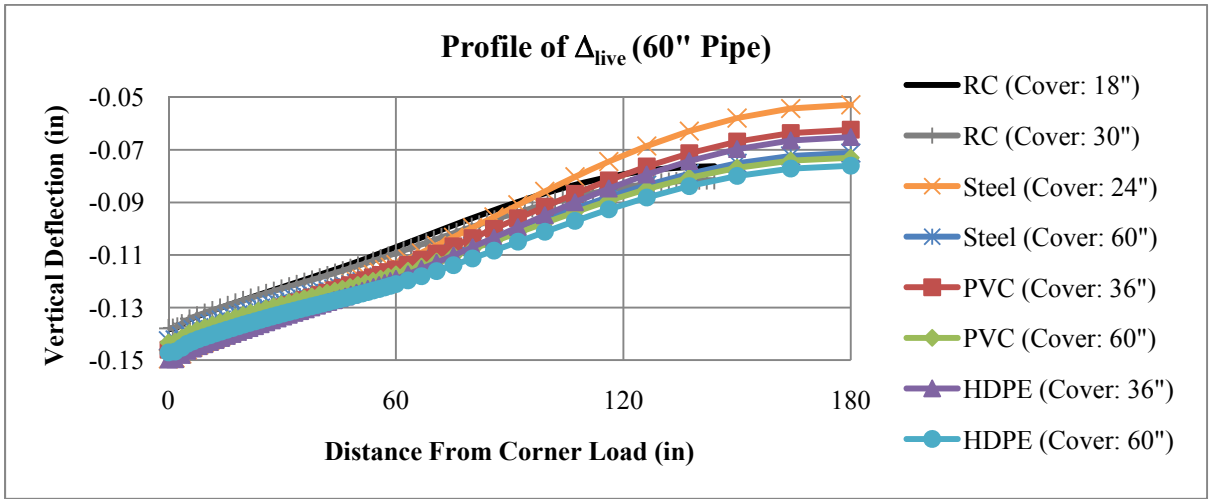

Figure 108
Profile of Δ_{live} for pipes with D = 60 in.

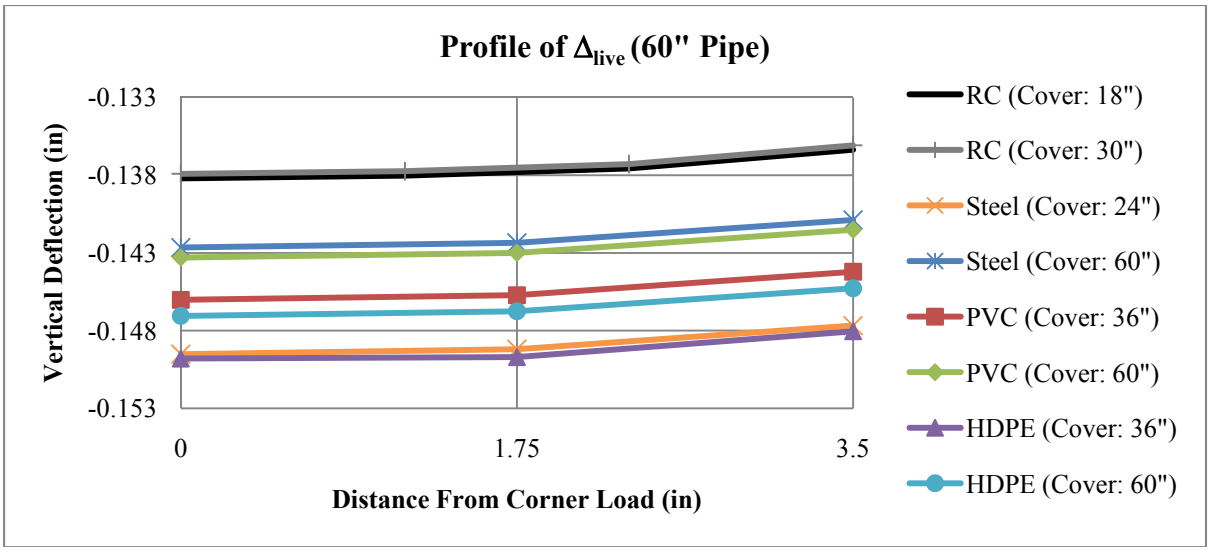

Figure 109
Profile of Δ_{live} for pipes with D = 60 in.: zoom view

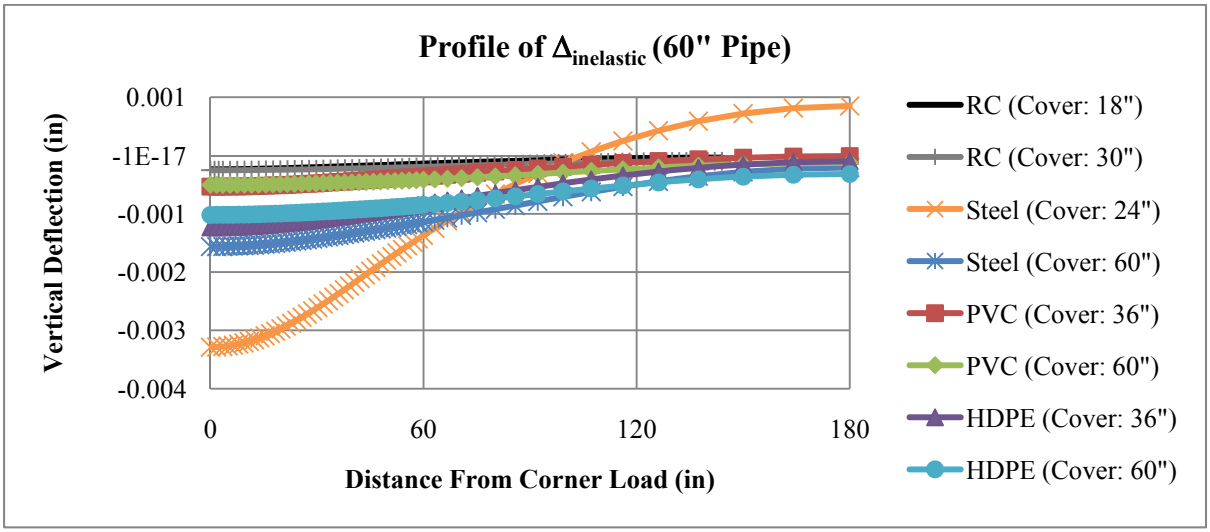

Figure 110
Profile of $\Delta_{inelastic}$ for pipes with D = 60 in.

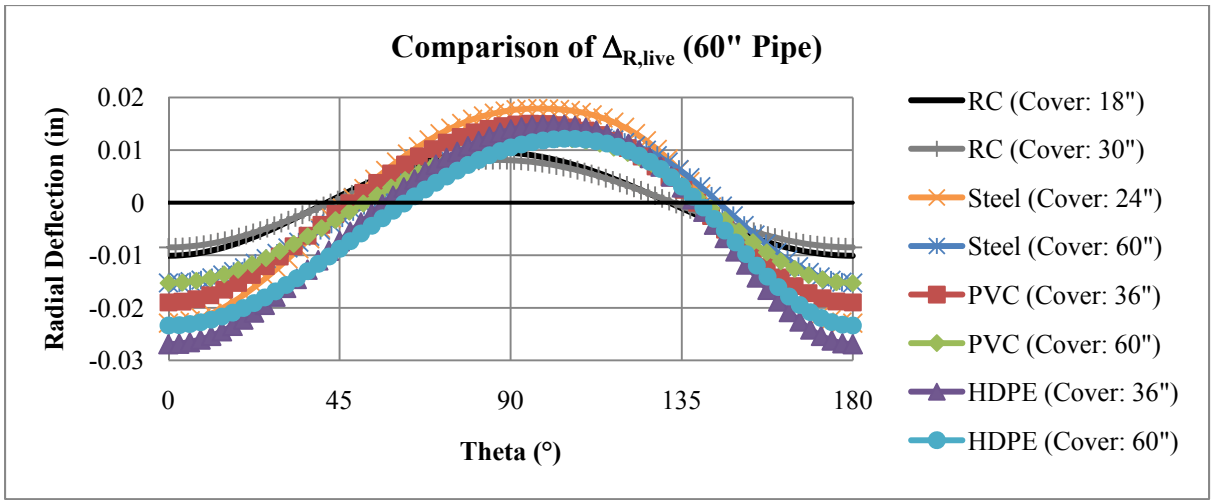

Figure 111
Comparison of $\Delta_{R,live}$ for pipes with D = 60 in.

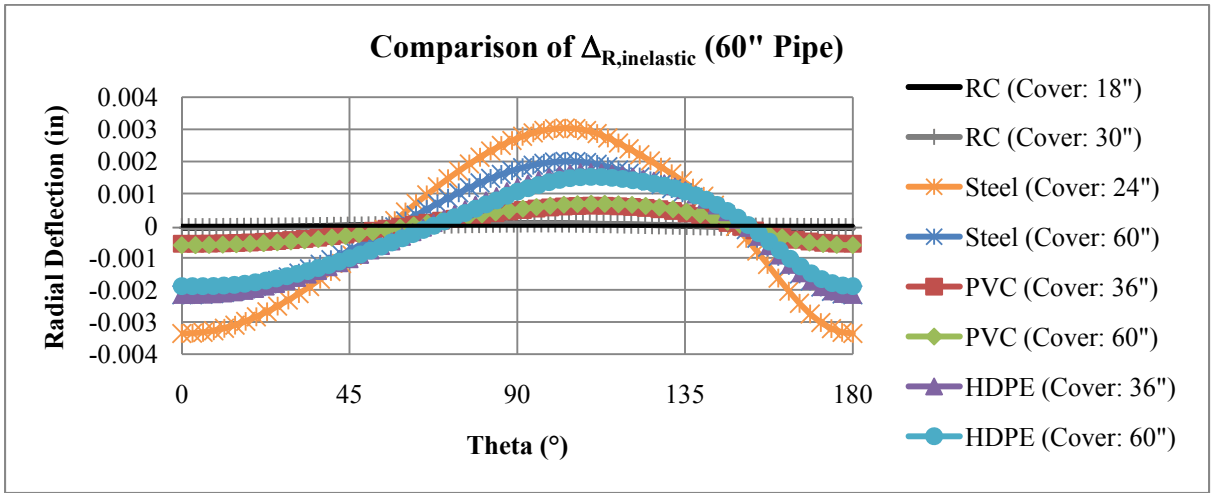

Figure 112
Comparison of $\Delta_{R,inelastic}$ for pipes with D = 60 in.

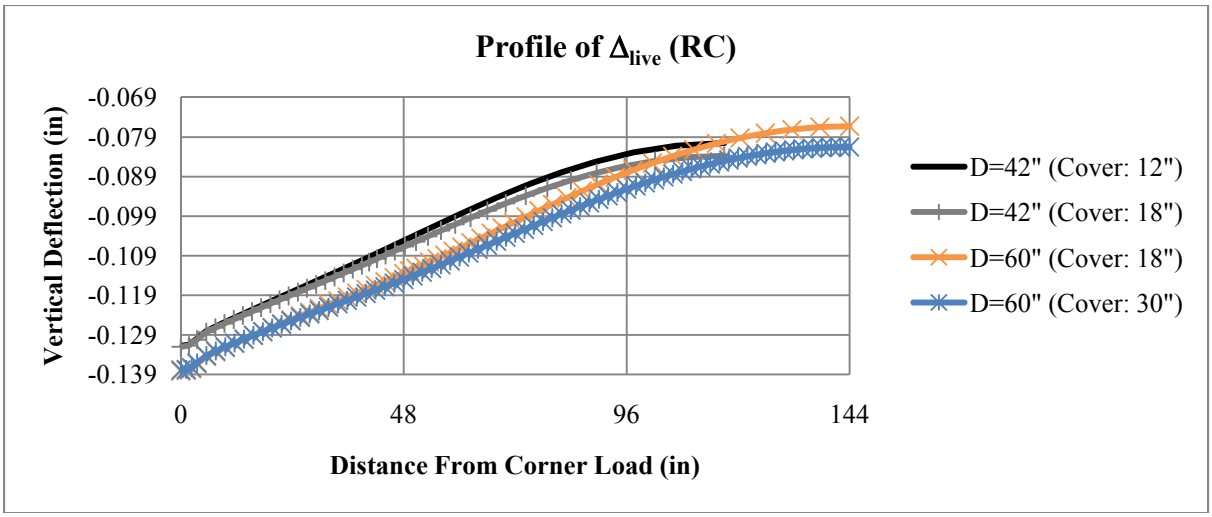

Figure 113
Profile of Δ_{live} for RC pipes

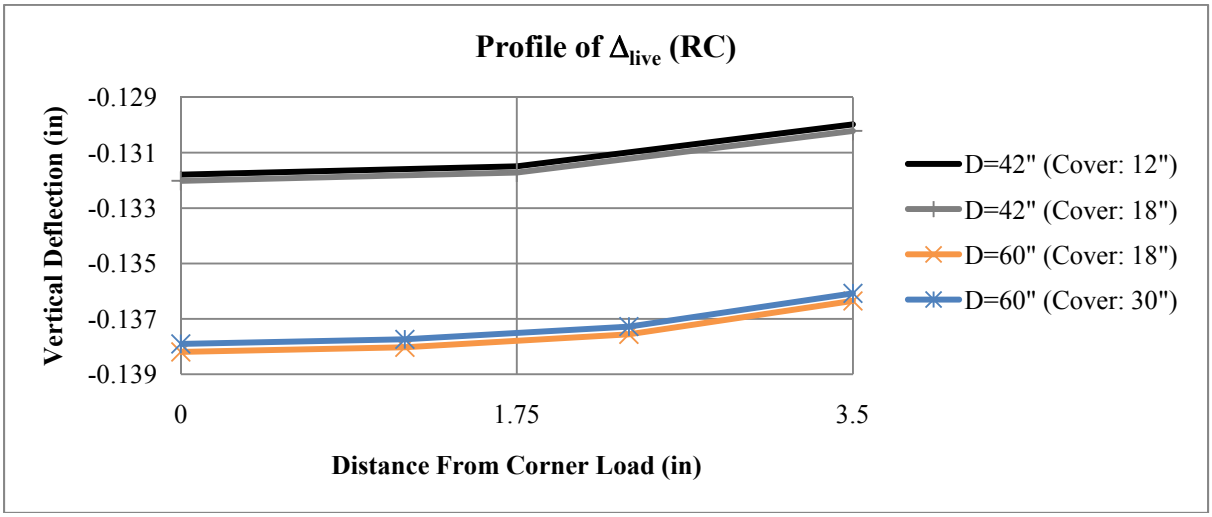

Figure 114
Profile of Δ_{live} for RC pipes: zoom view

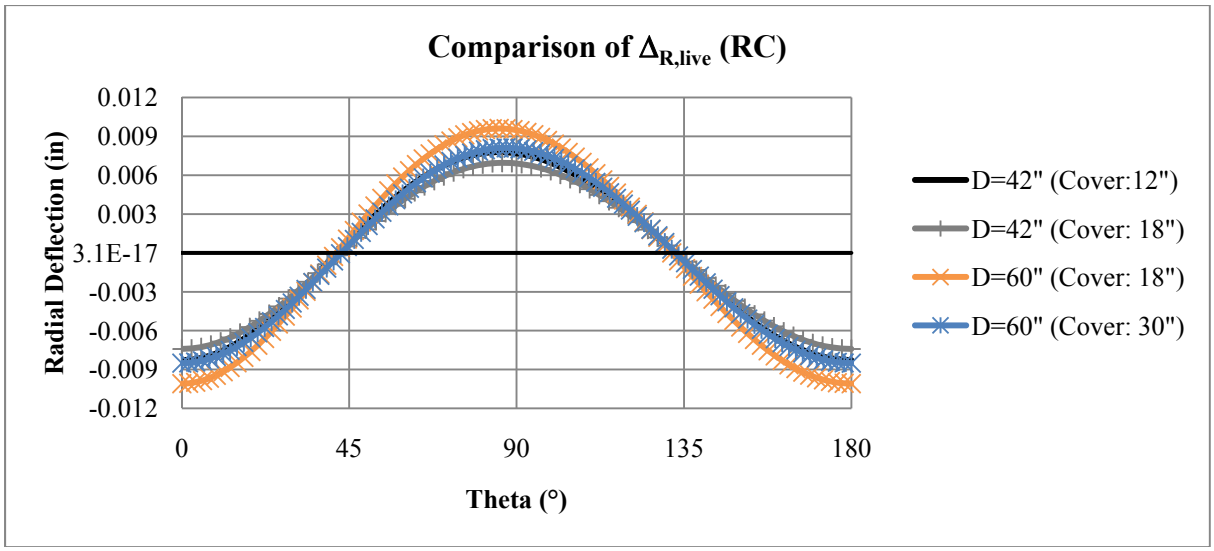

Figure 115
Comparison of $\Delta_{R,live}$ for RC pipes

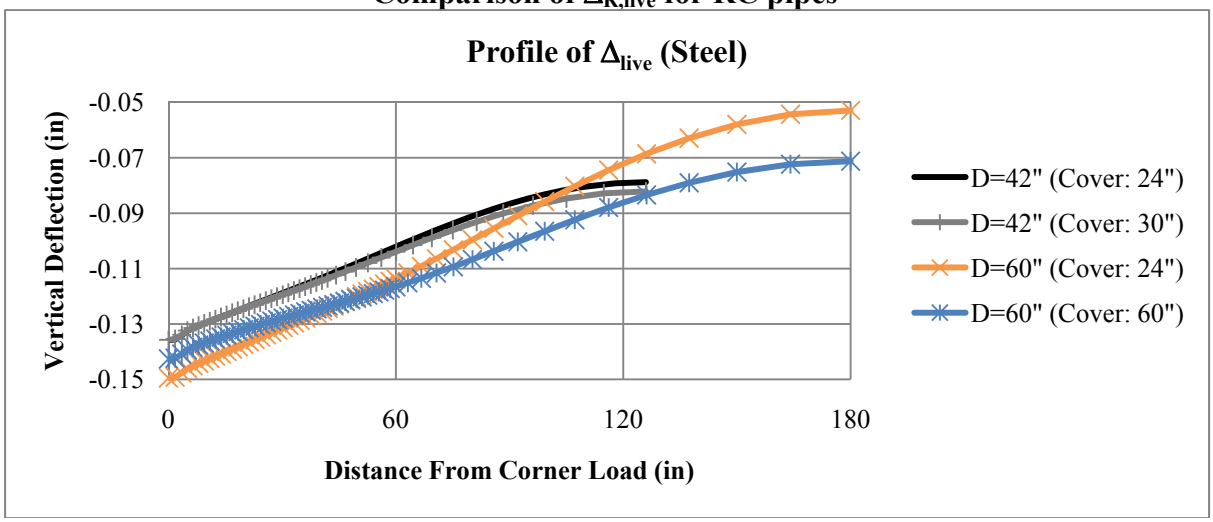

Figure 116
Profile of Δ_{live} for steel pipes

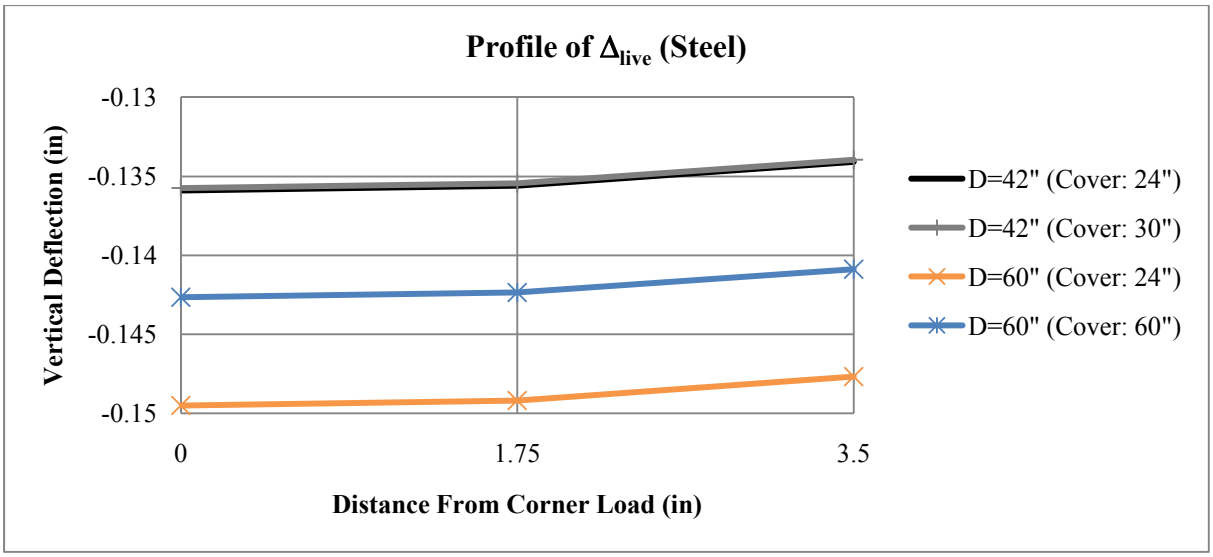

Figure 117
Profile of Δ_{live} for steel pipes: zoom view

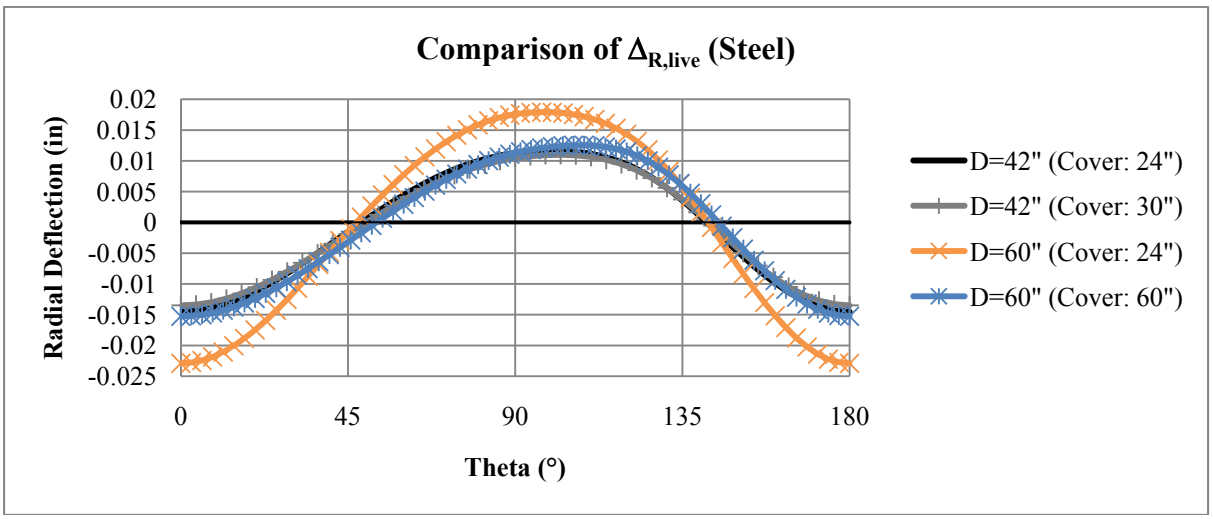

Figure 118
Comparison of $\Delta_{R,live}$ for steel pipes

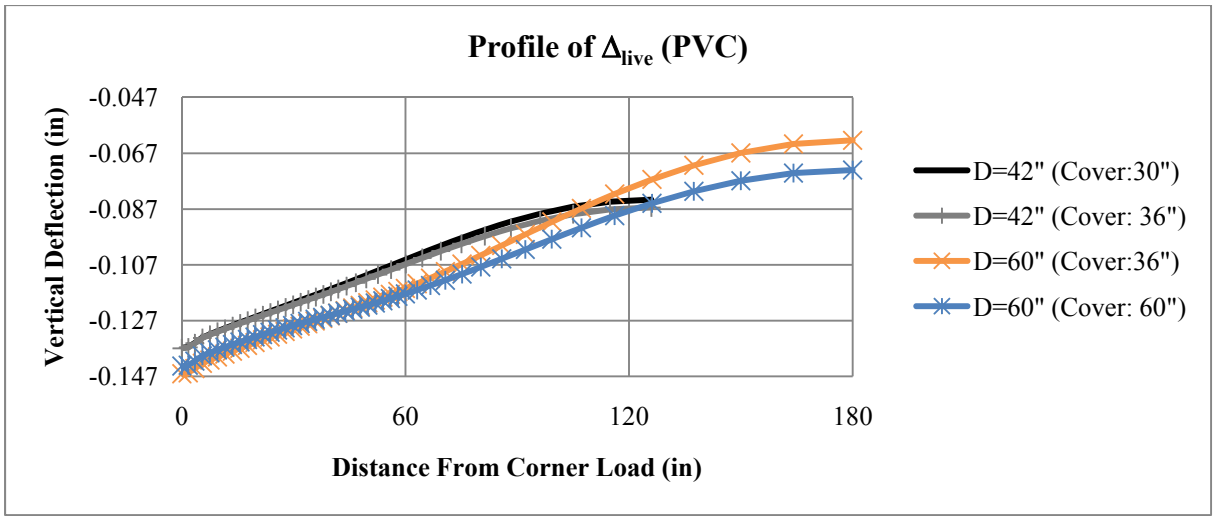

Figure 119
Profile of Δ_{live} for PVC pipes

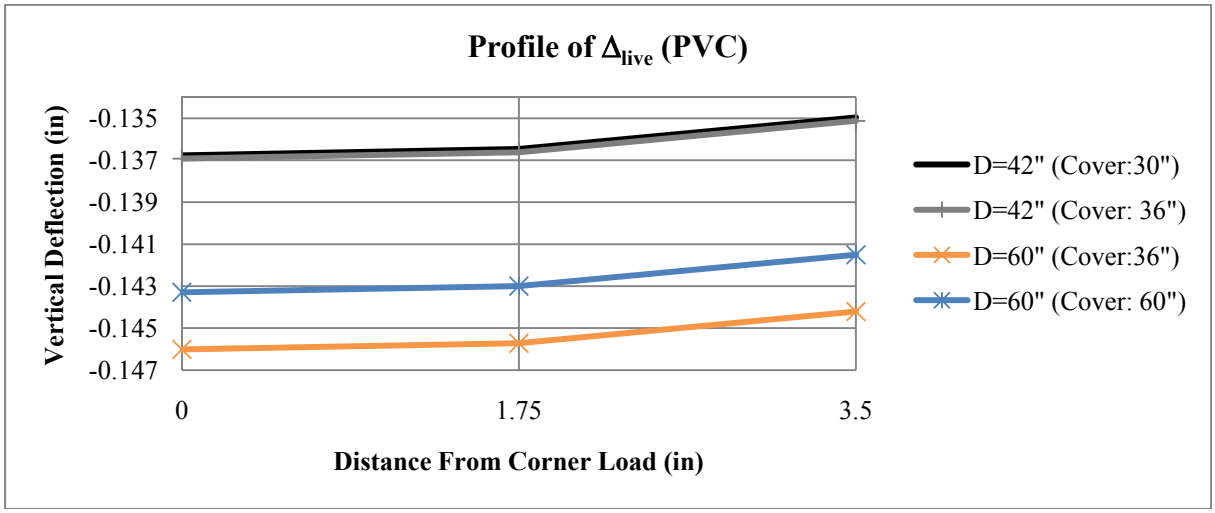

Figure 120
Profile of Δ_{live} for PVC pipes: zoom view

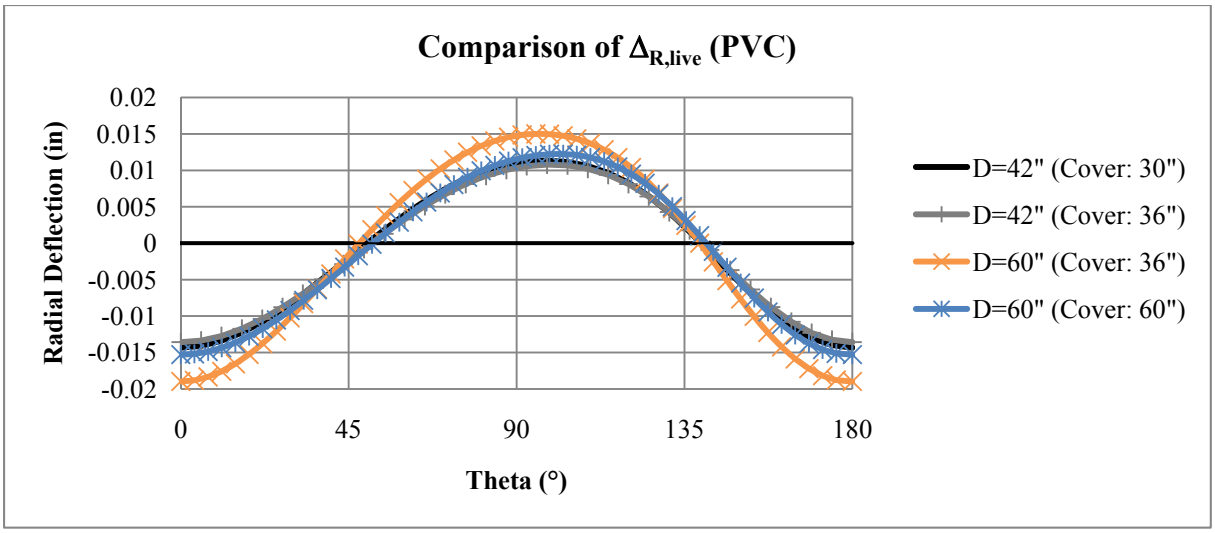

Figure 121
Comparison of $\Delta_{R,live}$ for PVC pipes

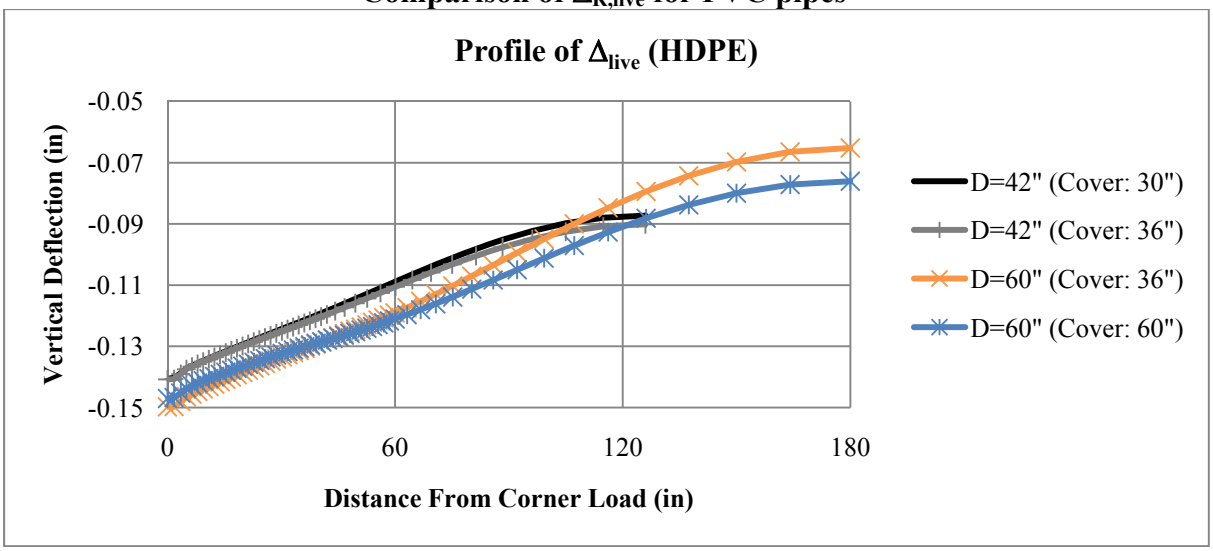

Figure 122
Profile of Δ_{live} for HDPE pipes

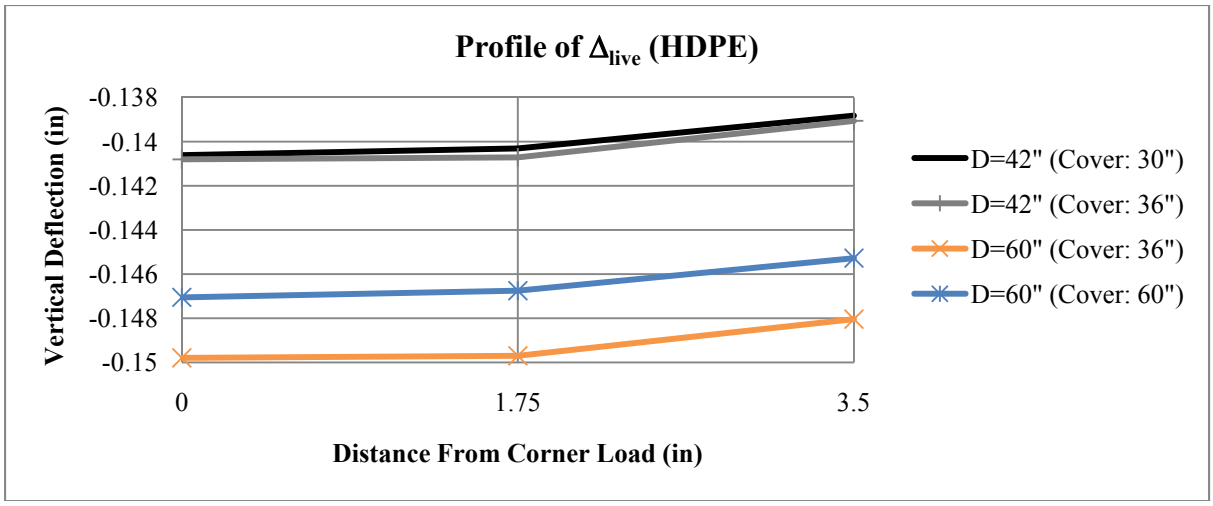

Figure 123
Profile of Δ_{live} for HDPE pipes: zoom view

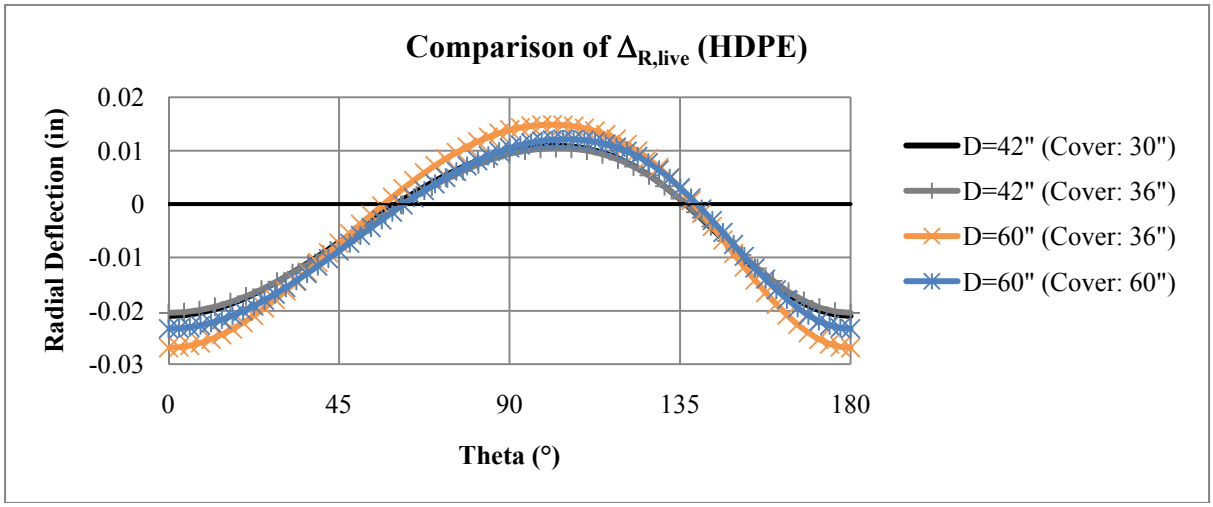

Figure 124
Comparison of $\Delta_{R,live}$ for HDPE pipes